
# Exploration of the thiosulphate process for the dissolution of gold from electronic waste and its recovery through ion-exchange

**Prepared by:**
Dasmi Maharaj

**Supervisor:** Jochen Petersen
**Co-Supervisor:** Thandazile Moyo

MSc Chemical Engineering

**Key Words:** E-waste, gold, PCBs, leaching, ion-exchange, resin, ammonium thiosulphate

A thesis submitted to the Faculty of Engineering and the Built Environment at the University of Cape Town, in fulfilment of the requirements for the degree of Master of Science in Engineering, in Chemical Engineering.

HYDROmet

minerals to metals

# Plagiarism Declaration

I know the meaning of plagiarism and declare that all work in the document, save that for which is properly acknowledged, is my own. This thesis/dissertation has been submitted to the Turnitin module (or equivalent similarity and originality checking software) and I confirm that my supervisor has seen my report and any concerns revealed by such have been resolved with my supervisor.

| Signed by candidate | 13 February 2022 |
| --- | --- |
| Signature | Date |

# Acknowledgements

First and foremost, I would like to thank my project supervisor and undergraduate lecturer, Professor Jochen Petersen for taking me in as a member of the growing Hydromet family. It was truly a privilege to be advised by him and under his guidance for the duration of this project. His insightful feedback pushed me to sharpen my thinking and ultimately brought my work to a higher level.

Furthermore, I would like to thank my co-supervisor, Doctor Thandazile Moyo for her advice and additional support who never refused my probing questions or assistance throughout my degree. Thank you for always checking in with me and for always willing to gently guide me in the right direction.

I would also like to express my sincere gratitude to Doctor Allan Nesbitt without whom none of my ion exchange laboratory experiments would have succeeded. I am extremely thankful and indebted to him for sharing his expertise, valuable guidance and the encouragement extended to me for the duration of this thesis.

Another heartfelt thank you to Kathija Shaik, the laboratory manager of the Hydromet research group. Thank you for your prompt responses to my laboratory based problems and for always being a helpful hand. I will cherish the long discussions about possibly anything and everything whilst in the laboratory.

I would also like to thank the SARCHi chair for the funding given to this project and not forgetting the National Research Foundation for their financial contributions.

Furthermore, I would like to thank Charney Anderson-Small from CAF Stellenbosch University and Shené Klink and Sandeeran Govender from the Analytical Lab at the University of Cape Town for analysing my countless samples and who contributed through their additional knowledge and emails. In addition, I would like to thank Miranda Waldron from the Electron Microscope Unit at UCT for further analysing my PCBs and Thelma Horsfield from Set Point Laboratories for my sample analysis. I would also like to thank Johanna van Deventer, without whom I would have had very little resins to work with. Thank you for imparting your knowledge and experience on ion exchange.

I would also like to thank the extended Hydromet family for their constant support be it via mock conference presentations or thesis guidance. Thank you all for the thoughtful comments and help throughout my degree.

Lastly, I would like to thank my family and friends. Thank you all for your unconditional support and understanding especially through the trying times. This degree is for you all.

# Abstract

Electrical and electronic equipment (EEE) has substantially grown over the past few years due to vast technological advancements and consequently so has electronic waste (e-waste). This growth has shown cause for concern with a generation of 53.6 million metric tonnes of e-waste globally in 2019 alone. Part of this concern may be due to the slow adoption of formal collection and recycling practices in developed countries whilst developing countries bear the brunt of the e-waste produced within the country and the e-waste imported from other countries. Furthermore, the burden of the increasing levels of e-waste has detrimental effects on the environment. In such cases, e-waste landfills have been known to leach metals, such as lead, into soil and groundwater of nearby regions thereby affecting human and animal life in the area. Despite the evident hazardous materials associated with e-waste, there is still value in this waste. The value is attributed to the metals such as gold, silver, copper and palladium found in e-waste. Printed circuit boards (PCBs) are a small but nonetheless crucial fraction of global e-waste making up 6% by mass. The gold content in this small fraction is of much higher concentrations than in typical primary gold ores thus PCBs represent the most economically attractive portion of e-waste.

Hydrometallurgical processing has previously been applied for the recovery of gold and copper from primary ores possibly due to it being considered environmentally friendly. Therefore, this thesis investigates a hydrometallurgical process for recovering gold from PCBs. Literature studies show ammonium thiosulphate to be a viable option in comparison to the more widely used cyanide leaching route (Aylmore & Staunton, 2014). Thus, the ammonium-thiosulphate system containing ammonia, ammonium thiosulphate and copper (II) sulphate pentahydrate was incorporated as a hydrometallurgical option for the recovery of gold. This study explores the formulation of synthetic gold solutions using gold powder as well as its application to PCB gold leaching in the same ammonium-thiosulphate system. Gold recovery using ion-exchange processes was investigated with the use of a medium-base (AuRIX®100) and two strong-base anion exchange resins (Purogold™ MTA5013SO4 and MTA5011SO4). The AuRIX®100 resin was specifically developed for and is currently used in the gold-cyanide system. The MTA5011SO4 resin is currently used in the Barrick Goldstrike operation for thiosulphate systems and the MTA5013SO4 resin was produced by Purolite® for thiosulphate-copper systems. In addition, two eluants (ammonium nitrate and ammonia) were tested to effectively elute gold from the resin. Furthermore, copper was monitored throughout the leaching and ion exchange experimentation due to its catalytic effect in the ammonium-thiosulphate system.

Determining the most appropriate dilution of the ammonium-thiosulphate solution after leaching to ensure solution stability in the periods between sampling time and analysis was explored as part of the investigation. In addition, gold powder dissolution from a 99.99% pure gold powder and gold leaching from PCBs were investigated. PCBs were cut by means of a bandsaw for the purposes of fitting them into a reactor whilst limiting copper liberation. Various additional background copper concentrations were introduced into the gold powder dissolution and leaching system to determine its effect on gold and copper extractions. For the ion exchange processes, capacity tests on all three resins were conducted to establish the resin operating capacities before loading and elution of synthetic gold solutions. Loading and elution tests were conducted at three flowrates (10 mL/min, 25 mL/min and 50 mL/min) and with two eluants; ammonium nitrate and ammonia. Kinetic and equilibrium experimental work was

investigated on the MTA5013 resin with the addition of chloride ions as a competing anion to loaded gold on the active sites of the resin. The MTA5011 resin was introduced into the experimental work for confirmatory results of the MTA5013 resin. This was necessary as both the Purogold™ resins are similar with the exception of particle size and thus were expected to behave in the same manner.

Gold concentrations of 141 ppm (representing 100% extraction) and 4.1 ppm (representing 91% extraction) after 24 hours was extracted for gold powder dissolution and PCB leaching experiments respectively. Background copper concentrations of 0.045 M and 0.1 M resulted in the highest gold and copper extraction values for gold powder and PCB respectively. In addition, the strong-base anion exchange resin (MTA5013) proved to be more suitable than the medium-base anion exchange resin for the ammonium-thiosulphate system. However, its low gold loading values of 8.06 meq/L (milliequivalents per litre of resin) and elution of 5.80 meq/L proved that it was ineffective in removing large gold amounts from the synthetic solution at a resin volume of 5 mL. Loading at low flowrates of 10 mL/min whilst eluting at 25 mL/min resulted in the highest loading and elution concentrations of both gold and copper. Copper loading and elution concentrations of 150 meq/L and 38.4 meq/L respectively were measured. This translated to 3.78% recovered in loading and 67.5% recovered in elution. High recoveries of gold and copper representing 75% and 67.5% respectively were achieved with ammonium nitrate as an eluant. Only 21.7% of the loaded gold was eluted when using ammonia as an eluant. Final kinetic and equilibrium test work revealed that the MTA5013 resin has an affinity for the aurothiosulphate ion over the weak chloride ion. This is attributed to low concentrations of chloride in solution therefore being ineffective in displacing the aurothiosulphate ion from the resin. Results from this study suggested that anions such as thiosulphate and tetrathionate competed strongly for the resin active sites and this was in agreement with Nicol & O'Malley (2002) who made the same postulation. Moreover, final gold loading concentrations were low (8.06 meq/L) given the operating capacities of the resin (0.77 eq/L). It was proposed that this may be due to other anions such as polythionates in the system occupying the active sites including the small resin volume. High concentrations of polythionates in solution compete for resin active sites despite the resin affinity for the aurothiosulphate ion over polythionates in the system.

It is concluded from this study that the ammonium-thiosulphate was efficient in leaching gold, obtaining almost 100% extraction in PCB leached solutions and 100% in gold powder synthetic solutions. Strong-base anion resins were proven to be ineffective in obtaining high gold recoveries for the system at low resin volumes and the resin indicating a high concentration of polythionate attachment relative to gold. However, the resin did demonstrate a higher affinity for the aurothiosulphate ion relative to copper species in the solution and given a larger resin volume: solution volume ratio, high gold recoveries are possible. Furthermore, an ammonium nitrate eluant is considered appropriate in removing high concentrations of gold from the resin.

# Table of Contents

# Table of Figures

# List of Tables

# List of Equations

# Nomenclature

## Abbreviations

| | |
|---|---|
| WEE | Waste electric and electronic equipment |
| E-waste | Electronic waste |
| PCB | Printed Circuit Board |
| IT | Information Technology |
| RIL | Resin-in-Leach |
| RIP | Resin-in-Pulp |
| PPE | Personal Protective Equipment |
| BSTR | Batch Stirred Tank Reactor |
| ZLC | Zero Length Column |
| ICP-AES | Inductively Coupled Plasma Atomic Emission Spectroscopy |
| ICP-OES | Inductively Coupled Plasma Optical Emission Spectrometry |
| ICP-MS | Inductively Coupled Plasma Mass Spectrometry |
| MP-AES | Microwave Plasma Atomic Emission Spectroscopy |
| SEM-EDS | Scanning Electron Microscopy – Energy Dispersive Spectroscopy |
| FWSV | Free West Settled Volume |
| MSDS | Material Safety Data Sheet |
| QEMSCAN | Quantitative Evaluation of Materials by Scanning Electron Microscopy |

## Chemical Formula

| | |
|---|---|
| Au | Gold |
| Ag | Silver |
| Cu | Copper |
| Fe | Iron |
| Al | Aluminium |
| Sn | Tin |
| Zn | Zinc |
| Pb | Lead |
| Pd | Palladium |
| B | Boron |
| Ba | Barium |
| Ca | Calcium |
| Co | Cobalt |
| K | Potassium |

| | |
|---|---|
| Mg | Magnesium |
| Na | Sodium |
| Ni | Nickel |
| Si | Silicon |
| Sr | Strontium |
| C | Carbon |
| H | Hydrogen |
| N | Nitrogen |
| $AuBr_3$ | Gold bromide |
| $Cl_2$ | Chlorine |
| $Br_2$ | Bromine |
| $S_2O_3^{2-}$ | Thiosulphate |
| $Cu(NH_3)_4^{2+}$ | Copper (II) amine |
| $Au(NH_3)_2^{+}$ | Gold (I) amine |
| $Cu(S_2O_3)_3^{5-}$ | Copper (I) thiosulphate |
| $Au(S_2O_3)_2^{3-}$ | Gold (I) thiosulphate |
| $NH_3$ | Ammonia |
| $Cu(NH_3)_2^{+}$ | Copper (I) amine |
| $Cu^{2+}$ | Cupric ion |
| $Cu^{+}$ | Cuprous ion |
| $H^{+}$ | Hydrogen ion |
| NaOH | Sodium hydroxide |
| NaCl | Sodium chloride |
| $Na_2SO_4$ | Sodium sulphate |
| $NO_3^{-}$ | Nitrate ion |
| $Cl^{-}$ | Chloride ion |
| $Zn(S_2O_3)_2^{2-}$ | Zinc (I) thiosulphate |
| $HNO_3$ | Nitric acid |
| HCl | Hydrochloric acid |
| $(NH_4)_2S_2O_3$ | Ammonium thiosulphate |
| $CuSO_4.5H_2O$ | Copper (II) sulphate pentahydrate |
| $NH_4NO_3$ | Ammonium nitrate |

**Symbols**

| | |
|---|---|
| $Q$ | Actual capacity (eq/L) |
| $\overline{C_e}$ | Gold concentration at equilibrium on resin (eq/L) |
| $b$ | Adsorption intensity constant |
| $C_e$ | Gold concentration at equilibrium in solution (eq/L) |
| $K_F$ | Freundlich adsorption equilibrium constant |
| $\bar{C}$ | Total resin capacity (eq/L) |

| | |
|---|---|
| $K_L$ | Langmuir adsorption equilibrium constant |
| $C$ | Total concentration of solution at equilibrium (eq/L) |
| $X_{Au}$ | Fraction of aurothiosulphate in solution at equilibirum |
| $K_{Au}^{Cl}$ | Selectivity coefficient for aurothiosulphate and chloride ion exchange |
| $\overline{X_{Au}}$ | Fraction of aurothiosulphate on resin at equilibrium |
| $K_{OH^-}^{Au(CN)_2^-}$ | Selectivity coefficient for aurocyanide and hydroxl ion exchange |
| $\alpha_A^B$ | Separation factor for B and A ion exchange |

# 1. Introduction

This thesis explores the dissolution of gold from printed circuit boards (PCBs) which make up an estimated 6% of the overall Waste Electrical and Electronic Equipment (WEEE) stream. In addition, recovery of gold via ion-exchange methods utilising strong- to medium-base resins is studied and is the focus of this investigation.

The purpose of this chapter is to provide context and background to the research leading up to problem statement. It also includes an overview of the subsequent chapters in this thesis.

## 1.1. Background to investigation

In the modern, developing world, technological advancements have resulted in a more convenient, independent and comfortable life. This fast-growing industry has estimated to generate 53.6 million metric tonnes of electronic waste (e-waste) per year (Forti et al., 2020). In South Africa alone, the total value of e-waste generated was documented to be approximately 416 kt in 2019 (Forti et al., 2020). Due to these rapid advancements, there is an increase in the demand of new products resulting in a shorter life span of said products. Subsequently, the environmental burden due to this “ecological baggage” has increased alarmingly causing unsafe and improper treatment and disposal of e-waste (Schwarzer et al., 2005). In addition to this, e-waste in this technologically advanced age, is still being transported from developed countries to developing countries. Often the e-waste entering these developing countries are processed via inefficient and rudimentary techniques to extract materials and components of value.

PCBs are a small but nonetheless key component of WEEE. They contain a large variety of precious and base metals. Base metals, such as copper and tin are found underneath the protective coatings of the board and precious metals, such as gold and silver to name a few, are present on the surface of the board. Gold, in PCBs, is typically found in high concentrations with some studies reporting figures as high as 903 g/t (Petter, Veit & Bernardes, 2014) while typical primary ores contain between 10 to 90 g/t (Jeffrey, Breuer & Chu, 2003; Arslan & Sayiner, 2018). Although there are reports of reduced use of precious metal in the manufacturing of PCBs, the stream can still outmatch primary ores whose grades are decreasing and whose minerology has become more complex. In addition, the value from this stream can far outweigh that from primary ore.

There are many challenges to the processing of PCBs. Some of these challenges include the complexity and heterogeneity of PCBs. Thus, industrial treatment of e-waste is carried out mainly via pyrometallurgical routes (Cui & Anderson, 2016). Although pyrometallurgical processes are currently in practice, this route does have its disadvantages mainly around the large energy requirements moreover the precious metals are only obtained at the very end of the process. Active research in the past 20 years has been carried out on hydrometallurgy as a viable option. This route has a low environmental impact and is easy to manage (Cui & Zhang, 2008). An ammonium thiosulphate system is one of the options in the hydrometallurgical route. The system is non-toxic as opposed to its competitor, the cyanide system and has shown to extract gold at much faster rates (Sullivan & Kohl, 1997). Recovery of gold from PCBs leach liquors such as cyanide uses the carbon adsorption or active carbon process. This process has reached high recoveries of 95% such as in Abbruzzese's et al.

(1995) study. However, there has been a shift to resin adsorption or ion exchange processes. These processes have been extensively used in the cyanide system for gold recovery with optimised resins such as Minix and AuRIX®100 being employed. Ion exchange is well suited to the ammonium thiosulphate system as it is environmentally friendly and requires no thermal regeneration of the resin (Kotze et al., 2005).

This thesis delves into the current technologies available for the safe and low-cost extraction of gold from waste printed circuit boards thus building on ongoing work within the Hydromet Research unit at the University of Cape Town. The ongoing work, depicted in Figure 1.1 below aims to develop and subsequently test a hydrometallurgical flowsheet for metal recovery specifically in ammoniacal solutions. The flowsheet investigates pre-treatment of the boards by means of cutting and thermal treatment as the initial step. Thereafter the flowsheet is divided between the acid and alkali circuit. The acid circuit removes the main metals, tin and lead, from the solders on the PCB. The alkali circuit is aimed at recovering copper, nickel and gold by means of both ammonium hydroxide and thiosulphate leachates. The effluent circuit investigates the removal of the remaining mixed metals subsequent to the acid and alkali circuits. The test work conducted within this thesis forms part of the Alkali Circuit (outlined in red) under extraction of precious metals. Pre-treatment of the PCBs including extraction of copper in the alkali circuit has been investigated and validated by previous earlier work.

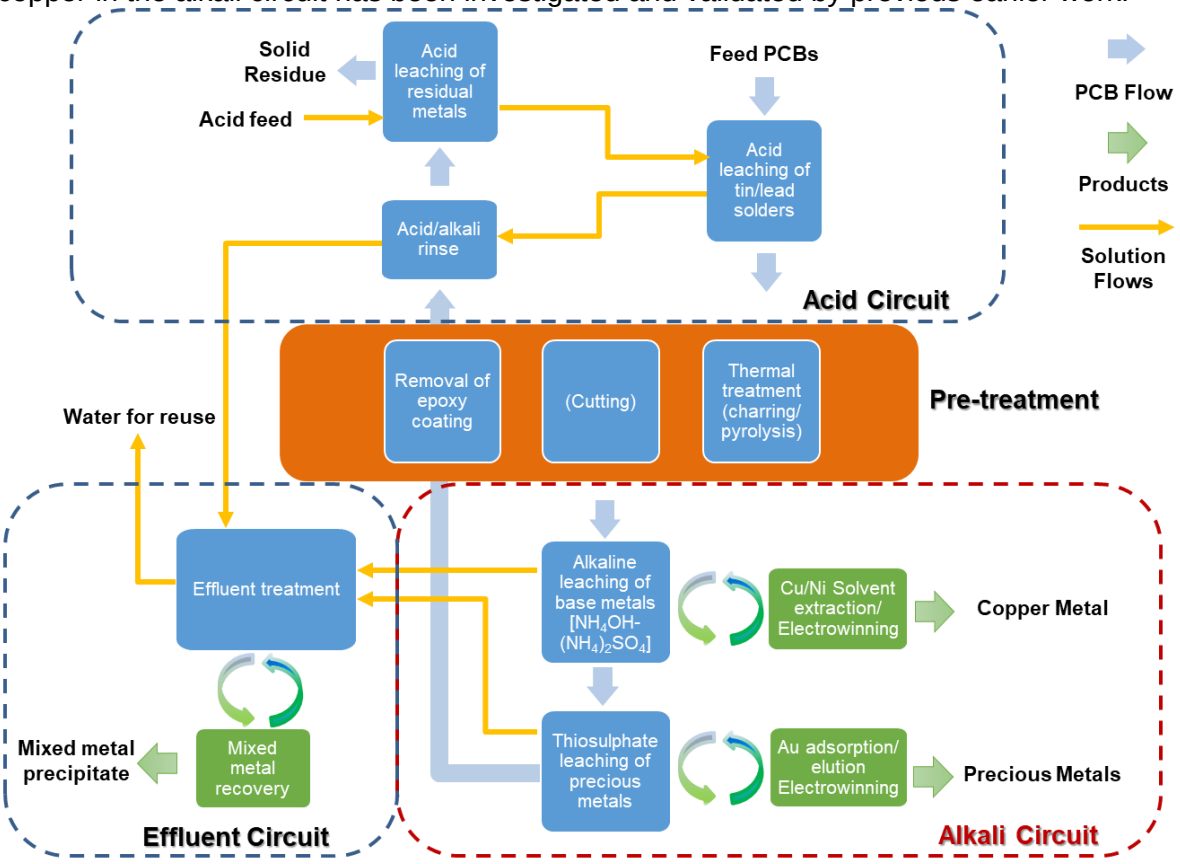


Figure 1.1: Proposed hydrometallurgical flowsheet for waste PCB recycling in the Minerals to Metals Research initiative

## 1.2. Problem statement

In order to elucidate the use of hydrometallurgical methods in the extraction of gold from e-waste, it is paramount to provide faults or limitations in the current methods. These promising

methods employ cyanidation and subsequent elution, electrowinning or cementation in the removal of gold from PCBs. Cyanidation as a technique for gold extraction has proven to be precarious, posing serious risks to health and environmental habitats whereas cementation has been known to produce slightly contaminated solid products necessitating further purification consequently increasing the costs. Thus, it is necessary that a viable method which is both environmentally friendly and economical is introduced and investigated in detail as an alternative to both cyanide leaching and gold cementation.

Ammonium thiosulphate leaching is one of the proposed methods to the leaching of gold. This process is non-toxic and environmentally friendly. Furthermore, literature findings have shown it to be faster than cyanide leaching (Aylmore & Muir, 2001; Jeffrey, Breuer & Choo, 2001). Employing the use of the thiosulphate leaching system, will subsequently necessitate an investigation into viable methods for analysing gold in the alkaline thiosulphate solution. Following leaching, gold is recovered from solutions using techniques such as solvent extraction and ion-exchange. Ion exchange is a leading method in water purification mainly due to its low cost and lack of need for thermal regeneration. In recent years, it has also proven to be a competitor to carbon adsorption in the extraction of gold (Zhang & Dreisinger, 2002). This method has the potential to be applied to an ammonia-ammonium thiosulphate system.

Hence, this thesis aims to provide an analysis into the thiosulphate leaching of gold from waste PCBs and its subsequent recovery using ion exchange processes for the beneficiation of precious metals from the PCB waste stream in a South African context.

## 1.3. Objectives

The project aims to test and validate the process for recovering gold from PCBs via thiosulphate leaching and ion exchange. To do this, gold leaching in thiosulphate is initially tested using a pure gold powder generating what is termed gold-thiosulphate synthetic leach solutions. This eliminates the effect of impurities especially on ion exchange which is conducted using resins typically employed in gold-cyanate chemistry.

The four main objectives are stipulated below:

- Evaluate the effectiveness of the alkaline thiosulphate system for gold leaching from PCBs.
- Determine the effect of background copper concentrations on PCB and gold powder leaching extractions and the role it plays in the chemistry.
- Investigate the effects, if any, of resin types and background ions on the recovery of gold from leachate generated in the above 2 objectives.
- Establish the effectiveness of different elution methods from the ion exchange resins.

## 1.4. Scope and limitations of investigation

The scope of this investigation will include the pre-treatment of PCBs for leaching of gold as well as the ammoniacal leaching of both PCB and gold powder. The recovery of gold powder from the leached solutions will be investigated by incorporating the ion-exchange method using medium- to strong-base resins as well as two different methods for elution. Gold powder that has undergone dissolving in an ammonium thiosulphate solution will be used to investigate the effectiveness of the ion exchange method in recovering gold. Investigation into

various parameters such as temperature, pH and time on leaching for both PCBs and gold powder will not be investigated including exploration of the most suitable conditions on ion exchange extraction.

## 1.5. Plan of development

This thesis consists of 5 Chapters. Chapter 1 is the first chapter in the thesis and introduces the thesis and provides background to the investigation. Thereafter Chapter 2, the literature review, provides a detailed analysis of literature by reviewing the various methods available for hydrometallurgical leaching including the thermodynamic and kinetics of the chosen ammonium thiosulphate leaching method. Current alternatives for downstream gold recovery are provided including a deeper analysis into the ion exchange method for the purposes of gold recovery. The key questions and hypotheses are then provided relative to the test work that was conducted in this study. Chapter 3 provides the research approach to the investigation. The experimental procedure performed is described for both leaching and ion exchange with an analysis on the type of equipment used including the conditions of the experimentation. Chapter 4 presents the results of all leaching and ion exchange experiments and includes a discussion that is expanded upon for each result sub-section. Chapter 5 provides the conclusions and any recommendations for further research. A reference list and an appendix containing additional information and experiment results are attached at the end of this report in the interest of clarity.

# 2. Literature Review

This purpose of this chapter is to outline and provide knowledge for the research in this study including identifying any gaps in the literature that the research work aims to address. Furthermore, it provides a framework of electronic waste (e-waste) as an increasing problem but still a resource that if managed and recycled properly can provide multiple avenues of income. Hydrometallurgy is introduced as an option for leaching printed circuit boards (PCBs) using an alkaline system and this is further expanded into current viable recovery methods for gold. Lastly, limitations are stated and discussed with each option and thus the chapter aims to provide a comprehensive overview of each step in the research process.

## 2.1. E-waste

E-waste is a great concern especially in the South African context where management of e-waste occurs in an informal and rudimentary manner. The sub-section below highlights the key issues surrounding e-waste and the alternatives methods that can be employed to develop e-waste as a resource contrary to viewing it as an obstacle in the developing world.

### 2.1.1. Overview

Waste Electrical and Electronic Equipment (WEEE) or e-waste is a growing worldwide concern in the technological industry. This can be attributed to the rapid advancements in the electronic world including the increasing availability of products open to the public and the obsolescence of said products in industry (Hadi et al., 2015). E-waste is formed when electrical and electronic equipment reaches its end-of-life and is no longer of any use. This consists of computers, mobile phones and television sets to name a few.

There is currently no standard definition for e-waste however this thesis will define e-waste as *'electronic and electrical equipment that utilises a power supply in order to perform its functions and has been disposed of by its original owner'* (Lydall, Nyanjowa & James, 2017). E-waste can be sub-divided into six smaller categories namely temperature exchange equipment, screens, lamps, large equipment, small equipment and small IT (Information Technology) and telecommunication equipment (Balde et al., 2017). In South Africa, there are two additional categories which are security and healthcare equipment as well as mixed waste electronic and electrical equipment (Lydall, Nyanjowa & James, 2017). All e-waste contains a mixture of various metals such as copper, gold, and aluminium as well as toxic metals namely lead and mercury (Hung Ha et al., 2010).

Equipment that has reached its end-of-life (e-waste) that is discarded or unused equipment such as fridges, cameras, printing machines and many others raise serious health and environmental risks, especially if not treated appropriately. In addition, the increasing level of electronic waste poses a significant concern to sustainable development. For instance, middle to low-income countries may be challenged by the considerable health and environmental risks associated with inadequately managed and inferior conditions for e-waste handling. The current trends state that e-waste generated will substantially increase over the next few years thus posing several challenges to the disposal of it. In addition, the environmental burden of these products is known to outweigh the burden due to other household material production (Schwarzer et al., 2005).

The generation of e-waste is expected to increase from 7.3 kg per capita annually in 2019 to 9 kg per capita by 2030 worldwide (Forti et al., 2020). Between 2014 and 2019, e-waste recycling was approximately 2 Mt per year therefore indicating that global recycling activities are evidently not keeping up with e-waste generation. Since 2014, global e-waste generated was approximately 44.4 Mt and this is expected to exceed 74 Mt by 2030 (Baldé et al., 2020). However, it is difficult to give an accurate value for e-waste generation in some cases due to non-existent data thus these quantities are an estimate. A large majority of the e-waste generated was most likely informally collected with no assurances of being conducted in an environmentally safe manner. A significant portion of the e-waste is managed outside of the official collection systems, with some being transported to third world countries. Thus, e-waste is subjected to improper disposal and treatment.

Though e-waste is a concern due to its fast growth, informal disposal and accumulation of hazardous substances in the ecosystem, metal beneficiation of e-waste is slowly becoming a more viable alternative source of gold next to mining primary gold-bearing ores. Extensive research into e-waste management has the potential to mitigate the extent of the problems associated with e-waste (Kiddee, Naidu & Wong, 2013). In addition, developing devices that are eco-designed, recovering and recycling material via safe methods, disposal of e-waste using suitable techniques and forbidding the transfer of e-waste to developing countries will be the driving force behind turning e-waste from a major concern into a resource.

### 2.1.2. Waste printed circuit boards (PCBs)

PCBs are an essential part of electronics and contain a range of base (copper, nickel and tin) and precious metals (gold and silver) (Ficeriová, Baláž & Gock, 2011). They are found in up to four of the six e-waste categories and according to Schwarzer et al. (2005), PCBs are approximately 6% of the total weight of e-waste. Despite presenting a small portion, they contain the most monetary value in the e-waste sector which can be largely attributed to the composition of the PCBs (Behnamfard, Salarirad & Veglio, 2013). Thus, most of the attention has been given specifically to PCBs due to the gold concentration being up to 100 times greater than that of primary gold ore (Kim et al., 2011). Therefore, this specific type of e-waste has multiple advantages if treated and recycled properly.

Figure 2.1 divides e-waste into the six different categories. In 2019, a total of 53.6 Mt of e-waste was generated of which Africa contributed 2.9 Mt (Forti et al., 2020). However only 9.3 Mt of the total was documented to be recycled and disposed of in a legal and environmentally safe manner (Forti et al., 2020). PCBs fall predominantly into the small IT category which is one of the smallest contributors to e-waste comprising of 8.8% but they do appear in most of the other categories as well, albeit in smaller quantities. The large equipment category consists of typical items such as washing machines, large printing machines and many others whilst the small equipment category includes toasters, shavers and electric kettles to name a few.

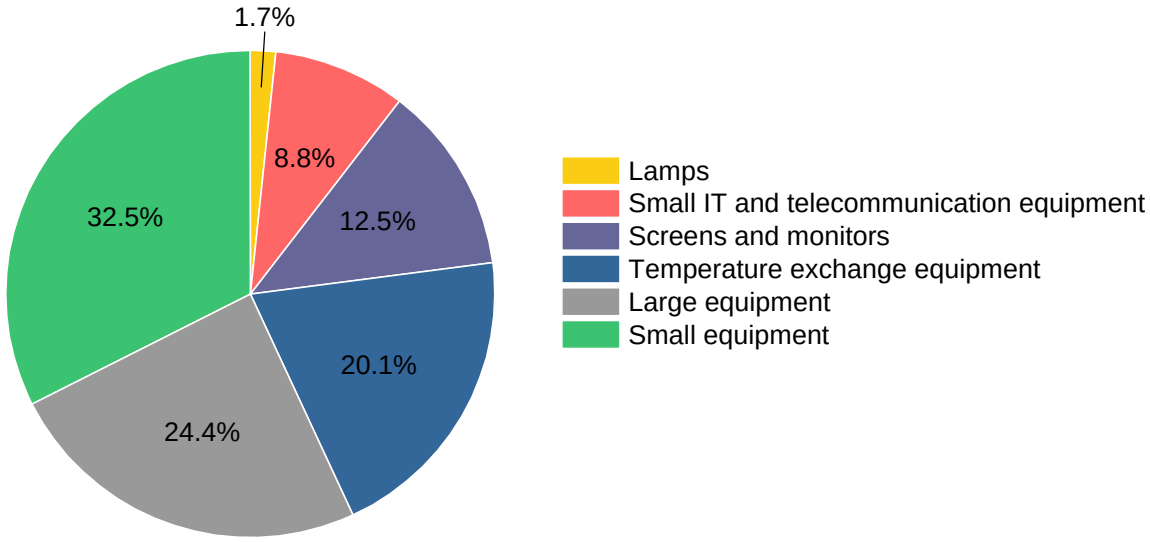


Figure 2.1: E-waste estimates per category in wt% for 2019 (Forti et al., 2020) .

Table 2.1 conveys the composition of PCBs for each respective element. The findings of these studies suggest that recycling of waste PCBs is the most lucrative due to the high precious metal compositions. Thus, the precious metal content can be seen as the main driving forces of developing advanced and safer metal recovery techniques.

Table 2.1: Weight compositions (wt%) of respective metals found in PCBs from various sources

| Element | PCB sample (1) | FR4 PCB (2) | PCB sample (3) | Mobile PCB (4) |
|---|---|---|---|---|
| Cu | 30.60 | 27 | 15.60 | 56.70 |
| Fe | 15.20 | 2 | 1.40 | 0.24 |
| Al | 11.70 | 1 | - | 1.42 |
| Sn | 7.36 | 3 | 3.24 | 1.40 |
| Ni | 1.58 | 0.20 | 0.28 | |
| Zn | 1.86 | 0.50 | 0.16 | 0.22 |
| Pb | 6.70 | 3 | 1.35 | |
| Ag (ppm) | 688 | 1000 | 1240 | 0.1 |
| Au (ppm) | 238 | 400 | 420 | 210 |

(1) Birloaga et al., 2013; (2) Hadi et al., 2015; (3) Zhang & Forssberg, 1997; (4) Tripathi et al., 2012

Gold constitutes between 200 - 400 ppm of the board shown by Table 2.1 and in some cases up to 900 ppm in comparison to typical primary ores which contain between 10 – 90 g/t (Petter, Veit & Bernardes, 2014; Arslan & Sayiner, 2018). Copper generally constitutes between 15% – 57% of the board which is the largest metallic fraction of the board. Given the relatively high gold concentrations found on PCBs and the associated incentive from a financial perspective, viable recycling methods to treat and subsequently remove gold and liberate other metals from the boards must be investigated.

### 2.1.3. Significance of recycling PCBs

Recycling of e-waste, specifically PCBs, is overregulated largely due it to being classified as toxic waste and is known to create additional hazards itself. In Europe, e-waste is exported to developing countries such as Ghana (Schwarzer et al., 2005; Birloaga et al., 2013). This contaminates the soil and groundwater in the nearby regions and largely affects the poor

communities such as an increase in metal (lead) levels observed in water bodies close to communities where rudimentary recycling occurs (Schwarzer et al., 2005). In the South African context specifically, majority of e-waste generated is disposed of in landfills causing environmental concern due to the hazardous metals associated with. The recycling of e-waste is largely through informal waste pickers and underdeveloped in terms of sophistication of automated recycling techniques (Schwarzer et al., 2005).

Much of the current literature on disposal of e-waste includes incineration which requires sophisticated scrubbers otherwise it is considered dangerous and toxic to the environment causing the formation of dioxins (Hadi et al., 2015; Lu & Xu, 2016). E-waste, specifically PCBs, consists of toxic and valuable precious metals therefore recycling and metal recovery from PCBs is necessary to prevent further environmental damage.

The incorporation of proper e-waste recycling advances the principles of a circular economy in addition to creating a more sustainable way of managing metal resources. The circular economy is a promising alternative cyclic flow model and describes the continuous flow of resources in a closed loop (Korhonen, Honkasalo & Seppälä, 2018). The model incorporates both the materials and energy throughout the product value chain thus integrating recycling as a means of handling e-waste and its metals in comparison to current and traditional methods of ‘extract-produce-use-discard’ which is unsustainable. Moreover, it will introduce an alternative to the management of metal resources from traditional primary ore mining.

Furthermore, from an economic perspective, recycling PCBs is extremely attractive due to the large copper, gold, silver and palladium content. However, the heterogenous and thus complex nature of PCBs are the main obstacles in recovering such metals. There are many routes to approach this problem such as firstly pre-treating the board either mechanically or chemically to upgrade the metal content in the board and secondly employing metallurgical processes such as pyro- and hydro-processes to attain the desired metal via extraction (Kim et al., 2011). A detailed analysis into both steps is provided in Section 2.3.

## 2.2. Current processes for PCB metal recovery

Current processes for PCB metal recovery includes pyrometallurgical and hydrometallurgical processes. Pyrometallurgy includes methods such as sintering, incineration and melting to extract the targeted metals from the PCBs (Birloaga et al., 2013). Hydrometallurgical processes involve the use of lixiviants such as cyanide, thiourea and thiosulphate to name a few. These lixiviants allow for the dissolution of the metals in an acid or alkaline medium. This subsequent leaching process is mostly not in industrial practice for the purpose of PCB gold metal recovery.

The current metal recovery process for PCBs consists of melting the materials in a lance furnace at extremely high temperatures (1200°C) and allowing reduction and oxidation processes to occur (Cui & Zhang, 2008). Copper is extracted in the final product using copper anodes in an anode furnace. A small amount of precious metals and other compounds deposit and form the anodic slime. Electrorefining is then incorporated to recover the precious metals such as gold from the anodic slime (Dönmez, Sevim & Çolak, 2001). The hydrometallurgical route will be considered in this study as an alternative to recovering gold from PCBs.

## 2.3. Pre-treatment methods.

Before processing the PCBs via hydrometallurgy, the PCBs need to be adequately prepared such that the highest dissolution rate can be achieved when leaching. Metal losses of 10% - 35% are known to occur when insufficient liberation is performed thus pre-treatment methods are incorporated before implementing hydro- and/or pyrometallurgical processes (Birloaga et al., 2013). The pre-treatment methods can be subdivided into two categories: mechanical and chemical pre-treatment methods.

### 2.3.1. Mechanical pre-treatment methods

Disassembly and mechanical pre-treatment often occur together. This allows for the liberation as well as separation of specific metallic components from their organic substance for the subsequent leaching processes (Zhang et al., 2012). It also aids in dividing the e-waste into more homogenous categories before metallurgical processing. The equipment which contains PCBs are first dismantled and the PCBs undergo the processes of shredding or separation. The PCBs are then subjected to a variety of pre-treatment separation methods such as eddy current separation, pneumatic separation, screening and electrostatic separation depending on the physical characteristics of the non-metals and metals present on the board to separate the metals from the board (Birloaga et al., 2013).

Hammer and ball mills are also known to be used in order to crush PCBs to smaller size fractions for better liberation. Ficeriová, Baláž & Gock (2011) investigated the effect of crushing PCBs using a hammer mill. It was found that leaching of ‘as received’ whole PCBs resulted in 12% gold recovery whereas leaching of PCBs that had undergone mechanical pre-treatment resulted in 98% recovery of gold. Thus, there is a large difference in the values obtained indicating the necessity of pre-treatment methods be it mechanical or chemical. However, it should be noted there is a concern dealing with mechanical separation due to the high energy cost and safety risks associated with this method (Mecucci & Scott, 2002).

### 2.3.2. Chemical pre-treatment methods

This method involves targeting base metals by dissolving them and leaving the precious metals in the residue. The precious metals are then isolated and purified from the residue. Nitric acid ($HNO_3$) or sulphuric acid ($H_2SO_4$) together with hydrogen peroxide are common chemical pre-treatments used before leaching (Zhang et al., 2012).

Mecucci & Scott (2002) performed pre-treatment experiments for the purpose of base metal leaching using $HNO_3$ of 1 M - 6 M. Copper and lead were specifically targeted in the PCBs. At 4 M concentration, 90% of lead and 83% of copper were recovered. Shredding the PCBs was incorporated to increase the efficiency of the stripping process to break up the multi-layered boards to expose more metal for leaching. In this study, incorporating chemical pre-treatment prior to actual leaching considers the nitric acid leaching step as pre-treatment.

Chemical pre-treatment for the purpose of metal liberation prior to leaching can also be considered. Such pre-treatment consists of utilising sodium hydroxide to remove the surface coating and liberate outer metal layers in addition to swelling the PCBs to liberate inner metals before leaching the targeted metal.

In this study, pre-treating will consist only of mechanical pre-treatment specifically cutting the boards into smaller sizes with the use of a bandsaw. Mechanical pre-treatment of the PCBs for the purposes of this study will primarily be referred to as size reduction of the PCBs.

## 2.4. Gold leaching of PCBs

Gold leaching can occur through various routes such as hydrometallurgical techniques and a combination of pyrometallurgical with hydrometallurgical techniques as mentioned previously. Hydrometallurgical processes are regarded to be predictable and can be easily controlled and scalable. In addition, there are less capital and operating costs associated with this option (Behnamfard, Salarirad & Veglio, 2013; Birloaga et al., 2013). Hence, there has been a shift in attention from a combination of pyrometallurgical and hydrometallurgical processes to solely hydrometallurgical processes for precious metal recovery in e-waste. A detailed analysis into the various hydrometallurgical routes is described below.

### 2.4.1. Cyanide leaching

Cyanide leaching has been used extensively for the dissolution of gold because of its low cost and ease of operation. Recently, there has been a shift towards the use of non-cyanide lixiviants in retrieving metals from ore bodies. This can be attributed to the serious environmental risks associated with cyanide leaching given its high toxicity to animal and human life (Petter, Veit & Bernardes, 2014). Furthermore, leaching with cyanide can require up to 24 hours to effectively leach gold from PCBs (Quinet, Proost & Van Lierde, 2008).

The cyanide leaching mechanism is an electrochemical process, taking place through a redox reaction. Equation 2.1, the Elsner equation, shown below is the reaction by which the gold cyanide complex is formed (Jeffrey, Breuer & Choo, 2001). It has been established by Jeffrey, Breuer & Choo (2001) that there is a critical cyanide concentration for the leaching reaction. Below this critical cyanide concentration value, gold leaching is limited by the cyanide concentration and if this value is exceeded, gold leaching is limited by the oxygen diffusion to the surface.

$$4Au + 8CN^- + O_2 + 2H_2O \rightarrow 4Au(CN)_2^- + 4OH^- \qquad \text{Equation 2.1}$$

Petter, Veit & Bernardes (2014) investigated the use of potassium cyanide in retrieving gold from mobile phone PCBs. The study reported gold recoveries of between 60% – 70% after 2 to 4 hours at ambient temperature. This translated to 540 – 590 g Au per ton of PCB. Quinet, Proost & Van Lierde (2008) investigated the use of cyanide in retrieving gold from crushed and milled mobile phones. After 3 hours at ambient temperature, Au leaching recovery was at 97%. Cyanide has also been used in downstream processes such as carbon adsorption incorporating new processes such as carbon-in-pulp and carbon-in-leach processes.

Though from literature the leaching recoveries using cyanide are generally relatively high, public concerns as well as various environmental incidents at gold mines dealing with the presence of cyanide in wastewater effluent have resulted in the increased exploration of non-cyanide lixiviants such as thiourea, halide and thiosulphate (Zhang et al., 2012).

### 2.4.2. Thiourea leaching

Thiourea, $SC(NH_2)_2$, is one of the more promising alternatives to cyanide leaching. It is a chemical compound that can be dissolved in an acid or water solution and in its aqueous form

it can react with gold to produce a soluble cationic complex (Birloaga et al., 2013). The reaction can occur using different oxidants such as ferric iron ($Fe^{3+}$) and hydrogen peroxide. However, the reaction kinetics have shown that ferric ions result in a lower dissolution rate in nitrate or chloride solutions than in an acid sulphate solution. The reaction in a sulphuric acid solution with ferric ions and thiourea can be achieved using Equation 2.2 below (Zhang et al., 2012; Birloaga et al., 2013).

$$2Au + 2Fe^{3+} + 4SC(NH_2)_2 + SO_4^{2-} \rightarrow [Au(SC(NH_2)_2)_2]_2SO_4 + 2Fe^{2+} \quad \text{Equation 2.2}$$

Birloaga et al. (2013) demonstrated that at 20 g/L thiourea, 10 g/L sulphuric acid and 6 g/L $Fe^{3+}$, 69% of gold was recovered with an agitation speed of 600 rpm. Jing-ying, Xiu-li & Wen-quan (2012) experimented on the effect of various factors on thiourea leaching of gold from waste mobile PCBs. Factors such as temperature, concentration of thiourea and ferric ions as well as particle size were investigated. Conditions for the optimum leaching of gold were found to be 24 g/L thiourea and 0.6% of $Fe^{3+}$ at 300 rpm. Under these conditions, 90% of the gold was recovered which was much greater than that found in Birloaga's et al. (2013) study.

The large difference in recoveries from the two studies may be attributed to the leaching time as Birloaga et al. (2013) recovered gold after 3.5 hours while Jing-ying, Xiu-li & Wen-quan (2012) recovered gold only after 2 hours. Jing-ying, Xiu-li & Wen-quan (2012) investigated the effect of leaching time on gold recovery and it was found that after 2 hours, gold recovery begins to decrease. Comparing the two results from both studies, it is evident that the leaching time played a significant role in the low recovery obtained from Birloaga's et al. (2013) study.

Thiourea leaching has many advantages and disadvantages in comparison with cyanide leaching. Some of the advantages include faster kinetics and a lower toxicity with less interference ions (Jing-ying, Xiu-li & Wen-quan, 2012; Lu & Xu, 2016). It is also environmentally friendly however, it is more expensive due to its high reagent consumption and the recovery of gold in this system requires further development (Zhang et al., 2012).

### 2.4.3. Halide leaching

Halide leaching incorporates the use of chlorine, bromine and iodine leaching. This method pre-dates cyanide leaching and all halogens besides fluorine have been experimented with for the recovery of gold. Gold forms gold (I) and gold (III) complexes ($Au^{+}$ and $Au^{3+}$ respectively) with the halogens and this is largely dependent on the solution conditions (Dönmez, Sevim & Çolak, 2001; Zhang et al., 2012).

Chlorine ($Cl$) as an oxidant and chloride ($Cl$) as a complexant has been extensively used on an industrial scale for the recovery of gold. However, it requires highly corrosive conditions necessitating the use of plastic pipes or tanks and glass-lined reactors. Low pH, high temperatures and high chlorine and chloride concentrations are required to achieve the high gold recovery rates (Pangum & Browner, 1996; Dönmez, Sevim & Çolak, 2001). In addition, aqua regia consisting of hydrochloric acid (HCl) and nitric acid as the oxidant is an option for acid halide leaching. Aqua regia is the most common reagent of choice in gold recovery from jewellery and other pure gold materials (Petter, Veit & Bernardes, 2014).

Iodine as a halogen forms the most stable complexes with gold and allows for easy regeneration of iodide due to iodine being reduced while gold is recovered. There is no corrosion associated with this type of leaching however it has high consumption rates, it is

quite expensive and efficiency of the gold electrolytic deposition still needs refinement (Zhang et al., 2012).

Bromine leaching can occur over a pH range of acidic to neutral and is non-toxic. The leaching process is a redox reaction and in many instances oxidants such as hypochlorite in conjunction with chlorine can be added to the solution. Therefore, allowing the regeneration of bromine (Sousa et al., 2018). The final redox reaction is shown below as Equation 2.3.

$$2Au + 3Br_2 \rightarrow 2AuBr_3 \qquad \text{Equation 2.3}$$

Bromine leaching is not as widely used due to the health and safety risks associated with the process thereby greatly restricting its application at an industrial scale (Zhang et al., 2012). Furthermore, oxidants used in bromine leaching have been known to cause high vapour pressure and corrosive reactions with minimal success in investigating alternative oxidants (Sousa et al., 2018).

It is evident that there are many alternatives (halide, thiourea) to leaching gold, each with its own advantages and disadvantages. Halide leaching has shown to have a much higher dissolution rate when compared to cyanide leaching however the high reagent costs and the difficulty in handling the solutions such as using strong corrosive chlorine has resulted in cyanide being a more promising industrial alternative. Thiourea on the other hand is a proven technology in leaching metals and has a higher dissolution rate and efficiency when compared to cyanide leaching (Gökelma et al., 2016). However, it has been known to show dissolution of heavy metals rather than gold and has a high reagent consumption in comparison to cyanide. Cyanide leaching though toxic still achieves high recoveries. A strong competitor to cyanide as well as halide and thiourea leaching is thiosulphate leaching (Petter, Veit & Bernardes, 2014). Thiosulphate has the ability to complex with not only gold but silver as well and is thus a promising substitute for cyanide. In addition, it is cheaper and has medium to low toxicity when compared to cyanide (Gökelma et al., 2016). Thiosulphate leaching as an alternative to standard cyanide leaching is expanded upon in the next section.

### 2.4.4. Thiosulphate leaching

Thiosulphate ($S_2O_3^{2-}$) is a chemical that is known to be used in pharmaceutical industries and in photography. It is non-toxic and can leach gold much faster than cyanide (Aylmore & Muir, 2001). Leaching using thiosulphate decreases some but not all of the interference from foreign cations such as antimony, zinc and copper (Jeffrey, Breuer & Choo, 2001; Zhang et al., 2012). Arslan & Sayiner (2018) stated that thiosulphate is a meta-stable species and readily undergoes decomposition in aqueous alkaline solutions.

There are two different types of thiosulphate leaching when recovering gold. These are: ammonium thiosulphate and sodium thiosulphate leaching. Ammonium thiosulphate is more widely used and has been researched and developed extensively in the past 20 years as an alternative to cyanide leaching (Petter, Veit & Bernardes, 2014). Ammonium thiosulphate is generally used as a fertiliser targeting soils with a low sulphur content. Sodium thiosulphate is not as common as ammonium thiosulphate for gold recovery. However, various experiments have been conducted to determine the kinetics and suitable conditions of leaching with sodium thiosulphate (Ha et al., 2014; Petter, Veit & Bernardes, 2014). Abbruzzese et al. (1995) studied gold leaching from gold-bearing ore at 2 M sodium thiosulphate, 0.1 M copper sulphate and 4

M ammonia. The study showed that an increase in temperature from 25°C to 60°C resulted in a decrease in gold recovery from 79% to 56% after 3 hours of leaching at 400 rpm, indicating that higher temperatures are not necessarily conducive for high gold recoveries.

Thiosulphate leaching is non-corrosive and has high selectivity. Furthermore, there is a lower consumption of the reagent without interferences from other ions during the leaching process in comparison to cyanide leaching (Aylmore & Staunton, 2014). However, many gold bearing ores typically occur with copper (similar to PCBs) which results in high reagent consumption with as much as 50% of the reagent lost in thiosulphate solutions containing copper ions (Aylmore & Muir, 2001). Moreover, there is no ideal accepted recovery method of gold from thiosulphate solutions.

#### 2.4.4.1. Chemical kinetics and thermodynamics

Ammonium thiosulphate leaching will be considered and investigated due to the readily available kinetics and thermodynamic analyses stipulated in literature. In addition to this, incorporating ammonium thiosulphate leaching will be advantageous for the subsequent ion-exchange step dealing with the recovery of gold from the leached solution as there are readily available resins such as MTA5011 produced for the thiosulphate system. This type of leaching is performed at alkaline conditions (pH 8 - 10) and at temperatures between 20°C and 60°C (Guerra & Dreisinger, 1999). Alkaline conditions are necessary to prevent the decomposition of thiosulphate into its degradation products (polythionates) such as trithionate and tetrathionate (Abbruzzese et al., 1995).

Gold dissolution in ammoniacal thiosulphate solution is a redox reaction catalysed by the presence of copper specifically cupric ions ($Cu^{2+}$). The cupric ions act as an oxidant and ammonia is utilised within the system to stabilise the cuprous ion ($Cu^{+}$) as the copper tetra-amine complex thus accelerating the anodic dissolution of gold into the gold-thiosulphate complex (Jeffrey, Breuer & Choo, 2001). In addition, ammonia is preferentially adsorbed on the gold surface forming the gold-amine complex and thereby reducing gold passivation (Arslan & Sayiner, 2018). Cuprous ions are further stabilised by complexing with thiosulphate. Thiosulphate stability generally decreases at low pH and high temperatures therefore alkaline pH and ambient temperatures are preferred to prevent degradation and ensure the stability of the cuprous-ammonia complex (Aylmore & Staunton, 2014).

The gold-thiosulphate complex is formed via two reactions, Equation 2.4 and Equation 2.5. Initially the gold-ammonia complex is formed on the gold surface before converting into the gold-thiosulphate complex (Equation 2.6). The overall dissolution reaction of gold in an ammonium thiosulphate solution in the presence of cupric ions is represented in Equation 2.6.

$$Cu(NH_3)_4^{2+} + Au + 3S_2O_3^{2-} \rightarrow Au(NH_3)_2^{+} + Cu(S_2O_3)_3^{5-} + 2NH_3 \quad \text{Equation 2.4}$$

$$Au(NH_3)_2^{+} + 2S_2O_3^{2-} \rightarrow Au(S_2O_3)_2^{3-} + 2NH_3 \quad \text{Equation 2.5}$$

$$Au + Cu(NH_3)_4^{2+} + 5S_2O_3^{2-} \rightarrow Au(S_2O_3)_2^{3-} + Cu(S_2O_3)_3^{5-} + 4NH_3 \quad \text{Equation 2.6}$$

The heterogenous redox reaction between oxygen and copper is shown below as Equation 2.7 (Fleming et al., 2003). In Equation 2.7, the cupric ion concentration eventually reaches steady state and at this point the rate of reduction of the cupric ions is matched by the rate of

oxidation of the cuprous ions by oxygen. Thus, the cuprous ions serve as both an oxidant and a catalyst in the leaching process.

$$4Cu(S_2O_3)_3^{5-} + O_2 + 16NH_3 + 2H_2O \rightarrow 4Cu(NH_3)_4^{2+} + 12S_2O_3^{2-} + 4OH^- \quad \text{Equation 2.7}$$

The overall redox reaction forming the gold-thiosulphate complex is shown below as Equation 2.8. The cupric-amine complex and the ammonia within the system is recycled therefore it is not present in Equation 2.8 (Xia, 2000).

$$4Au + 8S_2O_3^{2-} + O_2 + 2H_2O \rightarrow 4Au(S_2O_3)_2{}^{3-} + 4OH^- \quad \text{Equation 2.8}$$

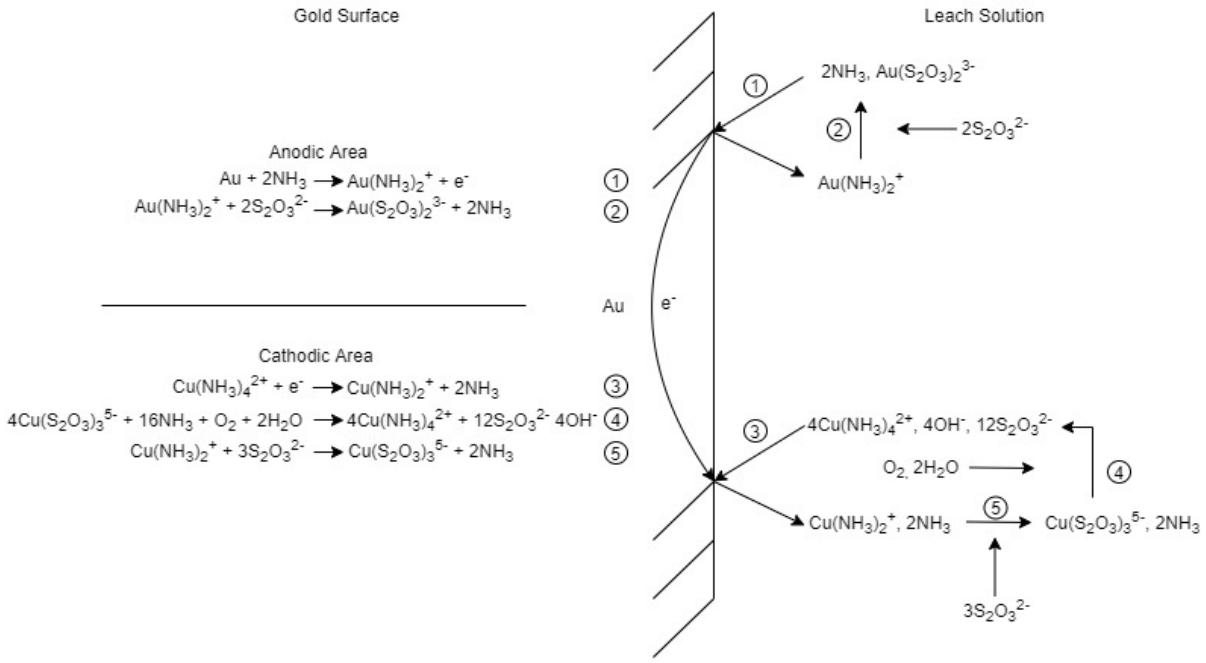


Figure 2.2: Electrochemical-catalytic mechanism model adapted from Xia (2000).

Figure 2.2 depicts the exchange of ions occurring in the cathodic and anodic area. The anodic area depicts the oxidation of gold to the gold-amine complex, $Au(NH_3)_2^+$, by the addition of ammonia. Ammonia is then substituted by the thiosulphate ion and the aurothiosulphate complex, $Au(S_2O_3)_2^{3-}$, is formed in the solution (Xia, 2000). The aurothiosulphate complex is the most stable gold soluble species in the process (Abbruzzese et al., 1995). In the cathodic area, the cupric-amine complex ion ($Cu(NH_3)_4^{2+}$) is reduced to the cuprous-amine complex ion ($Cu(NH_3)_2^+$) and the oxygen present in the ammonia solution oxidises the cuprous-thiosulphate complex ($Cu(S_2O_3)_3^{5-}$) back into the cupric-amine complex ($Cu(NH_3)_4^{2+}$). The cupric-amine complex, $Cu(NH_3)_4^{2+}$, catalyses the reaction of oxygen reduction and is more stable than the cuprous-thiosulphate complex when oxygen is sufficient (Xia, 2000). The relative concentrations of the species found in the solution greatly influence the predominant cathodic reaction. Ammonia present in the leaching process allows for the stability of the $Cu^{2+}$ ion especially in alkaline media by forming $Cu(NH_3)_4^{2+}$. Ammonia is also known to catalyse the reaction involving $Au^+$and $S_2O_3^{2-}$ in the anodic area of the process.

Thiosulphate when present in water is thermodynamically unstable and is partially oxidised to form its degradation products or polythionates. Equation 2.9 shows the degradation of thiosulphate into one of its degradation products, tetrathionate.

$$4S_2O_3^{2-} + O_2 + 2H_2O \rightarrow 2{S_4O_6}^{2-} + 4OH^- \quad \text{Equation 2.9}$$

Sulphate is the most stable form of the polythionates and when formed it is irreversible whereas tetrathionate and thiosulphate are metastable in aqueous solutions containing oxygen (Fleming et al., 2003). The reactions forming polythionates are undesirable mainly because the reagent is lost in these reactions and therefore additional thiosulphate must be added. In addition, the presence of polythionates in the leach liquor reduces the gold-thiosulphate loading on the resin by poisoning the resin in downstream recovery using ion-exchange (Zhang & Dreisinger, 2004).

There are various factors that can affect the leaching of gold from the PCBs some of these factors are the concentration of copper, ammonia and thiosulphate as well as temperature and pH. These are expanded upon below.

#### 2.4.4.2. Effect of copper concentration

Changing the copper concentration in the leaching solution can result in a faster reaction and thus a smaller leaching time for the gold dissolution in the thiosulphate system. Cuprous amine complexes have been known to cause an increase in the dissolution of gold for solutions containing ammonia (Tripathi et al., 2012).

Figure 2.3 below obtained from Tripathi et al. (2012) depicts the effect of copper sulphate on leaching of gold over 8 hours. It is evident that the presence of the copper ions in the solution has a significant impact on the dissolution of gold after 8 hours. There is a direct correlation between the copper sulphate concentration and the leaching rate indicating that the greater the concentration, the higher the gold recovery. This is fairly evident at 8 hours where a 0 M copper concentration results in about 4% gold recovery compared to the 35% gold recovery when incorporating 0.048 M Cu. However, high copper concentrations have been known to pose a risk by accelerating the decomposition reaction of thiosulphate in some instances (Hung Ha et al., 2010; Zhang et al., 2012).

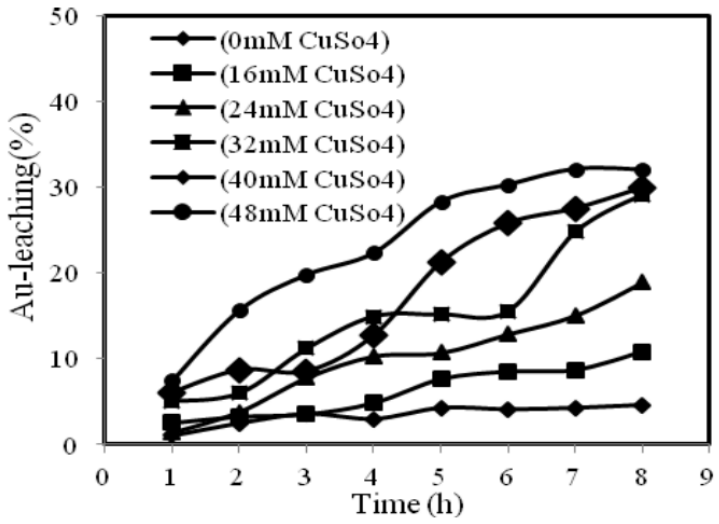


Figure 2.3: Graph showing the effect of copper on gold leaching rate (Tripathi et al., 2012).

#### 2.4.4.3. Effect of ammonia concentration

The ammonia concentration has also been known to greatly affect gold leaching recoveries. The effect of various ammonia concentrations on gold leach kinetics was studied by Breuer & Jeffrey (2000). From the graph below (Figure 2.4), it is evident that as the ammonia concentration increases, the gold leaching rate decreases. The role of ammonia in the thiosulphate system is to stabilise the cuprous ions as well as hinder the dissolution of gangue minerals found in gold bearing ores (Breuer & Jeffrey, 2000). It has been suggested that ammonia prevents gold passivation by being adsorbed on gold surfaces over thiosulphate. Therefore, the gold ammonia complex is formed before the gold thiosulphate complex as shown in Equation 2.3 and Equation 2.4. This evidently catalyses the reaction involving the gold and thiosulphate ions.

Hung Ha et al. (2010) found that increasing the ammonia between 0.1 M and 0.3 M, resulted in an increase in gold recovery. However further increase in ammonia caused lower gold recoveries, whilst maintaining the Cu concentration between 0.015 M – 0.03 M. Similar to what was found by Breuer & Jeffrey (2000) in Figure 2.4 below.

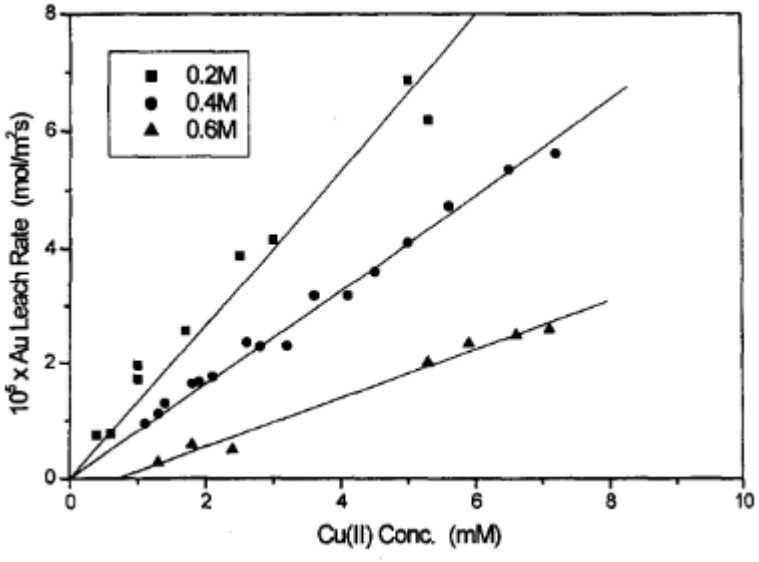


Figure 2.4: Graph showing the effect of ammonia on the gold leaching rate (Breuer & Jeffrey, 2000).

#### 2.4.4.4. Effect of thiosulphate concentration

The effect of thiosulphate concentration on the leaching kinetics is that at low thiosulphate concentrations the gold leaching rate is much slower. This is expected as at higher thiosulphate concentrations, the forward reaction stated as Equation 2.5 is favoured (Breuer & Jeffrey, 2000). Tripathi et al. (2012) stated that concentrations greater than 0.1 M thiosulphate result in a decrease in the gold leaching rate. This was attributed to the fact that at very high concentrations of thiosulphate, the formation of polythionates is promoted thus decreasing the leaching rate of gold. Figure 2.5 below shows the effect of various thiosulphate concentrations on the gold leaching rate.

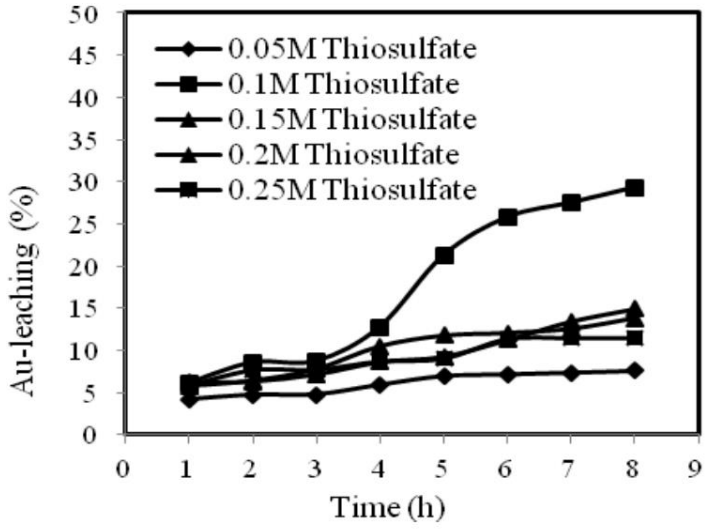


Figure 2.5: The effect of thiosulphate concentration on the gold leaching rate obtained from Tripathi et al. (2012).

It is also important to keep the ammonia to thiosulphate ratio well within 1-2 so as to allow

copper to play its catalytic role and transfer between its cuprous and cupric ion states (Black, 2006).

#### 2.4.4.5. Effect of temperature

Figure 2.6 shows that an increase in temperature results in an increase in the gold leaching rate within the range of 25°C - 40°C. This was expected for a chemically controlled reaction. Breuer & Jeffrey (2000) plotted an Arrhenius plot to determine the activation energy of the leaching reaction. The activation energy was found to be 60 kJ/mol which is greater than 25 kJ/mol generally associated with diffusion-controlled reactions. However, increasing temperature to increase the gold leaching rate poses reagent and energy consumption risks and thus a trade-off between the two is required.

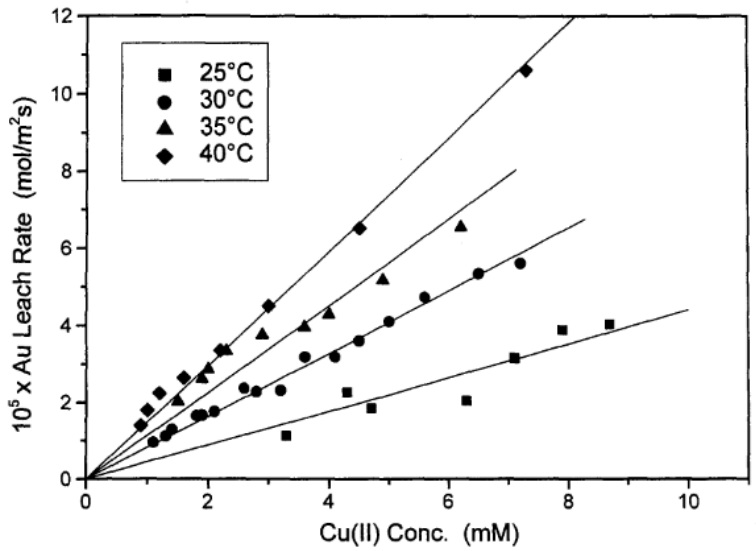


Figure 2.6: Effect of temperature on the gold leaching rate (Breuer & Jeffrey, 2000).

Abbruzzese et al. (1995) found that increasing temperatures between 25°C and 60°C resulted in decreased gold leaching rates. This was attributed to passivation by cupric sulphide formed in the reaction between the copper ions and thiosulphate. However, this decrease could also be ascribed to the loss of ammonia from solution at very high temperatures. In addition, high temperatures result in the degradation of thiosulphate therefore hindering the gold-thiosulphate complex formation. Consequently, high temperatures are generally not used due to being uneconomical and challenging to maintain ammonia in solution (Breuer & Jeffrey, 2000).

#### 2.4.4.6. Effect of pH

The effect of pH on the gold leaching rate was also studied. It is evident from Figure 2.7 that the higher the pH, the higher the gold leaching rate. The pH was measured by increasing the ammonia concentration in the solution. The addition of ammonium ions affects the kinetics of the cuprous-thiosulphate complex and the copper tetra-amine complex resulting in an increase in dissolution of gold in ammonium thiosulphate (Tripathi et al., 2012).

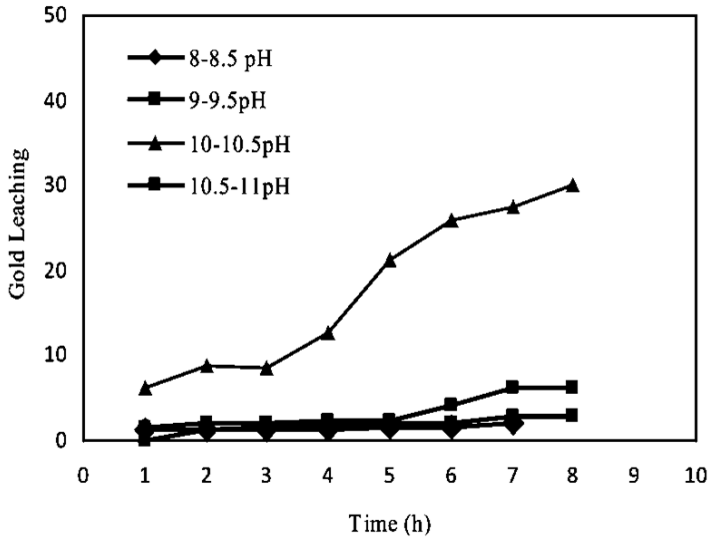


Figure 2.7: The effect of pH on the gold leaching rate (Tripathi et al., 2012).

For a pH greater than 10.5, Tripathi et al., (2012) states that there is a decrease in the thermodynamic stability of copper oxides. This leads to the removal of copper in solution including the widening of the thermodynamic stability regions of solid copper oxides on the gold surface therefore hindering its dissolution and causing low gold recoveries.

## 2.5. Recovery of gold

There are quite a few methods currently employed to recover gold from solution. Some of these methods are activated carbon adsorption and solvent extraction. The majority of these methods have first been applied to cyanide leach liquors before implementation in ammonium thiosulphate leach liquors. Therefore, there are varying degrees of success with each method and these are discussed in the next section.

### 2.5.1. Solvent extraction

This technique involves contacting the leach liquor with a solution of extractant in a water-immiscible organic solvent. The gold complex is separated into the organic phase and any other metals remain within the aqueous phase. The organic phase is first separated before being stripped and returned to the extraction process. Some of the extractants used for the thiosulphate system are primary alkyl-amines, tertiary amine oxides and phosphines (Zhao, Wu & Chen, 1998; Xu et al., 2017). One of the advantages of this recovery method include the enrichment of the aurothiosulphate ion when using these same extractants.

Solvent extraction has numerous disadvantages that limit its possible industrial applications. One disadvantage is that the extraction is limited to only clarified liquors that are free of any particulate matter. In order to clarify the liquor various, additional equipment and time is required resulting in a considerable increase in operating expenses and other costs including the addition of significant operational risk due to the high flammability of solvents (Zhang & Dreisinger, 2004).

### 2.5.2. Activated carbon

The activated carbon technique utilising the dicyanoaurate complex onto activated carbon has been incorporated into gold recovery for an extensive period. It is associated with having

relatively low costs and high efficiencies (Fleming et al., 2003). Granules of carbon are contacted with cyanide solution containing gold and are then recovered with the adsorbed gold. This step can occur in the presence of pulp or with clarified liquor (Kotze et al., 2005). The clarified liquor method is generally more costly and time consuming as opposed to utilising a mineral pulp. It was suggested, by Abbruzzese et al. (1995), that the gold adsorbed onto the carbon can be displaced by eluting with sodium hydroxide and deionised water.

Activated carbon is the most common method of gold removal however in the thiosulphate system, the gold-thiosulphate complex has been known to be poorly loaded onto activated carbon. This complex has a reduced affinity for carbon compared to the gold-cyanide complex. This may be due to the large size of the ion and the higher negative charge. Thus, rendering the widely used carbon-in-pulp technology less efficient (Fleming et al., 2003; Kotze et al., 2005).

### 2.5.3. Cementation

Cementation refers to the recovery of a dissolved metal in an aqueous solution via contact reduction and deposition of a more noble metal (Hiskey & Lee, 2003; Choo & Jeffrey, 2004). This recovery method has been widely used in the hydrometallurgy industry specifically for the recovery of gold. It has been used commercially to recover gold in the cyanide system using zinc known as the “Merill-Crowe Process” as well as using other metals such as iron and copper to recover gold (Dönmez, Sevim & Çolak, 2001; Hiskey & Lee, 2003; Cui & Zhang, 2008). Furthermore, all three metals (iron, zinc and copper) have been studied for its use in the thiosulphate system (Guerra & Dreisinger, 1999). Cementation using copper has proven to be a better alternative than zinc and iron (Choo & Jeffrey, 2004). Zinc and iron are foreign ions in the thiosulphate system and when used at high concentrations there is the possibility of gold precipitating in the thiosulphate solution during the cementation process. In addition, copper added during the cementation process can be oxidised into the cupric ion which is the oxidant in the leaching process. The reaction between gold and copper during cementation in the thiosulphate system is shown below (Choo & Jeffrey, 2004).

$$Au(S_2O_3)_2^{3-} + S_2O_3^{2-} + Cu \rightarrow Cu(S_2O_3)_3^{5-} + Au \qquad \text{Equation 2.10}$$

There are a few advantages and disadvantages to the use of cementation for gold recovery. One of the advantages include the low cost associated with the process however there is still some uncertainty with regards to the chemistry and reaction mechanism of the process (Hiskey & Lee, 2003). In the PCB context, due to the significant amounts of metallic copper on the board, gold cementation can occur during thiosulphate leaching of gold. Moreover, it is possible that zinc and aluminium from the board can also consume copper from the lixiviant (Lee, 2003).

It is evident that are various processes that can recover gold from solution after leaching such as solvent extraction, cementation and activated carbon each with its own advantages and disadvantages. In addition to these processes, ion exchange has recently been gaining interest in terms of gold removal. A few studies have conducted experiments using resins in the thiosulphate system and have shown promising results including the advantage of low water quality required by the system (Nicol & O’Malley, 2002; Zhang & Dreisinger, 2004; Dong et al., 2017) This process and its mechanism are expanded upon in the next section.

### 2.5.4. Ion-exchange

One of the most underdeveloped areas of hydrometallurgy is the use of ion-exchange specifically resin adsorption for the recovery of precious metals. Resin adsorbents are generally more expensive than carbon and require specialised equipment. However, ion-exchange is largely environmentally friendly and the resins utilised in the process have higher loading capacities, higher loading rates and require no thermal regeneration (Kotze et al., 2005; Murakami, Nishihama & Yoshizuka, 2015).

This technique has a relatively low requirement for water quality and is generally employed in the forms of resin-in-leach (RIL) and resin-in-pulp (RIP). The RIL method involves the adsorbent being added to the ore or PCB simultaneously with the leaching reagents required whereas the RIP method involves adding the adsorbent after an initial leaching period (Kotze et al., 2005). The resins are required to be stripped after being separated from the leach pulp/solution. The elution of the resin loaded with gold can occur at ambient temperature and generally no thermal reactivation is required. In addition, regeneration of the resin can occur simultaneously through the elution process depending on the chosen type of eluant (Fleming et al., 2003). It should also be noted that the functional groups of the resin can be suited for selectivity for a certain complex or ion depending on the resin.

#### 2.5.4.1. Ion exchange process

Ion exchange is defined as when cations or anions of a certain charge in solution are adsorbed onto a solid and replaced by equivalent quantities of other cations or anions of the same charge that are released by the solid material (De Dardel & Arden, 2012). The ion exchange process consists of recovering a desired ion by contacting a solution containing the desired ion with the resin. The desired ion is attracted to the resin and is adsorbed onto the resin leaving the solution. The non-desired ion present on the resin initially is then substituted for the desired ion and enters the solution. The adsorption of the desired ion onto the resin is known as loading (Murakami, Nishihama & Yoshizuka, 2015). To remove the desired ion from the resin, the loaded resin is then contacted with a solution known as the eluant. The eluant consists of similar ions which are adsorbed onto the resin allowing for the desired ion to enter the eluant. This process is known as elution of the resin and regenerates the resin by exchanging the desired ion on the resin for the non-desired ion in solution. The desired ion is now present in the eluant and the resin can then undergo the next loading process.

The amount of resin contacted with the loading/elution solution is known as the Free Wet Settled Volume (FWSV) (Nesbitt, 2016). The actual resin capacity is essentially the quantity of ions that the resin can hold and is generally contained within a column through which the loading solution or eluant can pass through (Kim et al., 2011). This actual capacity is slightly different from the general exchange capacity provided on the safety data sheet of the resin due to the conditions of the experiment such as temperature and resin quantity (De Dardel & Arden, 2012). This is further expanded upon in following sections.

#### 2.5.4.2. Resin types and structure

The ion exchanger or ion exchange resins consists of two main parts: the polymer matrix and the functional groups that interact with the ions present. These can be organic and inorganic ion exchange resins however the latter (consisting of zeolites) are not as widely used in extractive hydrometallurgy.

Polymer matrices can be polystyrene or polyacrylic. There are other types of matrices such as phenol – formaldehyde and polyalkylamine resins however these types are specifically suited towards intricate systems. Polystyrene matrices are made via the polymerization of styrene or vinylbenzene which yields linear polystyrene. Cross-linked polystyrene is formed when a proportion of divinylbenzene is then mixed with styrene (De Dardel & Arden, 2012). Polyacrylic matrices are obtained by polymerizing an acrylate or methacrylate with divinylbenzene.

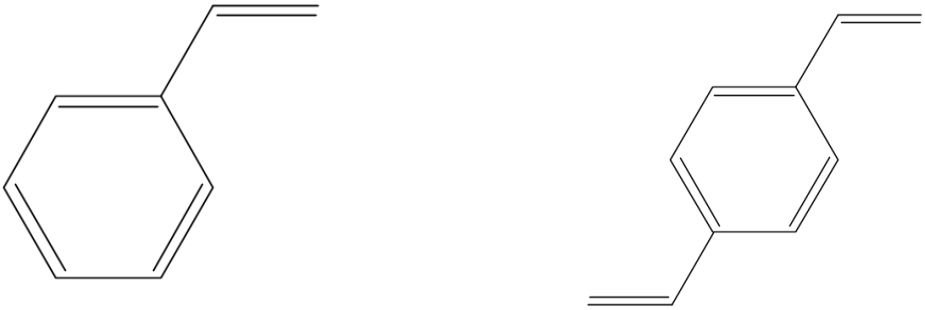

(a) (b)

Figure 2.8: (a) Styrene molecule (b) Divinylbenzene molecule

The functional groups of ion exchange resins can be cation or anion. Cation exchange resins can either be strongly acidic such as sulphonic groups or weakly acidic such as carboxylic groups. Similarly, anion exchange resins can be strongly basic such as quarternary ammonium groups or weakly basic such as amine groups (De Dardel & Arden, 2012). The cation exchange resins have an active site that attracts cations such as hydrogen ions whilst the anion exchange resins have an active site that attracts anions such as hydroxyl ions. There are other types of ion exchange resins known as chelating resins. These resin types can contain a variety of active groups such as thiol, amidoxime and aminophosphoric acid as well as many others. These resins can have cation or anion exchange groups or no ion exchange groups at all. With these specific active groups, selective absorption of metals is targeted and the resin is pH dependent (Kotze et al., 2005; De Dardel & Arden, 2012).

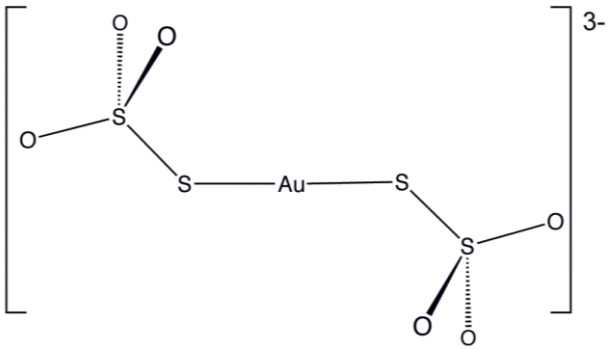


Figure 2.9: Aurothiosulphate ion chemical structure

In the ammonium thiosulphate system, gold is present as the aurothiosulphate ion, $Au(S_2O_3)_2^{3-}$, with a negative charge of 3 therefore anion exchange resins are applicable to the system as they allow for the attachment of anions only. Figure 2.9 represents the large aurothiosulphate molecule in the system. There are two different types of base anion

exchange resins that can be used for the attachment of this ion. These are strong- and weak-base anion exchange resins which are expanded upon below.

#### 2.5.4.2.1. Weak-base anion exchange resin

A weak-base anion exchange resin contains active groups that are generally derived from primary and secondary amines. Tertiary amines are denoted as intermediate or medium-base resins (De Dardel & Arden, 2012). The functional groups present on a weak-base resin must be protonated before any interaction with the anion and have no permanent charge. The greater the number of amine groups on the resin at a certain pH, the greater the potential for a high gold-loading capacity. Elution of a weak- or medium-base resin occurs by reversing the reaction (Kotze et al., 2005). An example of a medium-base anion exchange resin is the AuRIX®100 resin supplied by Cognis Corporation. This resin has been used in both RIL and RIP processes for recovery of gold in both silver and gold solutions in cyanide systems (Gray, Hughes & Abols, 2005).

Equation 2.11 to Equation 2.14 denote the deprotonation, protonation, loading and elution steps specifically for the AuRIX®100 medium-base resin in the ammonium-thiosulphate system. $R$ denotes the resin and $Gua$ denotes the active site for ion attachment. In the case of the AuRIX®100 resin, the active site is a guanidine group. The resin is presented in the hydrochloride form as Equation 2.11. When contacted with a highly caustic solution, the hydrogen ion detaches and the resin is thus deprotonated by removal of the hydrogen ion. The hydrogen and chloride ion both enter the solution and form water and sodium chloride. To protonate the resin as in Equation 2.12, the resin is contacted with deionised water where the hydrogen ion attaches onto the resin and the hydroxyl ions are left in solution. The resin is now ready to receive the anion of choice, in this instance the aurothiosulphate ion. Equation 2.13 and Equation 2.14 represent the loading and elution steps respectively. The aurothiosulphate ion attaches onto the protonated resin in the loading step and in the elution step, the resin is contacted with a highly caustic solution and the hydrogen ion is displaced into the solution along with the aurothiosulphate ion thereby deprotonating the resin. To load the aurothiosulphate ion on the same resin once again, the resin needs to be contacted with deionised water as in Equation 2.12.

$$R-(-Gua)HCl+NaOH \rightarrow R-Gua+H_2O+NaCl \quad \text{Equation 2.11}$$

$$H_2O+R-Gua \rightarrow R-(-Gua)H^+ + OH^- \quad \text{Equation 2.12}$$

$$3(R-(-Gua)H^+)+Au(S_2O_3)_2{}^{3-} \rightarrow Au(S_2O_3)_2{}^{3-}(R-(-Gua)H^+)_3 \quad \text{Equation 2.13}$$

$$Au(S_2O_3)_2{}^{3-}(R-(-Gua)H^+)_3+OH^- \rightarrow H_2O+R-Gua+\ Au(S_2O_3)_2{}^{3-} \quad \text{Equation 2.14}$$

#### 2.5.4.2.2. Strong-base anion exchange resin

A strong-base anion exchange resin contains active sites, which are quaternary ammonium groups with positive charges that are fixed. These resins can be divided into Type 1 and Type 2 resins (Figure 2.10 and Figure 2.11). Type 1 resins are strongly basic and contain benzyltrimethylammonium groups whilst Type 2 are less basic and contain benzyldimethylethanolammonium groups. Type 1 resins allow for total removal of anions. In the case of Type 2, in addition to total removal anions, these resins when contacted with sodium hydroxide release anions more easily during the regeneration process. Consequently, the resins have a high exchange capacity and regeneration efficiency. The disadvantage is

that they are less chemically stable and result in higher silica leakage than Type 1 (De Dardel & Arden, 2012).

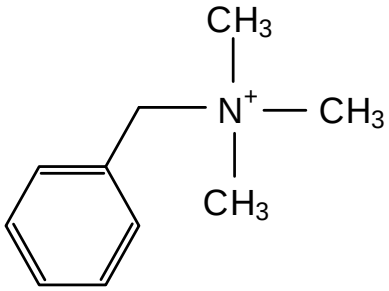


Figure 2.10: Type 1 Benzyltrimethylammonium functional group

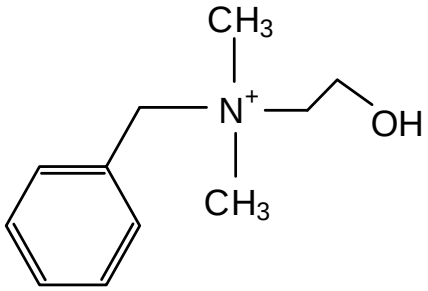


Figure 2.11: Type 2 Benzyldimethylethanolammonium functional group

In the gold ion exchange system, anion exchange resins are most suited due to the quaternary ammonium group or the amine group as gold exists as an anionic species (Kotze et al., 2005). The reaction occurs when the gold anion displaces the counterion associated with the positively charged site on the resin thus forming an ion pair. This reaction is dependent on the solution pH and therefore loading at alkaline pH does affect the performance of the resin (Kotze et al., 2005).

Equation 2.15 to Equation 2.17 denote the resin preparation, loading and elution steps for the Purogold™ MTA5013SO4/MTA5011SO4 resins. $R$ denotes the resin and $N(CH_3)_3$ denotes the active group. The Purogold™ resin is an example of a strong-base anion with a Type 1 quarternary ammonium group. The resin is generally in the sulphate form and is first converted to the hydroxyl form with contact of a sodium hydroxide solution. Once in the hydroxyl form, the resin is loaded with the aurothiosulphate ion as described by Equation 2.16. The hydroxyl ion is displaced by the aurothiosulphate ion during loading. In the elution process, the resin is contacted with a nitrate solution such as ammonium nitrate ($(NH_4NO_3)$) and the aurothiosulphate ion detaches from the resin and enters the solution whilst the nitrate anion is attached onto the resin.

$$[R-N(CH_3)_3]_2^+SO_4^{2-} + 2NaOH \rightarrow 2R-N(CH_3)_3^+OH^- + Na_2SO_4 \quad \text{Equation 2.15}$$

$$Au(S_2O_3)_2^{3-} + R-N(CH_3)_3^+OH^- \rightarrow [R-N(CH_3)_3]_3^+Au(S_2O_3)_2^{3-} + OH^- \quad \text{Equation 2.16}$$

$$[R-N(CH_3)_3]_3^+Au(S_2O_3)_2^{3-} + NO_3^- \rightarrow R-N(CH_3)_3^+NO_3^- + Au(S_2O_3)_2^{3-} \quad \text{Equation 2.17}$$

#### 2.5.4.3. Resin Capacity and adsorption

The theoretical or general exchange capacity of a resin is usually expressed in equivalents per unit volume resin and is a measure of the number of ions that are exchangeable given a fixed quantity of resin. One equivalent is the number of moles exchanged per ionic charge of that ion. The theoretical capacity of some basic anion resins ranges from 1.3 eq/L to 1.6 eq/L as shown by Table 2.2. In addition, the capacity values are based on the ionic form of chloride for the strong-base resin and in the free form for the weak-base resins.

Table 2.2: Typical general ion-exchange resin capacities adapted from De Dardel & Arden (2012)

| Resin Type | Capacity, $\boldsymbol{Q}$ (eq/L) |
|---|---|
| Strong basic Type 1 | 1.3 ($Cl^-$) |
| Strong basic Type 2 | 1.3 ($Cl^-$) |
| Strong basic acrylic | 1.3 ($Cl^-$) |
| Weak basic styrene | 1.25 (Free base) |
| Weak basic acrylic | 1.6 (Free base) |

The actual capacity or operating capacity of the resin is dependent on the application of the resin including many variables such as the concentration of the solution and ions to be adsorbed, the quantity of resin and temperature (De Dardel & Arden, 2012). Furthermore, the resin capacity is also a function of the service life of the resin. Thus, this actual capacity can be higher or lower than the general capacity. It is therefore necessary to determine the actual capacity of the resin before conducting any experimental work (O'Malley, 2002).

The moisture content of a resin is an indication of the kinetics, general capacity and mechanical strength of the resin. All resins contain fixed and mobile ions which are encompassed by water molecules situated on the inside of the resin (De Dardel & Arden, 2012). The moisture content is also a function of the degree of cross linking in the polymer and is generally given as a range. In the case of the AuRIX®100, a medium-base resin, the moisture content is between 47% and 53%.

#### 2.5.4.4. Selectivity of anions

Anion selectivity is an important aspect of ion exchange. It describes the ability of the resin to discriminate between different ions within the loading solution. In the ammonium-thiosulphate system, there are a variety of anions present in the PCB leach solution. Some of the anions present are $Au(S_2O_3)_2^{3-}$, $Cu(S_2O_3)_3^{5-}$, $Zn(S_2O_3)_2^{3-}$ and $OH^-$ in addition to many others. Thus, it is paramount that the targeted anion is allowed to load onto the resin in place of other anions. This is heavily dependent on the experimental conditions and can be determined via equilibrium tests on the resin. The loading of the aurothiosulphate ion in the ammonium-thiosulphate system will largely be dependent on the affinity of the resin for the anion relative to other anions present in the solution including the concentration of the anions (Zhang & Dreisinger, 2004).

The order of affinity in the thiosulphate system proposed by Eusebius, Ghose & Dey (1981) was lead > silver > copper > zinc. O'Malley (2002) suggested that the order would be gold, lead > silver > copper > zinc as the resin in the thiosulphate system would likely have the highest affinity for gold similar to the high gold affinity in the cyanide system. The study by Eusebius, Ghose & Dey (1981) used sodium thiosulphate at 1 M as the eluant with the strong-base anion Dowex 1-X8 resin however they did not investigate the gold ion. It was found that thiosulphate complexes loaded were copper, zinc, lead and silver. Gold was not examined in the study but was predicted to load onto the resins. After elution, copper, cadmium and zinc were easily removed but silver and lead were strongly held on by the resin. This is indicated in Table 2.3. The breakthrough volume refers to the volume of eluant that was passed through the resin column before the targeted metal ions could be detected in solution.

Table 2.3: Ion characteristics using sodium thiosulphate as an eluant adapted from Eusebius, Ghose & Dey (1981)

| Metal ion | Breakthrough volume (mL) | Eluant volume for maximum ion eluted (mL) | Eluant volume for complete elution (mL) |
|---|---|---|---|
| Cu | 3.5 | 15 | 140 |
| Zn | 5 | 60 | 380 |
| Ag | > 500 | - | - |
| Pb | > 500 | - | - |

In the case of sulphur species only, the order was tetrathionate, trithionate > thiosulphate > sulphate. This was established by Iguchi (1958) using hydrochloric acid as an eluant at various concentrations between 1 M and 9 M. It was found that 3 M HCl removed all trithionate ions whilst 6 M was required to remove the tetrathionate ions. Iguchi (1958) results were similar to experiments conducted by Zhang & Dreisinger (2002) where the presence of polythionates largely inhibited the gold loading ability of the resin. Thus, the degree of adsorbability of the ions increases with the number of sulphur atoms.

#### 2.5.4.5. Equilibrium models

There are many models that can be applied to the ammonium-thiosulphate system to describe the loading of gold onto resin and the affinity of the gold relative to other anions in the system. Some of these isotherms or models are the mass action law, the Langmuir model and the Freundlich model. These models largely depend on the gold concentrations in solution at equilibrium and the actual resin capacity which are key independent variables.

The Freundlich model or isotherm is one of the equilibrium expressions that is applicable to the ion exchange system. For this isotherm, a linear relationship is expected between $\ln(\overline{C_e})$ and $\ln(C_e)$. This relationship was based on the adsorption being achieved when the rate of ions adsorbed onto the resin is the same as the rate of desorption from resin (Cui & Zhang, 2008).

$$\overline{C_e} = K_F(C_e)^b \qquad \text{Equation 2.18}$$

$K_F = Freundlich\ adsorption\ equilibrium\ constant$
$b = adsorption\ intensity\ constant$
$\overline{C_e} = gold\ concentration\ at\ equilibrium\ on\ resin\ (eq/L)$
$C_e = gold\ concentration\ at\ equilibrium\ in\ solution\ (eq/L)$

Gomes, Almeida & Loureiro (2001) found that the Freundlich isotherm represented the equilibrium data with good accuracy for a cyanide solution and weak-base resin. It was stated that the model was best represented between 20°C and 50°C and the model does not predict a limit for the resin capacity and would likely fail if applied to the elution process. A $K_F$ value of 1294 g fluid/mg Au and $b$ value of 0.405 was calculated for the gold cyanide system. Chaparro et al. (2015) found that for the AuRIX®100 resin, $K_F$ = 0.33 mg/g and $b$ = 0.43 in 3 hours. The study by Chaparro et al. (2015) concluded that the Freundlich model was a good fit for the experimental data with a correlation of 0.97 that simulated the adsorption of gold.

The Langmuir isotherm balances the rates of adsorption and desorption, that is dynamic equilibrium. It was initially derived to describe solid-gas phase adsorption but it is also used to quantify the capacity of various adsorbents (Ayawei, Ebelegi & Wankasi, 2017). The behaviour of non-ionic adsorbents is found to be similar to the behaviour of ion exchangers or resins in the presence of non-electrolyte solutions hence the applicability of the Langmuir isotherm (Gomes, Almeida & Loureiro, 2001). The model is also based on an equilibrium relationship between species in solution, species adsorbed on specific sites and free sites. The Freundlich model in comparison is largely empirical and is more commonly used in non-specific adsorption such as in soils or organic matter. The Langmuir isotherm equation is shown as Equation 2.19.

$$\overline{C_e} = \frac{\bar{C} K_L C_e}{1 + K_L C_e} \qquad \text{Equation 2.19}$$

$\bar{C} = Total\ resin\ capacity\ (eq/L)$
$K_L = Langmuir\ adsorption\ equilibrium\ constant$

The model is based on the assumption that the resin has homogenous active sites, equivalent adsorption energies and no interaction between adsorbed species (Cui & Zhang, 2008). The Langmuir constant can be correlated to the surface area of the ion exchange and the pore volume. For a large surface area and pore volume, the adsorption capacity will be higher (Ayawei, Ebelegi & Wankasi, 2017). This model is widely used for metal biosorption but not as common in the hydrometallurgy route (Cui & Zhang, 2008). Adsorption onto biomass is purely surface adsorption whereas in ion exchange there is subsurface diffusion and inner resin effects which might render the inner sites less effective than those at the surface.

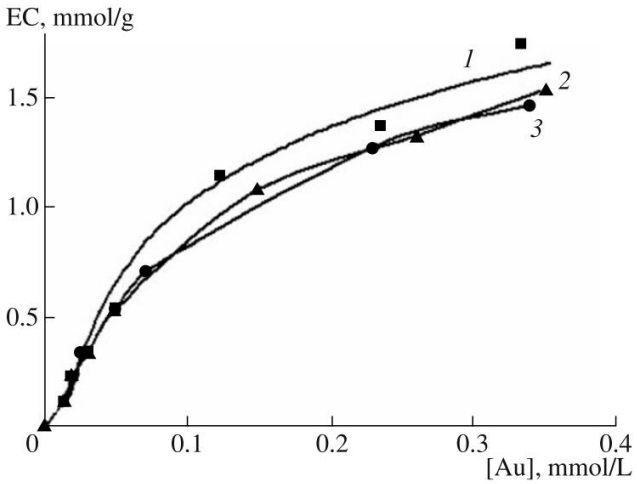


Figure 2.12: Application of Langmuir model in gold-thiocyanate system with three resins in $Cl^-$ form (Krinitsyn et al., 2008)

Figure 2.12 displays the solution isotherms of gold concentration in mmol/L against the loaded Au at equilibrium in mmol/g resin. Resin 1 and 2 were strong-base anion resins whilst resin 3 was a weak-base anion resin. Krinitsyn et al. (2008) found that the exchange capacity and the high adsorption selectivity are independent of the resin type in the cyanide system. It was also stated that the actual resin capacity corresponded to the exchange capacity at equilibrium of each resin with respect to the chloride ions.

The mass action law is the fundamental equilibrium model for ion exchange resins. The equilibrium behaviour of strong-base anions are generally similar to the mass action law (De Dardel & Arden, 2012). This model accounts for the active site of the resin, the adsorbing ion and the desorbing ion in the system. When the adsorbing ion and desorbing ion have a valency of 1 each, it is called a mono-monovalent exchange. If dissimilar valence ions exchange, then the system can be mono-divalent or mono-trivalent or even di-trivalent depending on the valency of both ions. The complexity of the model increases with the variation of valencies.

For the ammonium-thiosulphate system, an exchange between the aurothiosulphate ion and the chloride ion is depicted in Equation 2.21. In this case, the adsorbing ion is the chloride ion and the desorbing ion is the aurothiosulphate ion based on the reaction given by Equation 2.20. The selectivity coefficient differs for each different pair of ions. This is based on the resin affinity for an ion and is thus governed by the size of its hydrated form. A large ion such as the aurothiosulphate ion would require the resin bead to expand to accommodate it (De Dardel & Arden, 2012). This expansion is thus opposed by the cross-links within the resin and consequently a large ion will require a greater force to penetrate the resin compared to a small ion such as the chloride ion.

$$[R-N(CH_3)_3]_3^+Au(S_2O_3)_2{}^{3-} + Cl^- \rightarrow R-N(CH_3)_3^+Cl^- + Au(S_2O_3)_2{}^{3-} \quad \text{Equation 2.20}$$

$$\frac{\overline{X_{Au}}}{(1-\overline{X_{Au}})^3} = K_{Au}^{Cl} \times \left(\frac{\bar{C}}{C}\right)^2 \times \frac{X_{Au}}{(1-X_{Au})^3} \quad \text{Equation 2.21}$$

$\overline{X_{Au}} = \ Fraction\ of\ aurothiosulphate\ on\ resin\ at\ equilibrium$
$X_{Au} = Fraction\ of\ aurothiosulphate\ in\ solution\ at\ equilibrium$
$C = total\ concentration\ of\ solution\ at\ equilibrium\ (eq/L)$
$K_{Au}^{Cl} = selecitivity\ coefficient\ for\ Au(S_2O_3)_2^{3-}\ and\ Cl^-\ exchange$

Gomes, Almeida & Loureiro (2001) found that the mass action law accurately describes the equilibrium data presented from the Purolite® A-100 strong-base anion resin and that it is applicable to the elution process. They (Gomes, Almeida & Loureiro, 2001) reported a $\bar{C}$ value of 2.28 mmol Au/ g dry resin and $K_{OH^-}^{Au(CN)_2^-}$ value between the aurocyanide ion and hydroxyl ion of 9.44. In addition, they found that each active resin site attracts a single aurocyanide ion whilst the silver cyanide complexes requires up to three active resin sites. Thus, the resin showed a higher capacity for removing gold than for the silver complexes.

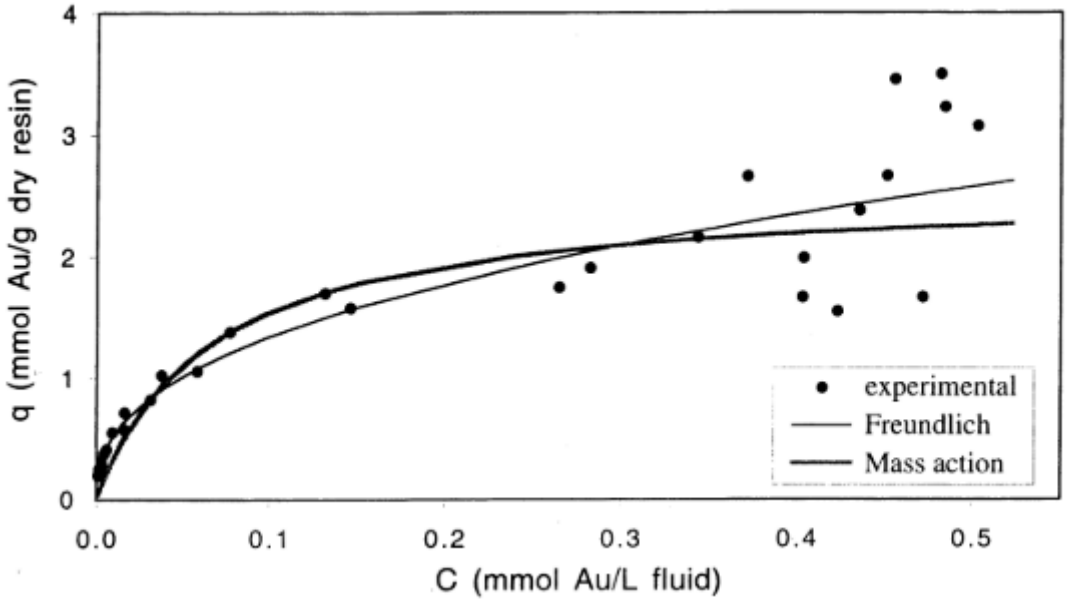


Figure 2.13: Experimental equilibrium points and the mass action and Freundlich isotherms for the gold-cyanide system (Gomes, Almeida & Loureiro, 2001)

Figure 2.13 depicts the equilibrium models for the gold cyanide system indicating significant scatter of data at high loadings. This is typical of these systems and ultimately limits the accuracy of any of the models at high loadings. Gomes, Almeida & Loureiro (2001) found that the mass action isotherm was preferred over the Freundlich isotherm mainly because the Freundlich isotherm does not predict a limit for the resin capacity.

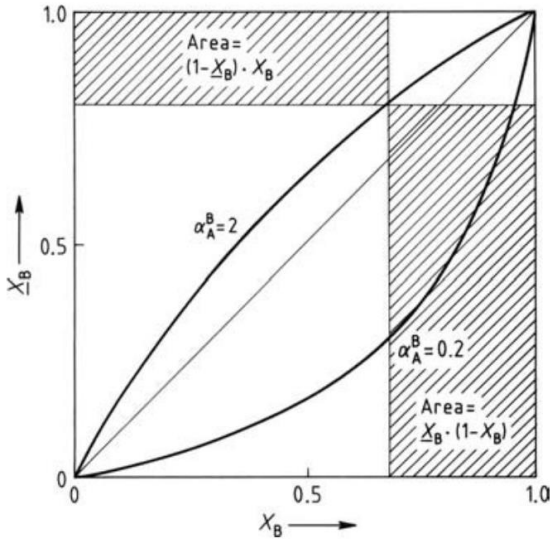


Figure 2.14: General case for ion exchange isotherms in a mono-monovalent system (De Dardel & Arden, 2012)

Figure 2.14 depicts the general case expected using the mass action law. The separation factor, $\alpha_A^B$, for a mono-monovalent system is the same as the selectivity coefficient. For the mono-trivalent system, the separation factor is a function of the term $K_{Au}^{Cl} \times \left(\frac{\bar{C}}{C}\right)^2$. Therefore, a high selectivity co-efficient will result in a large separation factor and a bow and arrow graph similar to Figure 2.14 where a separation factor of 2 is depicted above the parity line.

#### 2.5.4.6. Effect of copper concentration and solution flowrate

Loading gold onto the resin can be affected by the presence of copper in the solution. Zhang & Dreisinger (2004) experimented with the effect of copper on the loading of gold onto resin by measuring the amount of gold present in the effluent after being pumped through the column. A 0.1 M ammonium thiosulphate solution containing 20 ppm Au at pH 11 was used. In the case of no copper present, virtually no gold was detected in the effluent. As most of the solution passed through the column, the loading of gold increased as shown in Figure 2.15. The legend refers to resins Dowex G51 and and Dowex 21K used in the experiments at flowrates of 14 BV/h and 13 BV/h respectively, where BV/h refers to bed volume per hour.

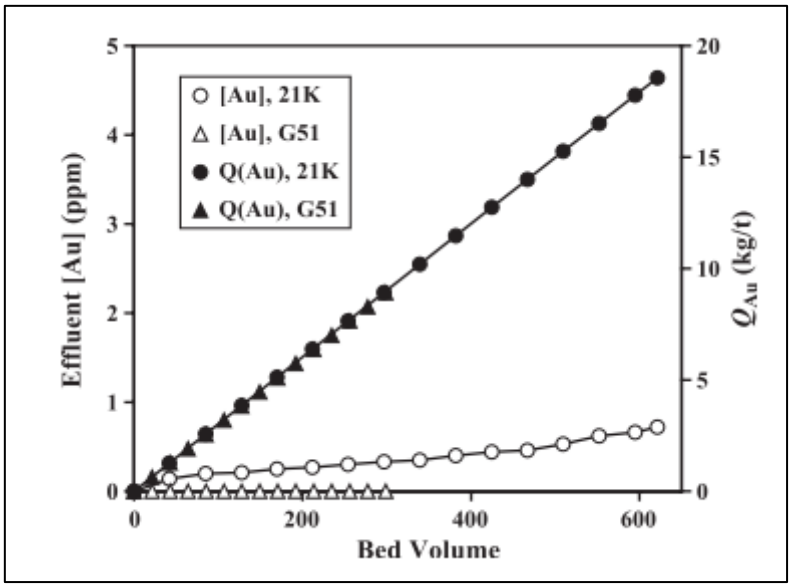


Figure 2.15: Loading of gold onto columns from an ammonium thiosulphate solution (Zhang & Dreisinger, 2004)

In the presence of copper, the capacity for gold on the resin was much lower due to the competing effect of the adsorption of the copper complex. Furthermore, the flow rate at which the solution was passed through the column affected the gold loading. With a high flow rate, saturation of the column was achieved at a later stage. This is attributed to the residence time of ions spent in the column. A small residence time results in a less complete exchange of ions and thus more solution was required to saturate the column (Zhang & Dreisinger, 2004).

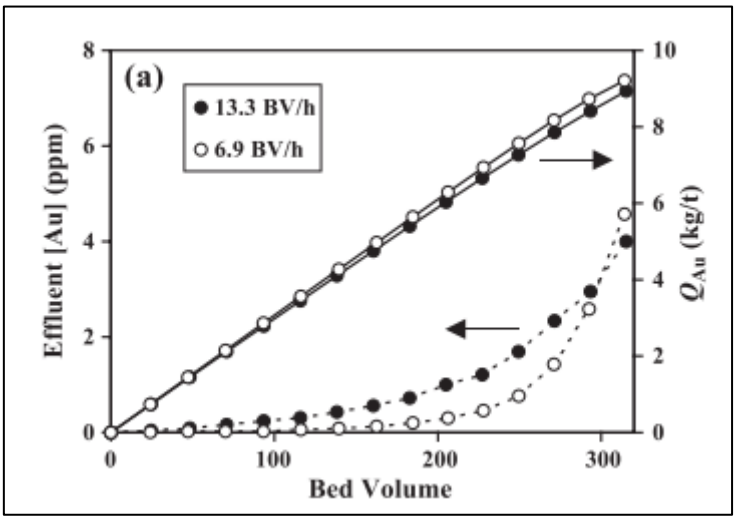


Figure 2.16: Loading of gold in the presence of copper (Zhang & Dreisinger, 2004)

A solution containing 0.1 M ammonium thiosulphate, 20 ppm gold and 500 ppm Cu at pH 11 was utilised for the loading of the resin in an open system. Figure 2.16 shows the loading of gold at different flowrates as well as the gold composition in the effluent. It is clear that a higher flowrate results in a higher gold concentration in the effluent and thus a lower gold loading value.

## 2.6. Research importance

The background research provided in the literature review emphasizes that the ammonium-thiosulphate system has demonstrated to be an effective system for gold leaching and recovery and therefore has potential for application in PCB processing. Researchers such as Aylmore & Muir (2001) and Tripathi et al. (2012) have investigated and improved the ammonium-thiosulphate system for gold recovery by exploring multiple leaching parameters (temperature, pH, copper concentration). In addition, studies by Hung Ha et al.( 2010) and Jing-ying, Xiu-li & Wen-quan (2012) delved specifically into waste PCBs and the gold that can be retrieved once suitable conditions are employed. In comparison, Petter, Veit & Bernardes, (2014) scrutinized the same ammonium-thiosulphate system but on PCBs gold-bearing ores and effectively demonstrated that the gold recovered from PCBs (up to 903 g/t) far outweighs the gold recovered in Abbruzzese et al.'s (1995) study from gold-bearing ores (41.2 g/t) . This suggests that recovery from PCBs is gradually becoming an attractive alternative due to the gold yield from ores in comparison to the potential of gold in the e-waste industry.

The efficiency of the ammonium-thiosulphate system is largely based on the copper present on the board and the copper concentration of the lixiviant. Thus, it is paramount to understand the electro-catalytic mechanism of the system and the behaviour of the additional leached copper from PCBs during the leaching process. Furthermore, the ion exchange downstream processes are impacted by the high copper and polythionate concentrations. Therefore, a detailed experimental analysis can be conducted such that the most suitable resin type and eluant is employed for the unstable system. Nicol & O'Malley (2002) assessed the leachate from an ammonium thiosulphate system for gold recovery via ion-exchange and reported that there is still minimal understanding on the effect of polythionates in the ion exchange system and as such an exhaustive understanding of the chemistry is required. This in turn will allow for better gold recoveries to be achieved.

Gold leaching from PCBs using ammonium thiosulphate has been extensively researched however the importance of this research lies in the recovery aspect in relation to ion-exchange. This aspect is not as expansive especially in the ammonium-thiosulphate system context. Therefore, experimentation conducted in this sector will prove to be fruitful in terms of the knowledge gained and the importance of formal recycling of e-waste in the South African context.

## 2.7. Key questions

There are 5 main questions that this study aims to answer. These are stated below:

1. What is the effect of co-dissolving ions in gold leaching from waste PCBs in ammonia-ammonium thiosulphate solution?

Copper is the most abundant metal in PCBs therefore the second key question relates specifically to this ion.

2. What is the effect of background copper concentrations on PCB leaching and gold powder dissolution extraction and how do they compare?
3. What is the performance of the different resin types in recovering gold from leachate?
4. What is the resin affinity to background ions?
5. To what degree do the different eluants effect gold recovery in the elution process?

## 2.8. Hypothesis

A hypothesis is a limited statement regarding the cause and effect of a certain situation. The Hypothesis for this study is stated below:

It is hypothesised that a strong-base anion exchange resin with an ammonium nitrate and ammonia eluant will result in the highest gold recovery from the thiosulphate leached solution. The strong-base resin has a quarternary ammonium group which allows for easy removal of anions from solution. The gold present in the eluant is a gold-thiosulphate complex and is the most stable species in the system. In addition, the presence of ammonia in the eluant further stabilises the cuprous ammonia complex and allows for the gold-thiosulphate complex to remain in solution.

# 3. Research Approach

This chapter outlines the experimental procedure including the materials and methods used in this research. The experimental study aimed to validate the hypothesis and fulfil the project objectives. The experimental work was carried out in three phases namely:

- Pre-treatment of PCBs – Necessary to reduce PCB size for the purposes of fitting into the reactor and limiting copper liberation
- Leaching – to dissolve gold via
    - ♦ Dissolution of gold powder as a proxy for the gold present on PCBs
    - ♦ Leaching of gold from PCBs
- Recovery of gold – to remove gold from leached solution
    - ♦ Using three different resin types
    - ♦ Evaluating two types of eluants

The chapter defines each phase with the materials and equipment utilised for the experimentation.

## 3.1. Materials

There were three types of materials used throughout this study namely, gold powder for the gold dissolution experiments, PCBs for the leaching experiments and anion exchange resins for the subsequent ion exchange gold recovery. Each material is described in the following sub-sections. The last sub-section consists of the reagents used in this study.

### 3.1.1. Premion® gold powder

Gold powder utilised in the study was produced by Alfa Aesar and supplied by Industrial Analytical. The powder was available at Premion® 99.99% on a metal basis and a total of 4 g was needed for all gold powder dissolution experiments. The gold powder was utilised in the pure metal dissolution experiments and to prepare feed solutions for all ion exchange experiments.

Figure 3.1 below illustrates the gold powder in a solution containing only ammonia, $NH_3$, and ammonium thiosulphate, $(NH_4)_2S_2O_3$. The powder is present as small gold flecks before being dissolved.

Figure 3.1: Gold powder in solution prior to copper addition

The gold powder was stored at ambient conditions and experimental work was conducted only when wearing proper Personal Protective Equipment (PPE) such as safety glasses and appropriate protective latex gloves and a laboratory coat.

### 3.1.2. Printed circuit boards

Printed circuit boards are a complex and heterogeneous type of e-waste and require thorough analysis before being incorporated into experiments. The physical description and the elemental analysis on the standardised PCBs used in the gold leaching experiments are expanded upon below.

#### 3.1.2.1. Physical description

The PCBs used in all experiments were custom made boards manufactured by Trax Interconnect (Pty) Ltd. The dimension of the boards was 142 x 105 x 1.55 mm. All boards were of the same composition, dimension and framework and were manufactured from the same type of materials, thus ensuring that accurate comparison and reproducibility of the experiments could be accomplished. Figure 3.2 below shows both the top-side and the bottom-side of the board. For the purposes of this study, only unpopulated boards, as in Figure 3.2, were used.

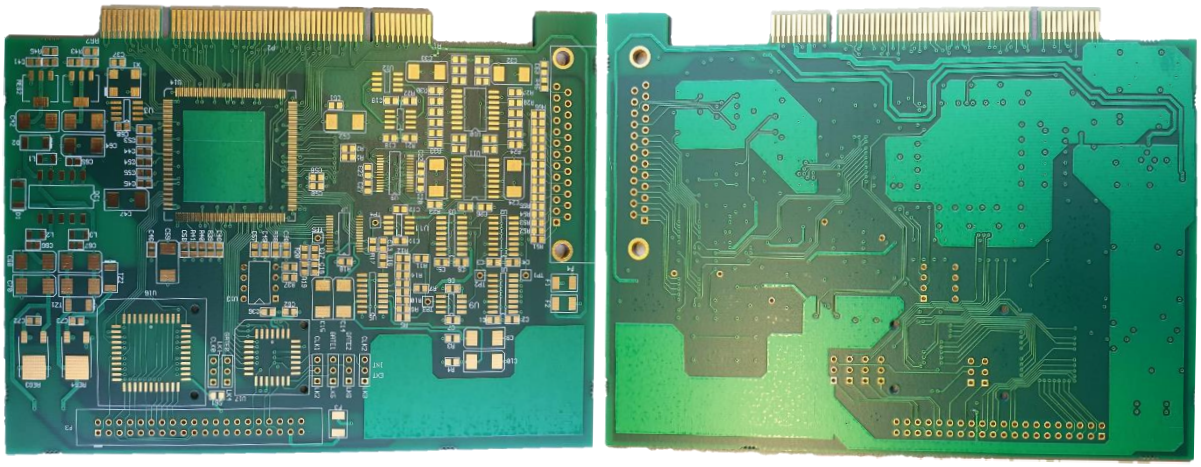

(a) (b)

Figure 3.2: (a) Front view of PCB obtained from Trax Interconnect (b) Back view of PCB obtained from Trax Interconnect

The PCBs are comprised of four distinct layers which aid in the function of the board. The illustration below (Figure 3.3) details the simplified inner layers of the PCBs. The thickness of the entire board is 1.63 mm with the inner-most layer (FR4 core) constituting the majority of the thickness at 0.937 mm. The average weight per board was 52.24 g (Prestele, 2020).

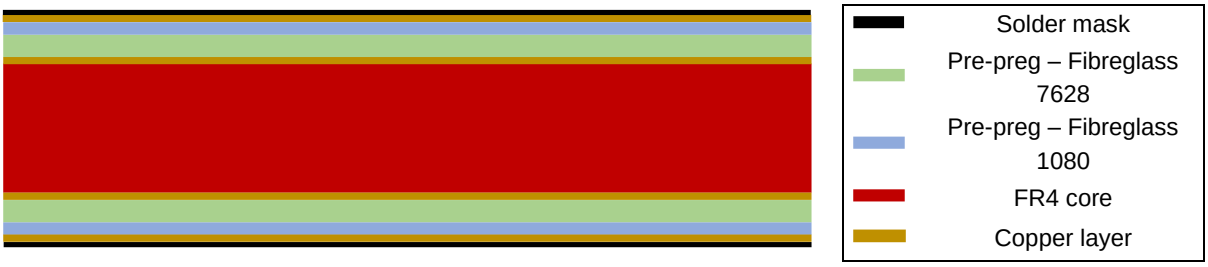


Figure 3.3: Various layers of the custom-made cross-section PCBs from Trax Interconnect (Adapted from Prestele, 2020)

The four layers constitute the unpopulated PCBs with an outer layer on the top and bottom of the PCBs consisting of the solder mask. The solder mask is a combination of solvents and

polymers that make up the ink mask. The ink undergoes photo imaging such that specific areas of the board are covered with the ink (Chirume, 2019). The ink mask in this case is that of a green colour shown in Figure 3.2. On the inside of the solder mask layer, lies a copper layer. This copper layer is essentially a copper foil layer of rolled-annealed copper that is thermally pressurised onto the pre-impregnated (pre-preg) composite layer.

The pre-preg layer in Figure 3.3 consists of fibreglass or electrical grade glass that has been embedded within an epoxy matrix. The epoxy matrix is fundamentally epoxy resin formed by polymerization of monomers into polymers (Prestele, 2020). The FR4 core laminate forms the innermost layer of the PCB only after the pre-preg layer has been pressurised at high temperatures (300°C) to create a strong bond between the inner core and the copper foil layers. The FR4 core is the most common type of core found in PCBs, mainly due to its suitability for a wide range of applications (Sanapala, 2008).

A blueprint of the PCB layers is shown below in Figure 3.4. A large amount of the copper is found within the inner PCB layers, shown as (b) and (c), whilst the remaining copper is within the top and bottom layers, (a) and (d).

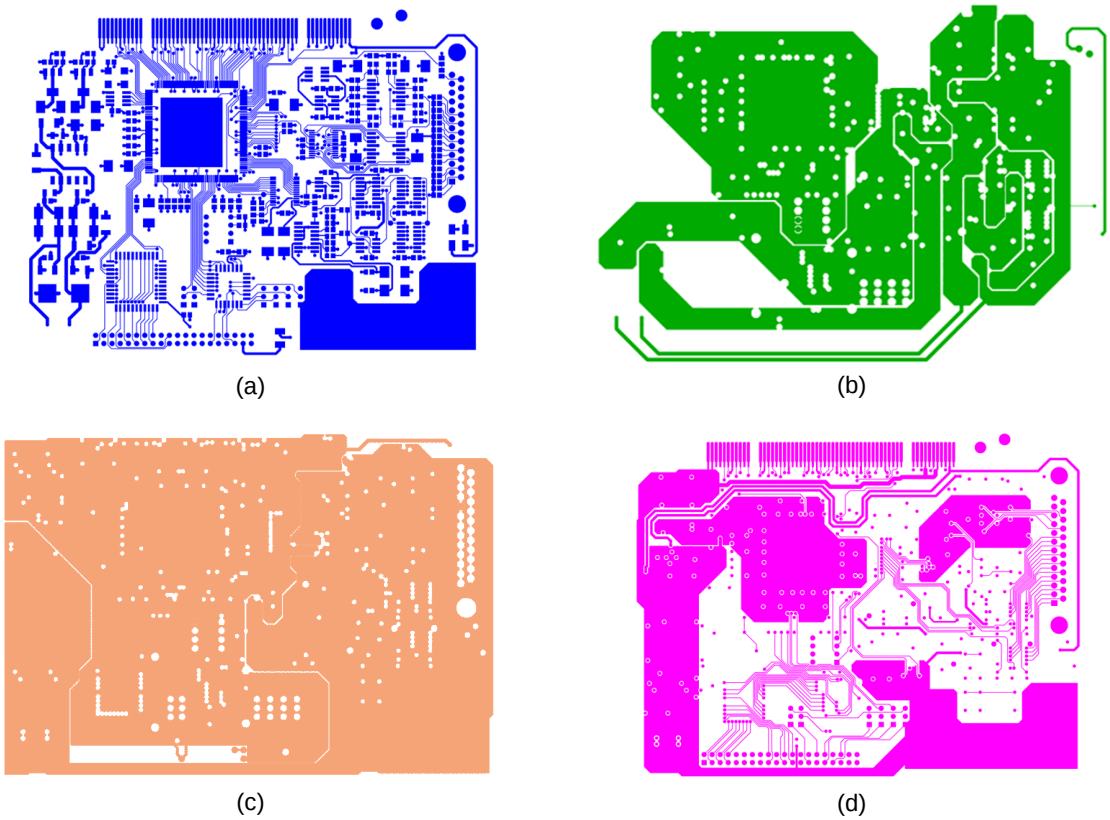

(a) (b)

(c) (d)

Figure 3.4: Blueprint of copper PCB layers (a) Top layer (b) Top-Inner layer (c) Bottom-Inner layer (d) Bottom layer

The blueprint of the solder mask top layer is shown as Figure 3.5.

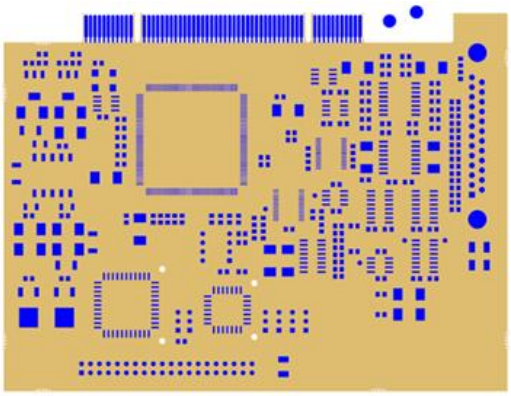

Figure 3.5: Mask blueprint of PCB top layer

The blue coloured areas indicate the gold-nickel alloy that has been plated onto the board and the non-blue areas are indicative of the green ink mask that is present in Figure 3.2. The exposed copper, found on the board in Figure 3.4 (a) is electroplated with nickel and the nickel is electroplated with gold in the manufacturing process. Thus, the gold present on the board is in the form of a nickel-gold alloy. The gold-nickel alloy is present on the surface or vias of the board and is therefore already exposed to any interaction between the gold and the leach solution. All layers are then combined to form the complete whole PCB utilised in all experiments.

#### 3.1.2.2. Elemental analysis

To quantify the composition of elements on the PCBs, a head-grade experiment was conducted. Ammonia-ammonium thiosulphate PCB leaching was conducted under standard conditions used in this study (Section 3.3.2.1) at an ammonium concentration of 0.5 M and a background copper concentration of 0.02 M for 6 hours. The pre-treated PCBs obtained after ammonia-ammonium leaching were then pulverized using a ring mill until a homogenous coarse powder was obtained. This was then split into eight individual solid samples using a Rotary microriffler. Two of the samples obtained from the Rotary microriffler were combined and further leaching experimentation was conducted on these two samples only. This included first acid leaching the sample using reverse aqua regia in a $HNO_3$: HCl ratio of 5 M: 1 M on a heated Lasec magnetic stirrer. The experiment was conducted for 24 hours. In the first 3 hours, temperature remained constant between 60°C - 70°C thereafter the heat was switched off and the leaching continued at an ambient temperature of 25°C. The leachate was stirred at 300 rpm for the entire leaching period.

The sludge obtained from the reverse aqua regia experiment was further leached using regular aqua regia. The concentration of HCl and $HNO_3$ was 3 M and 1 M respectively. A solid to liquid ratio of 1:10 was used for both leaching steps. This method followed a similar process as that of the reverse aqua regia leaching step. After which, the sludge was then dried overnight and finally roasted in a microwave oven at 250°C for 3.5 hours. Solution samples were taken at each acid leaching step for Inductively Coupled Plasma Atomic Emission Spectroscopy (ICP-AES) analysis and the dried solid sample was sent for Inductively Coupled Plasma Mass Spectroscopy (ICP-MS) analysis. The results from the leaching and roasting step are shown in Table 3.1. Detection limits and sample preparation are stated in Appendix A. The ammonia-ammonium thiosulphate experiment was not repeated however the subsequent leaching steps were repeated twice using smaller samples of the same PCB.

Table 3.1 tabulates the gold and copper mass recovered in the three leaching steps and the final roasting procedure of the investigation. Size reduction of the board by means of cutting was required before the first leaching step and this resulted in a total mass loss of 7.3% in the first step. Size reduction was necessary for the purposes of fitting the PCB into the reactors. This was a significant amount that was lost (3.77 g) however mechanical pre-treatment by means of cutting was necessary to reduce the size of the board whilst limiting the liberation of copper that could occur from the inner layers of the PCB. The first leaching step using ammonia and ammonium thiosulphate was required to determine the gold that can be recovered in this specific system. Reverse aqua regia and aqua regia leaching were incorporated to ensure that all gold present on the PCB had completely dissolved into solution and aided in oxidising the gold for better dissolution. The roasting step was required to completely dry the leach solid residue and remove the plastic residue to determine the remainder of undissolved gold via ICP-MS analysis as well as ignite any organic material such that only metal remained. The gold in the roasted sample was measured by acidifying and digesting the sample in 2% nitric acid. Table 3.1 indicates the mass of gold and copper recovered from a single PCB at each step in the experiment.

Table 3.1: Gold and copper recovered mass for leaching and roasting

| | Au mass recovered (mg/PCB) | Cu mass recovered (g/PCB) |
|---|---|---|
| Ammonium thiosulphate leaching | 1.20 | 1.56 |
| Reverse aqua regia leaching | 2.18 | 9.65 |
| Aqua regia leaching | 0.14 | 0.56 |
| Roasting* | $8.56 \times 10^{-2}$ | $3.09 \times 10^{-3}$ |
| Total | 3.61 | 11.77 |

*Measured after roasting the leached sample

The first leaching step recovered 1.20 mg and 1.56 g of gold and additional copper respectively. The reverse aqua regia leaching step recovered the largest amount of both gold and copper as was expected given that gold is known to be completely digested in aqua regia (Petter, Veit & Bernardes, 2014). Across the three leaching steps, a total of 3.52 mg and 11.76 g of gold and copper respectively were extracted. The roasting step contained the smallest mass of both gold and copper. The total mass loss accounted for across the entire experiment was 14.9 g which approximated to 37% of the board. In total, the gold recovered amounted to 3.61 mg whilst the copper was much higher at 11.77 g. This was expected given that copper is found in four of the layers of the PCB whilst gold is plated only on the surface of the PCB. It was possible that the gold and copper masses on a single PCB might be slightly higher than the total reported in Table 3.1 due to the PCB mass loss over all steps including the 10% manufacturing thickness tolerances stated by the supplier. In addition, size reduction by use of a bandsaw could have resulted in some gold being lost granted that the gold is present on the surface and the sawing from the tool would dispense with a significant amount of gold lost.

Another method to determine the gold mass on a board utilised the thickness of the gold plating on the board as well as the square meter area of the gold on the top and bottom layer only. The gold plating thickness was taken to be 0.07 µm provided by Trax Interconnect. Incorporating the gold density in addition to the gold area and thickness, produced the mass

of gold for a single board. Table 3.2 contains both the area and mass of gold on the outer layers.

Table 3.2: Gold distribution in area and mass on the top and bottom layer of a single PCB

| | Area ($m^2$) | Au mass (mg) | Gold distribution (%) |
|---|---|---|---|
| Top layer | $2.33 \times 10^{-3}$ | 3.15 | 74.78 |
| Bottom layer | $7.87 \times 10^{-4}$ | 1.06 | 25.22 |
| Total | $3.12 \times 10^{-3}$ | 4.22 | 100 |

It is evident that the mass of gold is slightly higher at 4.22 mg compared to the 3.61 mg obtained from the leaching experiments. However, these values are considered acceptable with a difference of only 0.61 mg equating to a variance of 14%. Since it was not feasible to determine the exact gold content for each PCB after cutting in order to account for the losses in calculations, a decision was made to use 4.22 mg as the initial gold concentration of the samples, neglecting the minimal losses due to cutting which were not expected to be uniform across samples. Gold extractions and recoveries were compared to the initial Au gold on the board. Therefore, the mass of gold present on a single PCB was 4.22 mg given that the first method of gold determination resulted in some mass loss over the entire investigation. The mass of copper present on a single board was taken to be 11.8 g from the first method of gold and copper mass determination.

Concentrations of the remaining elements were taken from Chirume (2019) and are tabulated with the Au and Cu results from above in Table 3.3. The board was found to be composed of 26 elements of both precious and base metals. Table 3.3 tabulates the majority average elemental composition of the boards. The board is largely copper based and a large amount of this copper can be found in the inner two layers whilst gold is found on the surface of the board as depicted in Figure 3.2 and Figure 3.3.

Table 3.3: Average composition of elements found on the Trax custom made PCB (Adapted from Chirume, 2019; Cu and Au result from this study)

| Elements | Average mass (wt%) |
|---|---|
| Al | 5,31 |
| Au | $8 \times 10^{-3}$ |
| B | 0,85 |
| Ba | 0,22 |
| Ca | 20,28 |
| Co | 1,12 |
| Cu | 22.52 |
| Fe | 2,59 |
| K | 0,17 |
| Mg | 0,26 |
| Na | 0,17 |
| Ni | 1,15 |
| Pb | 0,30 |
| Si | 0,15 |
| Sr | 0,07 |
| Zn | 0,36 |

### 3.1.3. Resin

The project utilised three different types of resins namely the AuRIX®100 resin and two resins, Purogold™ MTA5013SO4 and Purogold™ MTA5011SO4, obtained from Purolite®.

The AuRIX®100 resin was manufactured and supplied by Cognis Corporation. This resin was produced for the sole purpose of removing gold in the form of $Au(CN)_2^-$, the aurocyanide ion, in the gold-cyanide system (Gray, Hughes & Abols, 2005). The trialkylguanidine resin is essentially a styrene di-vinyl based resin and the resin is functionalised with guanidine groups. The chemical structure of the resin is shown in Figure 3.6 where $R'$ denotes the different alkyl groups and thus active sites for anion attachment whilst $N$ and $H$ are nitrogen and hydrogen respectively.

The resin has the appearance of tan beads and is spherical in shape with a particle size of approximately 600 µm. Figure 3.7 shows the resin beads with their colour when dry. The resin has a moisture retention between 47% and 53% on a chloride basis and has a general capacity of between 0.25 eq/L to 0.35eq/L stated by the manufacturer. It is generally transported in the hydrochloride form and is a weak- to medium-base anion exchange resin. Appendix C.1 contains the MSDS of the resin.

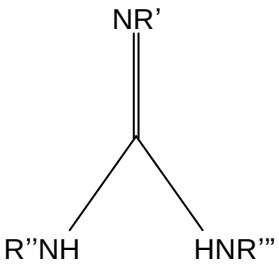


Figure 3.6: Chemical structure of the AuRIX®100 resin guanidine group

Figure 3.7: Tan spherical resin beads

The resin typically operates between a pH of 9 - 11.5 and is ideally suited for gold recovery from alkaline cyanide leach liquors to retrieve $Au(CN)_2^-$. Despite the resin being specifically for the gold-cyanide system, it was still used in testing on the gold thiosulphate complex for reference. Being a weak-base resin, it is first required to be protonated before loading with the aurocyanide ion in the gold-cyanide system similar to Equation 2.11 to Equation 2.14.

The resins obtained from Purolite® are strong-base anion exchange resins. They are manufactured and supplied by Purolite® in the sulphate ionic form and are polystyrenic macroporous resins. These resins are similar to the AuRIX®100 resin as they are crosslinked with di-vinylbenzene however the functional group is Type 1 Quartenary Ammonium. Figure 3.8 illustrates the chemical structure of the resin where $X$ represents the attachment site for the anion $C$, $H$ and $N$ represent carbon, hydrogen and nitrogen respectively.

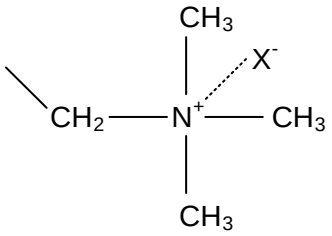


Figure 3.8: Chemical structure of the Purogold™ functional group

This type of resin has a moisture retention of between 54% - 61% in the chloride form and its capacity is 1.15 eq/L. Figure 3.9 and Figure 3.10 provide images of both the Purogold™ MTA5013SO4 and Purogold™ MTA5011SO4. Both images illustrate large tan spherical beads with the only difference being the particle size range between the two resins. MTA5013SO4 has a particle size range of between 1000 - 1600 µm whilst MTA5011SO4 has a particle size range of 800 - 1300 µm (Appendix C.2 and C.3). Both resins were manufactured for an RIP process system and have the advantage of having a larger bead size with superior mechanical strength.

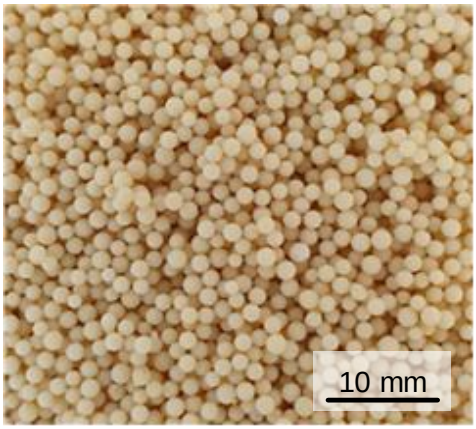


Figure 3.9: MTA5013SO4 Resin

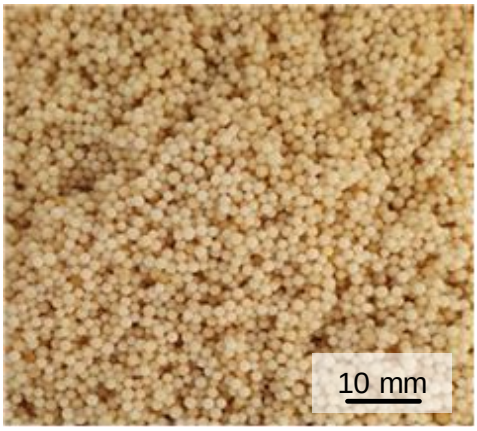


Figure 3.10: MTA5011SO4 Resin

### 3.1.4. Reagents

Several reagents were used throughout the study. Ammonium thiosulphate, 25% ammonia solution and copper (II) sulphate pentahydrate were required for the leaching experiments. $HNO_3$ and HCl were also obtained for the purposes of acid leaching. In the ion exchange experiments, sodium hydroxide (NaOH) and sodium chloride (NaCl) were required. Other reagents included $NH_4NO_3$, $H_2SO_4$ as well as methyl red indicator for the purposes of titration. All reagents were acquired from Merck Chemicals (Pty) Ltd with the exception of the ammonium thiosulphate which was provided by Sigma Aldrich. All reagents were prepared with the appropriate amount of deionised water to achieve the required molar concentrations for each solution. Deionised water was available in the experimental laboratory. A breakdown of the calculations can be found in Appendix B.1 with all reagents being of reagent grade.

## 3.2. Equipment

The equipment utilised in the leaching and dissolution experimentation consisted of a batch stirred tank reactor (BSTR) and a water bath. Ion exchange experiments required a BSTR, Zero Length Column (ZLC), a water bath and a rotary console drive pump. A detailed description of the equipment is provided below.

### 3.2.1. Batch stirred tank reactor

The BSTR was utilised in both leaching and ion exchange experiments. For the purposes of the leaching and gold powder dissolution experiments, an overhead stirrer and a water bath was connected to the BSTR. A total of three 1 L BSTRs were utilised and the experimental reactor set up is displayed in Figure 3.12. A simplified diagram of an individual BSTR is shown as Figure 3.11. All three reactors in the reactor configuration were connected to a water bath, shown on the left in Figure 3.12, to maintain similar temperature within the reactors. This allowed for temperature-controlled water to be circulated between each reactor before returning to the water bath. The overhead stirrers were set at the same speed and a 2-blade metal stirrer allowed for continuous mixing. In addition, air was used as the oxidant and was passed through each reactor. The air level was monitored by the flow meter shown on the right.

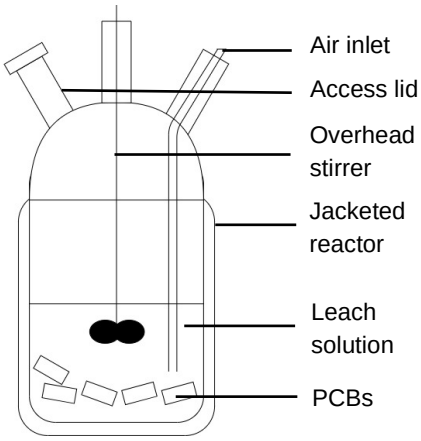


Figure 3.11: Diagram of BSTR

Figure 3.12: Experimental set up of batch stirred tank reactors

For the ion exchange experiments, one 0.5 L BSTR was utilised with a magnetic stirrer in addition to the water bath. This set up was mainly used for kinetic and equilibrium experiments carried out on the MTA5013SO4 resin. The set up will be expanded upon in Section 3.2.2.

### 3.2.2. Zero Length Column (ZLC)

A ZLC was used to conduct the ion exchange experimentation utilising resin. The ZLC consists of a small bed of resin connected to inlet and outlet tubes that allow for the metal containing solution to flow through the resin bed (Figure 3.13 and Figure 3.14). This mechanism assumed no longitudinal dimension and therefore is not a plug flow arrangement. The ZLC can hold approximately 5 mL of resin and the direction of flow was upwards to prevent the formation of bubbles. Figure 3.14 illustrates the actual ZLC utilised in all ion exchange experiments. The twist mechanism allows for easy access to load or remove resin within the mechanism.

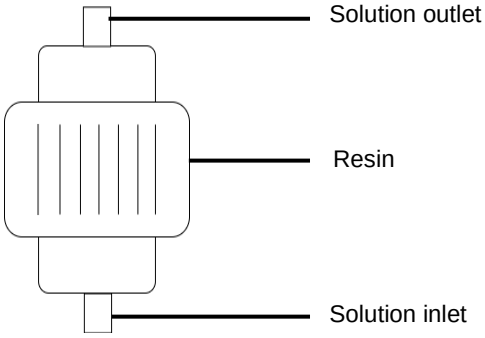


Figure 3.13: Diagram of ZLC

Figure 3.14: ZLC utilised in all experiments

The experimental rig set up for ion exchange is shown as Figure 3.15. A water bath was utilised together with the ZLC, BSTR, magnetic stirrer and peristaltic pump for kinetic and equilibrium experiments. In the case of the capacity, loading and elution experiments only the pump and ZLC was required along with two large 1 L pyrex beakers and a 1 L measuring cylinder. A benchtop pH meter was utilised for all experiments to measure temperature, pH and the conductivity of the solutions. The meter was supplied by Hanna Instruments (Pty) Ltd.

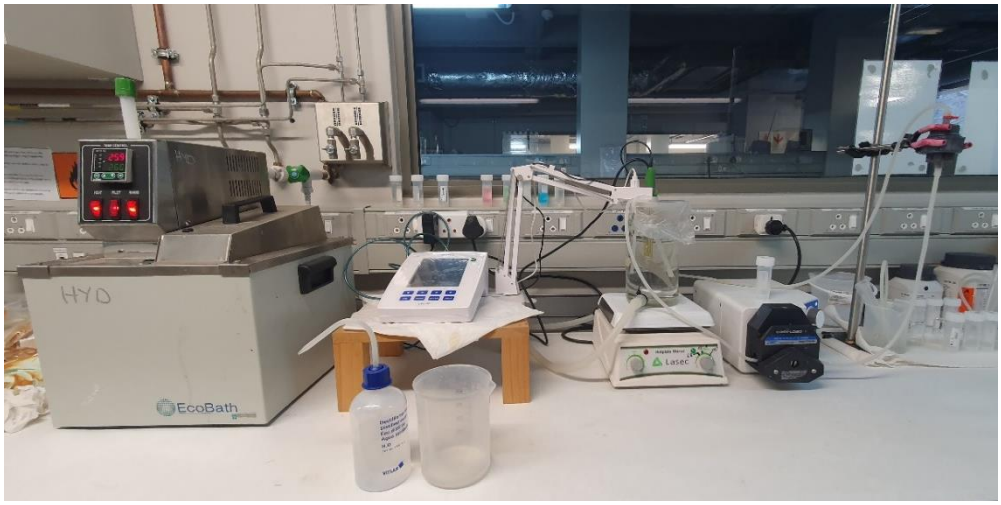


Figure 3.15: Experimental set up for ion exchange experimentation

The peristaltic pump was calibrated before any experimentation could be conducted. The pump required simple operation with a single-turn speed control setting and was provided by Masterflex®. Deionised water was passed through the pump for 5 minutes to calibrate the flowrates at 10 mL/min, 25mL/min and 50 mL/min and collected in a measuring cylinder.

In addition to the above-mentioned equipment, titration equipment consisting of a 50 mL pipette and a 50 mL burette was required for capacity testing along with two 250 mL Erlenmeyer flasks and a pipette filler. This equipment was required only for capacity tests on the resin.

## 3.3. Methods

A detailed description of all experiment methods is provided within this section. These methods include size reduction of the PCBs, gold leaching and ion exchange for loading and elution as well as kinetic and equilibrium tests conducted.

### 3.3.1. Size reduction of PCBs

Size reduction involved manually cutting the PCBs with the use of a bandsaw. This was necessary to reduce the PCB size for the intention of fitting into the 1 L reactor. The cutting technique was favoured mainly due to the reduced amount of copper that would be exposed when compared to shredding the PCBs. Liberation of copper was not expected, in the case of cutting the PCBs, except along the edges of the cut PCBs. Since the gold is present on the surface of the board, extensive mechanical treatment was not required to liberate the gold and thus the PCBs were cut into 1.5 x 3 cm pieces before being leached. Figure 3.16 below shows the PCBs prior to and post size reduction.

(a) (b)

Figure 3.16: (a) PCBs prior to size reduction with demarcated lines (b) PCBs after size reduction

The methodology incorporated for size reduction was as follows: the uncut PCBs were weighed using an electronic mass scale and its weight was recorded. The PCBs were then marked into 1.5 x 3 cm rectangles with a permanent black marker. The boards were cut along the demarcated lines using a bandsaw with the assistance of the Chemical Engineering workshop. The plastic bag was weighed and the PCB pieces were then weighed in the plastic bag using the same electronic mass scale. Both masses were recorded for the purposes of PCB mass loss investigation in the pre-treatment step.

### 3.3.2. Leaching experiment

The leaching experiments were conducted in multiple phases and using various conditions. These experiments involved the use of an ammonium and ammonium thiosulphate system with the addition of copper (II) sulphate pentahydrate. Leaching experiments, where possible, were repeated three times to test reproducibility of the experiments. The phases are shown below:

Phase 1: Gold analysis method experiments (Appendix A)
Phase 2: Elemental mass balance for gold and copper (Section 3.1.2.2)
Phase 3: Gold powder dissolution for 6 and 24 hours at various added Cu concentrations
Phase 4: PCB leaching for 6 and 24 hours at various background Cu concentrations
Phase 5: Gold powder dissolution for ion exchange experimentation

#### 3.3.2.1. Gold powder dissolution and PCB leaching experiments

In the leaching experiments, ammonia and ammonium thiosulphate was used and copper (II) sulphate pentahydrate was added in small amounts to catalyse the reaction (Section 2.4.4.2). Table 3.4 lists the various conditions for all leaching experiments on gold powder and PCBs.

A standard solution consisting of ammonium thiosulphate, ammonia and copper (II) sulphate pentahydrate was first prepared for the 24 hour gold powder experiment. The concentrations of the lixiviants used were as follows: 0.5 M ammonium thiosulphate, 0.5 M ammonia and 0.02 M background copper sulphate (II) pentahydrate. A 2 L standard solution was prepared in a 2 L volumetric flask with 151.2 g of ammonium thiosulphate, 9.987 g of copper sulphate and 75.7 mL of 25% ammonia solution. Once all reagents were measured appropriately using an electronic mass scale, a weighing boat and a graduated cylinder, they were added into the volumetric flask and topped with deionised water to the 2 L mark. The solution was then stirred using a magnetic stirrer until it was completely dissolved and had attained a deep dark blue colour.

Table 3.4: Lixiviants and conditions for ammonia-ammonium thiosulphate leaching

| Lixiviants/Conditions | Units | Values |
|---|---|---|
| $(NH_4)_2S_2O_3$ concentration | M | 0.5 |
| $CuSO_4.5H_2O$ concentration | M | 0.008/ 0.02/ 0.045/ 0.1 |
| $NH_3$ concentration | M | 0.5/ 1 |
| pH | - | 9 - 10 |
| Temperature | °C | 25 |
| Time | Hours (h) | 6/24 |
| Stirring speed | Revolutions per minute (rpm) | 400 |
| Volume | mL | 500 |
| Compressed air flowrate | L/min | 0.07 |
| Solid to liquid ratio* | - | 1:10 |
| Gold powder** | mg | 56 |

*Applies only to PCB experiments. **Applies only to gold powder experiments

Premion® 99.99% gold powder (56 mg) was weighed using a weighing boat and an electronic mass scale. Three jacketed reactors in series were set up for the experiment as depicted in Figure 3.12. The reactors were connected to a water bath which was switched on and allowed to maintain a steady temperature of around 25°C for the duration of the experiment. Exactly 500 mL of the standard solution was measured and added into each reactor followed by the gold powder. Overhead stirrers were required for mixing of the solution at 400 rpm stated in Table 3.4. Oxygen ($O_2$) was supplied as compressed air at a flowrate of 0.07 L/min per reactor. Once all reactors were set up a vacuum sealant was applied to the reactor lid and the reactor was sealed shut with only a small outlet for air.

Sampling of 6 mL leachate occurred at 15 minutes intervals for the first hour, 30 minute intervals in the second hour and every hour up until the 6 hour mark. Samples were then taken again every hour from the 21 hour mark up until 24 hours. Sampling occurred using a silicon tube, a 10 mL syringe and 0.2 µm nylon syringe filter. The syringe filter was utilised to prevent solids entering the solution bottle. As discussed in Appendix A, the solution samples were further diluted in a 1:1 ratio using a 10 mL Eppendorf pipette with a fresh solution of 0.5 M

ammonium thiosulphate and 0.5 M ammonia before being refrigerated until analysis. This was necessary to stabilise the solution over long periods of time prior to analysis. To ensure a constant 500 mL volume in the reactor, 6 mL of the initial fresh 2 L standard solution consisting of ammonium thiosulphate, ammonia and copper (II) sulphate pentahydrate was added back into the reactor at each sampling time. The pH was monitored at the start and the end of the 24 hour experiment. Solutions samples were then analysed for both gold and copper using ICP-AES.

Each experiment was terminated by stopping the magnetic stirrers and switching off the water bath. The compressed air tap was closed and the reactor lid was gently slid off. The remaining solution, in the reactors, was then disposed of.

The 6 hour experiments conducted on the gold powder followed a similar procedure to the 24 hour experiments. Four tests were run at the various copper concentrations shown in Table 3.4. Sampling occurred exactly the same as the 24 hour experiment up until 6 hours at which point the experiment was complete.

Leaching tests conducted on the PCBs followed the same procedure. In both the 24 hour and 6 hour experiments, one pre-treated PCB was leached in each reactor. The blade of the overhead stirrer was immersed into the solution allowing for it to be slightly above the cut PCBs whilst at the same time allowing continuous mixing of the solution.

Once the experiment was completed, the solution and PCBs were separated via a vacuum filter using a compressor, a Buchner funnel and filter paper. The mass of the PCBs was recorded once they were completed dried.

#### 3.3.2.2. Gold powder dissolution for ion exchange

Dissolution of gold powder using ammonia-ammonium thiosulphate solution similar to what was described in Section 3.3.2.1 was conducted for the purposes of downstream ion exchange experimentation. This type of experiment utilised the same ammonia-ammonium thiosulphate system. The concentration of ammonia and ammonium thiosulphate was 0.5 M each. Copper sulphate was added at a low concentration of 0.02 M. All other experimental conditions are as stated in Table 3.4 and the experiments were conducted for 24 hours to ensure completely dissolved gold powder.

Sampling occurred at the start and end of the experiment only. Only 5 mL of solution was extracted and diluted in a 1:1 ratio with 0.5 M ammonia and 0.5 M ammonium thiosulphate solution. The synthetic solution containing the dissolved gold was collected at the end of the experiment and dispensed into 500 mL Schott bottles. The bottles were kept in the refrigerator until the ion exchange experimentation could be conducted.

### 3.3.3. Ion exchange experiments

The ion exchange experiments were conducted using all three resins namely, the AuRIX®100 resin, the Purogold™ MTA5013SO4 and Purogold™ MTA5011SO4. Capacity, loading and elution tests were conducted on all three resins. Kinetic and equilibrium tests were only conducted on the MTA5013SO4 resin and testing on the MTA5011SO4 resin was purely for confirmatory tests on that of the MTA5013SO4 resin.

#### 3.3.3.1. Free Wet Settled Volume (FWSV)

The Free Wet Settled Volume (FWSV) of the resin was first measured before depositing the resin into the ZLC. An estimated volume of 5 mL of dry resin was deposited into a 10 mL measuring cylinder. The cylinder was filled to just below the brim with deionised water and the top was sealed and inverted to allow the resin particles to suspend freely in solution. The cylinder was returned to the upright position and the particles were allowed to completely settle at the bottom for 1 minute. Once the resin was completely settled, the exact volume in millilitres was recorded from the measuring cylinder graduations. This value was the FWSV. The resin was then deposited into the ZLC by slowly pouring and ensuring no loss of ion exchange resin beads.

This method was applied before conducting any new ion exchange experiments. Once the ZLC was loaded with the measured resin and sealed tight, ion exchange experiments were carried out.

#### 3.3.3.2. Capacity test experiments

Capacity tests were measured regularly and are a necessity before any ion exchange experiments can be conducted on the resin. The capacity tests determine the active sites available for attachment of the targeted ion. Capacity tests were conducted at the start of the experiments after measuring the FWSV once the ZLC had been packed with the resin.

The experimental set up for an open circuit capacity test is illustrated in Figure 3.17. A rotary pump, measuring flask and a beaker were required for the experimentation. The magnetic stirrer was required only at the start and end of the experiment to ensure that the solution was thoroughly mixed. The measuring flask was required in the final step of the experiment. Beakers were used in all other steps to collect the effluent from the ZLC. Additional titration equipment was required for capacity tests on the MTA5013SO4 and MTA5011SO4 resins. All experiments were conducted at ambient temperature and the flowrate was kept constant at 25 mL/min. The FWSV of the resin was determined before starting experiments on all three resins. Once this was conducted, the resin was deposited into the ZLC and the ZLC was screwed shut to prevent any loss of solution or air.

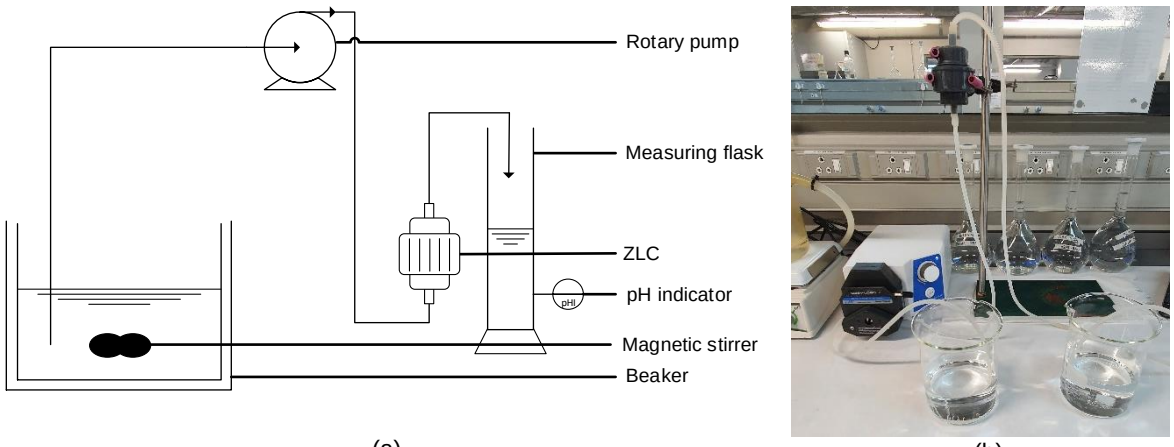


(a) (b)

Figure 3.17: (a) Diagram of an open circuit ion exchange system (b) Experimental set up for capacity testing

Capacity tests, for the AuRIX®100 resin, were completed using two methodologies. These methodologies were investigated to determine the effect on the final resin capacity value. Both

types of methodologies utilised 1 M NaOH, deionised water and 0.1 M NaCl. The first method consisted of five steps. Once the FWSV was determined and the ZLC had been packed with the appropriate amount of resin, the capacity test was conducted. The AuRIX®100 was available in the hydrochloride form. In the first step, 1 L of the NaOH solution at a flowrate of 25 mL/min was passed through the ZLC using a pump. This was required to convert the resin into the free-base form. At the start, the ZLC was lightly tapped to ensure that all bubbles escaped and all NaOH solution had been pumped out of the ZLC before proceeding with the next step. This method of tapping the ZLC and pumping all fluid out at the end was applied to all steps in the experiment.

Once the NaOH step was complete, deionised water was flushed through the ZLC until the pH was between 9 and 10. This required 1 L – 1.5 L of deionised water. The pH of the deionised water at the start and end of the step was measured. Flushing the resin with deionised water is necessary to remove all excess anions present in the system. The third step utilised 1 L of the 0.1 M NaCl solution which was passed through the ZLC. Thereafter deionised water was used again to flush out any excess ions whilst still monitoring the pH such that the effluent pH was between 9 and 10. In the final step, 1 M NaOH at a volume of 1 L was pumped through the ZLC. The final step was necessary to detach the chloride ions attached onto the resin. A 10 mL sample of the NaOH effluent was analysed for chloride ions using a Gallery™ Discrete Photometric Analyser. The analytical range of the analyser was 3 – 50 mg/L Cl.

The second method employed the same solutions and concentrations as the first method however only the first three steps of the methodology were carried out. The final step 3 was conducted in a closed circuit such that the NaCl solution was circulated between the beaker and ZLC for 40 minutes at 25 mL/min. The solution was mixed using a magnetic stirrer at 300 rpm before extracting a 10 mL sample for analysis. The NaCl effluent sample was analysed using the photometric analyser to determine the final concentration of chloride ions in solution.

The capacity tests for the Purogold™ MTA5013SO4 and Purogold™ MTA5011SO4 resins were conducted in a similar manner. Both resins were available in the sulphate form. Only three steps were required for this experiment and the same reagents were used. NaOH was required at a concentration of 2 M and NaCl was present at 0.5 M. The concentration of NaCl in the capacity tests for all three resins was chosen to ensure that there would be a large excess of chloride ions in solution for attachment onto the resin. This concentration was calculated based on the resin general capacity provided in the MSDS for all three resins (Appendix C). The capacity tests for the Purogold™ resins included a titration experiment after the final step to determine the chloride ions in solution. The titration utilised 1 M HCl as the titrant for the MTA5013 and 0.1 M for the MTA5011 experiments. Both experiments required methyl red as the indicator and the NaCl effluent from the ZLC as the analyte.

100 mL of the alkaline NaCl solution containing hydroxyl ions prior to step 3 was titrated against the 1 M HCl using a 100 mL pipette, a 250 ml Erlenmeyer flask and a 50 mL burette. This solution is known as the blank sample. 1 L of fresh NaCl was pumped through the ZLC and beaker and the solution was stirred. 100 mL of the mixed effluent at 40 minutes was then pipetted into an Erlenmeyer flask. A few drops of methyl red was added into the solution and the now yellow solution was titrated with HCl until it turned a red-pink colour. The volume of HCl in mL required for the colour change was recorded in both the blank sample and the

effluent sample. Equation 3.1 was then applied to calculate the actual capacity of the resin in eq/L.

$$Q = \frac{10 \times \left(V_{effluent} - V_{blank}\right) \times N_{HCl}}{FWSV} \quad \text{Equation 3.1}$$

$Q = Actual\ resin\ capacity\ (eq/L)$
$V_{effluent} = Volume\ of\ HCl\ added\ to\ neutralise\ the\ effluent\ sample\ (mL)$
$V_{blank} = Volume\ of\ HCl\ added\ to\ neutralise\ the\ blank\ (mL)$
$N_{HCl} = Concentration\ of\ HCl\ (mol/mL)$
$FWSV = Free\ Wet\ Settled\ Volume\ of\ resin\ in\ the\ bed\ (L)$

#### 3.3.3.3. Loading and elution experiments

Loading and elution experiments were conducted on all three resins using the standardised leached solutions on gold powder. These experiments were important to determine the performance of the resin in removing the aurothiosulphate ion from solution for gold recovery.

Testing on the AuRIX®100 was first conducted in four steps in an open circuit. The conditions and lixiviants used are shown in Table 3.5. Once the FWSV experiment and capacity test had been completed the loading experiment was conducted. A 0.5 L solution of 1 M NaOH was pumped through the ZLC before passing 0.5 L of deionised water. Thereafter, the dissolved gold powder synthetic solution was loaded onto the resin by being pumped through the ZLC. To limit the possibility of precipitate formation, the dissolved gold powder synthetic solution was always prepared within 24 hours of the ion exchange experiment. A 5 mL sample of the dissolved solution was taken at 10 minute intervals for the duration of 20 minutes. Thus, three samples were collected and diluted in a 1:1 ratio with 0.5 M ammonia and 0.5 M ammonium thiosulphate solution. The resin was eluted with 0.5 M NaOH using 0.5 L of solution. Samples of the eluant were taken in the same manner however these were not diluted. The pH was recorded at the start and end of all steps. Deionised water was used to remove any excess ions present in the ZLC. All samples were sent for ICP-AES analysis for gold and copper. The same resin was used for all loading and elution for the AuRIX®100 resin.

Table 3.5: Loading and elution experiment conditions for AuRIX®100 resin

| Lixiviants/conditions | Units | Values |
|---|---|---|
| NaOH concentration | M | 1/0.5 |
| NaOH volume | L | 0.5 |
| Deionised water volume | L | 0.5 |
| Leachate volume | L | 0.5 |
| Flowrate | mL/min | 25 |
| Temperature | °C | 25 |

Loading and elution experiments, on the Purogold™ resins, were conducted in a similar technique of four steps in an open circuit. Loading solutions consisted of dissolved gold in solution from the dissolution experimentation in Section 3.3.2.2. The method followed that of the AuRIX®100 resin except for the sodium hydroxide concentration. Exactly 1 L each was required for the sodium hydroxide and deionised water step. Sodium hydroxide was required

at a high concentration of 2 M to dislodge the large sulphate ions present on the resin. Loading and elution steps were conducted at a volume of 0.5 L. All experiments occurred at ambient temperature. The pH was recorded at the beginning and end of each step (Appendix D.4). Two different eluants were introduced for experimentation on the MTA5013 resin at various flowrates. The MTA5011 resin tests were conducted using one type of eluant at a 25 mL/min flowrate. Samples were taken in the same manner as that of the AuRIX®100 resin. Figure 3.18 illustrates the loading step of the experimentation.

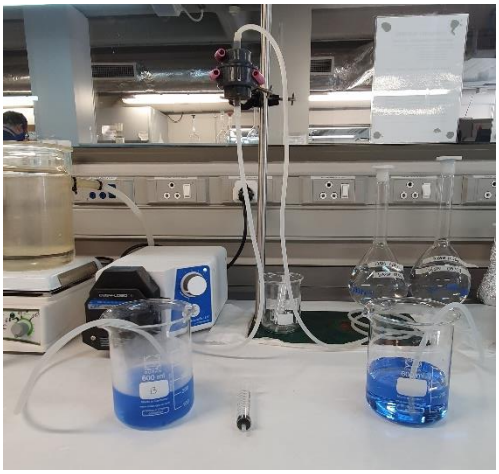

Figure 3.18: Loading step of ion exchange experimentation

The two eluants used, in the experimentation on the MTA5013SO4 resin, were ammonium nitrate ($NH_4NO_3$) and $NH_3$. In the first method, 2 M $NH_4NO_3$ was used to elute the aurothiosulphate ion from the resin. Ammonium nitrate at a concentration of 2 M was used to remove the large aurothiosulphate ion from the resin. These tests were run at three different flowrates (10 mL/min, 25 mL/min and 50 mL/min), for the loading and elution step only. Fresh resin was used with each change in flowrate.

The second method was completed in five steps. In this instance, $NH_3$ at 1 M concentration was utilised after the loading step to remove any copper ions that may have attached onto the resin. Thereafter, 1 M $NH_4NO_3$ was used to desorb the aurothiosulphate ion. This was conducted at a flowrate of 25 mL/min and at ambient temperature. Fresh resin was used in this experiment. In both methodologies, samples were taken from the loading step and diluted at 1:1 ratio of 0.5 M ammonia and 0.5 M ammonium thiosulphate before analysing using ICP-AES. Effluent samples consisting of the eluant from the elution step were also collected and analysed using ICP-AES

#### 3.3.3.4. Kinetic and equilibrium experiments

Kinetic and equilibrium experiments were conducted on the Purogold™ MTA5013SO4 resin only. A new batch of resin was required for both the kinetic and equilibrium experiments. Kinetic experiments were conducted in a closed circuit. A thermostated jacketed BSTR, a water bath and a magnetic stirrer was used as illustrated in Figure 3.19. These tests occurred at three different flowrates: 10 mL/min, 25 mL/min and 50 mL/min. A capacity test was performed before any kinetic experiments could be conducted. This ensured that the resin was in the chloride ion form before loading. Table 3.6 lists the conditions for the kinetic experiments.

Table 3.6: Ion exchange kinetic experiment conditions

| Conditions | Units | Values |
|---|---|---|
| Temperature | °C | 25 |
| Speed | rpm | 300 |
| Time | h | 2 |
| Leachate volume | L | 0.5 |
| Flowrate | mL/min | 10/25/50 |

Once the resin was in the chloride ion form, the water bath was switched on and allowed to maintain a constant temperature of 25°C. A volume of 0.5 L of dissolved gold synthethic solution from Section 3.3.2.2 was poured into the BSTR. The pH and temperature probe were placed into the solution and both measurements were automatically recorded every minute. The inlet and outlet tubes connected to the ZLC were placed inside the BSTR and the reactor top was sealed using parafilm. The magnetic stirrer was switched on at 300 rpm. The rotary peristaltic pump was switched on and the pH/EC meter was set to collect data. Samples were taken in 15 minutes intervals for the first half an hour thereafter they were collected in 30 minutes intervals. A 5 mL sample was extracted at each interval thus a total of 30 mL was removed from the reservoir. All samples were diluted in a 1:1 ratio of 0.5 M **(**$(NH_4)_2S_2O_3$ and 0.5 M $NH_3$ and sent for ICP-AES analysis. After 2 hours, the resin was eluted with 0.5 L of 1 M $NH_4NO_3$ in an open circuit at the same temperature and flowrate. This method was repeated thrice for all flowrates.

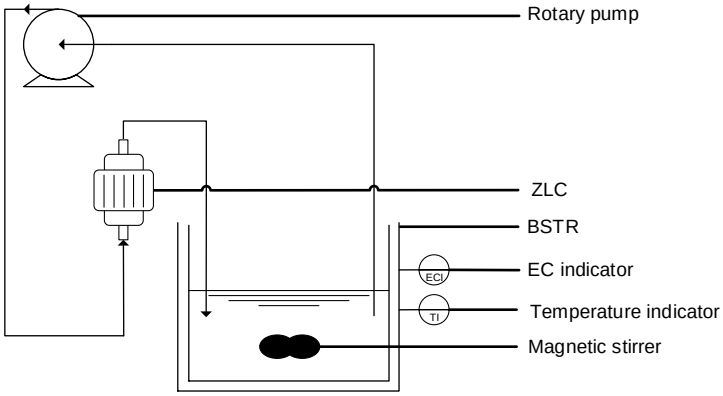


Figure 3.19: Diagram of a closed circuit ion exchange system

Equilibrium experimentation was conducted on a new batch of resin after its FWSV had been determined. This experimentation was conducted in five steps. Three different excess capacities were tested: 50%, 100% and 200%. Excess capacities were based on the resin general capacity provided in the MSDS. The calculations in determining the excess capacities are provided in Appendix B.2. Testing was conducted using the same experimental set up as in Figure 3.19 with the same additions as in the kinetic experimentation. The first step required 1 L of 2 M NaOH to convert the resin into a hydroxyl form. Exactly 1 L of deionised water was flushed through the system to remove any excess ions. A 0.5 L of leached solution prepared in Section 3.3.2.2 was passed through the ZLC as the gold saturated loading solution. This allowed for any aurothiosulphate ions in solution to attach onto the resin. These three steps

were conducted in an open circuit. The conditions for the experimentation are listed in Table 3.7.

Table 3.7: Ion exchange equilibrium experiment conditions

| Conditions | Units | Values |
|---|---|---|
| Temperature | °C | 25 |
| Speed | rpm | 300 |
| Time | Hours | 4 |
| Flowrate | mL/min | 25 |
| NaCl volume | L | 0.5 |
| Excess capacities | % | 50/100/200 |

A thermostated (25°C) BSTR was equipped with a pH and temperature probe and a conductivity meter. The NaCl solution, at various concentrations, was added into the reactor and agitated using a magnetic stirrer at 300 rpm. This solution was allowed to flow between the ZLC and BSTR in a closed circuit. Figure 3.20 illustrates the experimental set up for the ion exchange equipment. This step was conducted for 4 hours and the pH, conductivity and temperature were automatically recorded every minute. The final step consisted of eluting the resin with 1 M $NH_4NO_3$ in an open circuit.


Figure 3.20: Experimental set up for equilibrium ion exchange tests

At the end of step 4, all liquid was allowed to return into the BSTR before switching off the pump, the magnetic stirrer, the pH/EC meter and finally the water bath. Samples were then taken at the end of the experiment and analysed for both gold and copper. No dilution of samples was required.

## 3.4. Analysis techniques

There are various types of equipment available for analysing the samples obtained from experimentation. This study utilised various analytical methods for both solid and liquid samples from the experimentation to determine mainly the gold and copper present. In some instances, chloride ions were also analysed.

ICP-OES/AES/MS can determine the composition of elements in majority water dissolved samples (Guo et al., 2011). This analysis type includes high analysis speed and is a technique that incorporates using both plasma and a spectrometer. Analysis for gold was conducted using ICP-AES Thermo iCAP 6000 in the Central Analytical Facilities at the University of

Stellenbosch. Generally, dilution or acidification, using Ultra- pure $HNO_3$, of liquid samples are required prior to analysis for the purposes of dissolving all particles present in the sample and to allow for sample concentrations to be within the analytical range of the equipment (Thermo Fischer Scientific, 2021). For this study, deionised water was required for dilution of samples (Appendix A). The Agilent 4200 MP-AES was used in addition to ICP-OES for comparison analysis of a few samples. MP-AES/ICP-MS analysis is similar to ICP-AES, however this type of equipment allowed for a lower detection limit thus smaller concentrations on ppb level of the targeted metal could still be analysed. The detection limit for ICP-AES and ICP-OES was 50 ppb.

In the ion exchange experiments, measurement of chloride ions present in solution was conducted using the Thermo Scientific™ Gallery™ Discrete Analyzer. This analysis was conducted by Set Point Laboratories. Mercury (II) thiocyanate was employed in the analysis and the reaction of this compound with chloride produces a soluble compound. The thiocyanate ions that are then released and react with iron (III) nitrate to form a stable colour. This is then measured spectrophotometrically at a wavelength of 480 nm and is related to the chloride concentration by means of a calibration curve.

Solution pH was measured at the beginning and end of each experiment using the Hanna Professional Benchtop pH/EC meter. The Hanna meter was calibrated for pH every day using Hanna pH technical calibration buffer solutions of pH 4.01, 7.00, 9.01 and 12.00. This ensured accurate and precise readings when measuring the sample solutions from the experiments.

Electrical Conductivity (EC) analysis was conducted on the same Hanna Professional Benchtop meter as the pH analysis. EC was measured mainly in the ion exchange equilibrium experimentation conducted. The EC probe was calibrated every second day using calibration buffer solutions of 1413 µS/cm and 12880 µS/cm.

Scanning Electron Microscopy with Energy Dispersive Spectroscopy (SEM-EDS) analysis was used for the solid samples. This type of analysis was conducted by the Electron Microscope Unit at the University of Cape Town. The SEM analysis used the FEI Nova NanoSEM 230 and the EDS was done using an Oxford X-max 20 $mm^2$ detector and Oxford INCA software. The samples were mounted on 12 mm aluminium SEM stubs and carbon coated before viewing in the SEM. Carbon coating is necessary to make the samples conductive. SEM analysis was conducted on mainly 3 samples to determine the presence of gold. This provides a visual type of analysis of the sample surface and contributes to the identification of any unknown material present.

## 3.5. Error analysis

Pre-liminary experiments had revealed the necessity for developing a dilution method to analyse for gold in solution. Gold error results in leaching prior to incorporating the dilution method were close to 100% as the analysis method compromised the stability of the ions in solution thus making accurate and reproducible analysis for dissolved gold in solution impossible. Thus, introducing the dilution method for the gold powder dissolution and PCB leaching experiments significantly reduced the error (Appendix A). Error results for gold across all leaching and gold powder dissolution experiments were in the range of 0 – 15% with some outliers allowing up to 43%. There was a significant reduction in the gold error analysis when

compared to pre-liminary experiments thus further demonstrating the need for the dilution method. Copper error results for PCB leaching was between 0.48% and 10% with the incorporation of the dilution method. Most of the data fell between this margin of error with some outliers reaching up to 32%. Copper error analysis remained within the same error range (0.48 - 10%) and did not increase with the addition of the dilution method.

Furthermore, there was a remainder residual error associated with the gold (112 ppm) standard solutions prepared for the ion exchange experiment. Dissolved gold solutions exceeding the concentration of 112 ppm was assumed to be 100% of gold (56 mg) dissolved into the solution. Ion exchange recoveries were reported relative to the measured final concentration of each standard solution.

# 4. Results and Discussion

This chapter outlines the results for all experiments mentioned in Chapter 3 and discuss and interpret these results. The chapter is divided into two main sections (leaching and ion exchange) and is further sub-divided into the relevant sections corresponding with the sections mentioned in Chapter 3. In addition, this chapter highlights the key challenges encountered.

## 4.1. Gold powder dissolution and leaching experimentation

This section details the gold powder dissolution experiments and the PCB leaching experiments for both the 24- and 6-hour time periods. Detailed experimental conditions are stated in Chapter 3. For each experiment in this section, experimental conditions are summarised, results are stated, key points are outlined and thereafter a discussion follows.

Figure 4.1 depicts the gold extraction over 24 hours for gold powder dissolution and PCB leaching using the ammonia-ammonium thiosulphate system in the presence of 0.5 M ammonia and ammonium thiosulphate and 0.02 M background copper sulphate. Additional conditions were stated in Table 3.4 (Section 3.3.2.1). The curve for the dissolution of gold powder shows a sharp increase within the first 2 hours, thereafter a small but gradual increase until 21 hours after which the extraction declines. Within the first 2 hours, a fast dissolution rate was expected due to the fast leach kinetics of the system as proposed by Breuer & Jeffrey (2000) in the presence of oxygen and this was evident in Figure 4.1. The decline in the concentration after 21 hours of leaching was unexpected and is thought to be due to thiosulphate decomposition within the system therefore hindering gold staying in solution. This is in line with observations made by Senanayake (2004) and Feng & van Deventer (2006) who found that over time gold losses increase due to the oxidation of thiosulphate into polythionates.

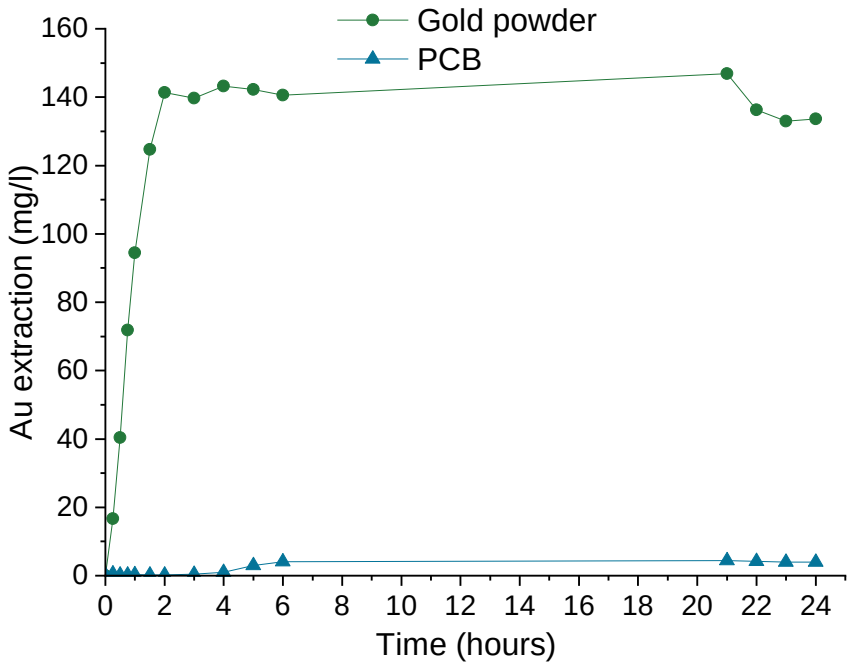


Figure 4.1: Graph comparing the Au extraction from PCB and gold powder dissolution for 24 hours

Results from Figure 4.1 served as confirmation that ammonia-ammonium thiosulphate solutions were promising for the leaching of gold from PCBs. Within 24 hours, the gold powder

was completely dissolved in the ammonia-ammonium thiosulphate system. The maximum extraction of gold for the gold powder dissolution experiment was achieved at 21 hours, with 147 mg/L of gold dissolved.

Results from the PCB leaching experiment in Figure 4.2 showed a similar trend to that of gold powder dissolution. There was an increase in extraction up to 4 mg/L within the first 6 hours followed by a period of not sampling. Further sampling at 21 hours suggests that the concentrations showed only a slight increase and thereafter started to decrease. The increase within the first 6 hours was much slower than the first 6 hours of the gold powder dissolution experiment. The dissolution rate for the first 6 hours in the gold powder dissolution experiment was 11.7 mg/h whilst that of the PCB leaching experiment was 0.34 mg/h. The PCB experiment (Figure 4.2) reached a maximum concentration of 4.4 mg/L (52%) at 21 hours indicating that half of the gold had been extracted from the PCB. Between 6 and 21 hours, there was a slower increase in gold extraction and at 24 hours the gold extraction was 47% which correlated to 4 mg/L.

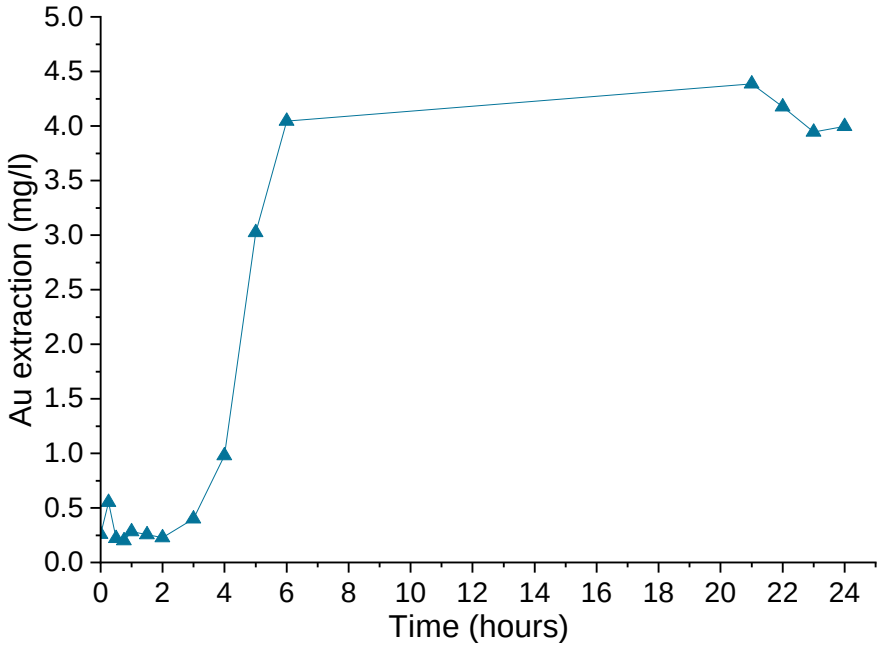


Figure 4.2: Graph showing Au extraction from PCB leaching over 24 hours

The high dissolution of gold powder was promoted by the absence of competing ions for the thiosulphate complex formation in the gold powder experiment. Background copper present in the solution at the start of the experiment was approximately 0.02 M. No additional Cu ions were present when the gold powder was dissolved therefore additional Cu was not in competition with the gold for the thiosulphate ion. Moreover, there was no additional Cu available to catalyse the oxidation of thiosulphate ions. The additional copper from leaching the PCB could have hindered the gold leaching process as copper is known to compete with gold in forming a thiosulphate complex thereby consuming thiosulphate present in the solution and reducing the cupric ion concentration available for complexing with ammonia in the process (Ha et al., 2014). Furthermore, the PCB contained other ions such as nickel and zinc which compete with gold ions for complexation with the thiosulphate ion. It was also evident that around 21 hours both the gold powder and PCB experiments each attained their highest gold extractions. The increase in gold extraction between 6 and 21 hours for the gold powder dissolution experiment was 141 mg/L and 147 mg/L respectively whilst the PCB leaching experiment extractions at the same time were 4.1 mg/L and 4.4 mg/L respectively. Although

the maximum extraction was at 21 hours, the increase between 6 and 21 hours was minimal and these experiments could have been terminated at 6 hours. Thus, it can be deduced that complete gold extraction in both the gold powder and leaching experiments was achieved at 6 hours at the conditions of 0.5 M $NH_3$, 0.5 M $(NH_4)_2S_2O_3$ and 0.02 M background $CuSO_4.5H_2O$.

The decline in extractions for both the gold powder dissolution and gold from PCB leaching after 21 hours may be due to the consumption of thiosulphate as well as loss of ammonia in solution. Consumption of thiosulphate is attributed to the ion being meta-stable in addition to being “easily oxidised by the cupric ions” (Xu et al., 2017). Furthermore, both Molleman & Dreisinger (2002) and Xu et al. (2017) reported that thiosulphate consumption was a cause for low gold extractions. Loss of ammonia could also be a contributor to low gold extractions as this disrupts the ratio of thiosulphate to ammonia thereby inhibiting the regeneration of the cuprous ion. The pH of the solution decreased from 9.51 to 9.33 for the gold powder dissolution experiment and 10.11 to 9.16 for PCB leaching over the 24 hours (Appendix D.3). Thus, it is possible that low gold extractions can be attributed to ammonia loss especially in the PCB leaching experiment. Thiosulphate and ammonia are the dominant ligands of both the cupric and cuprous ions and as such need to be maintained for copper regeneration (Equation 2.4 and 2.5).

Figure 4.3 compares gold to copper concentration over 24 hours of PCB leaching. Copper extraction proceeded faster than the gold extraction reaching a value of 6.6 g/L in 24 hours. Copper was not liberated from between the inner layers of the board and can only be etched from the edges of the cut board pieces in contact with the solution. Copper extraction was subsequent to gold extraction because gold is essentially plated onto the available copper surfaces. The trend overall was similar to the gold extraction trend however there was a sharper increase in copper extraction between 6 and 21 hours when compared to the gold extraction. The copper extraction in Figure 4.3 refers only to the copper sulphate extracted from the PCB.

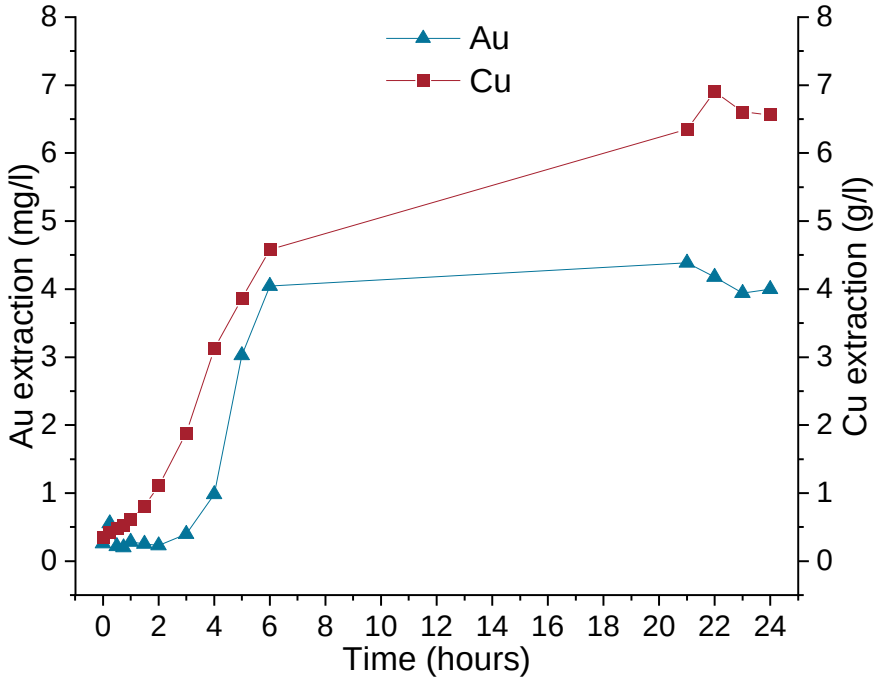


Figure 4.3: Graph comparing the Au and Cu extraction from PCB leaching over 24 hours

The maximum copper extraction occurred at 22 hours with 6.9 g/L of copper being extracted. At 24 hours, the concentration of copper in solution had declined to correspond with 29% of copper extracted from the entire PCB. There was also a very slight decline in copper concentration after the peak at 22 hours, in a similar manner to the decline in gold extraction after 21 hours. The copper dissolution rate was 0.38 g/h in 6 hours compared to the gold powder dissolution rate of 0.34 mg/h. The peak in copper concentration at 22 hours can be attributed to copper being leached preferentially over gold thus resulting in a simultaneous decrease in gold extraction. This is made possible when ammonia is lost from solution thus limiting the regeneration of the cupric ions into the cuprous amine complex and resulting in the copper thiosulphate complex stabilising (Xia, 2000). This is conveyed in Figure 2.2 where the ratio of cuprous ammonia complexes to thiosulphate ions is 1:3. Moreover, ammonia is known to catalyse the reaction between gold and thiosulphate in the anodic area in Figure 2.2 and thus a decrease in ammonia would cause a decrease in gold extraction (Tao, Jin & Shi, 1993; Molleman & Dreisinger, 2002; Hung Ha et al., 2010).

Figure 4.4 investigated the effect of background copper (II) sulphate concentration on gold extraction in the gold powder dissolution experiment. Four different background copper concentrations with 56 mg of gold powder each were introduced into the system and the gold powder dissolution experiment was conducted over a 6 hour period. The data presented in the Cu concentration graphs (Figure 4.4 - Figure 4.6) were based on the mean of all three experiments conducted at each background Cu concentration. Error bars were removed from the background Cu concentration graphs for better clarity of the graph trends. Figure D.4 in Appendix D.4 depicts the gold extraction from gold powder dissolution with error bars.

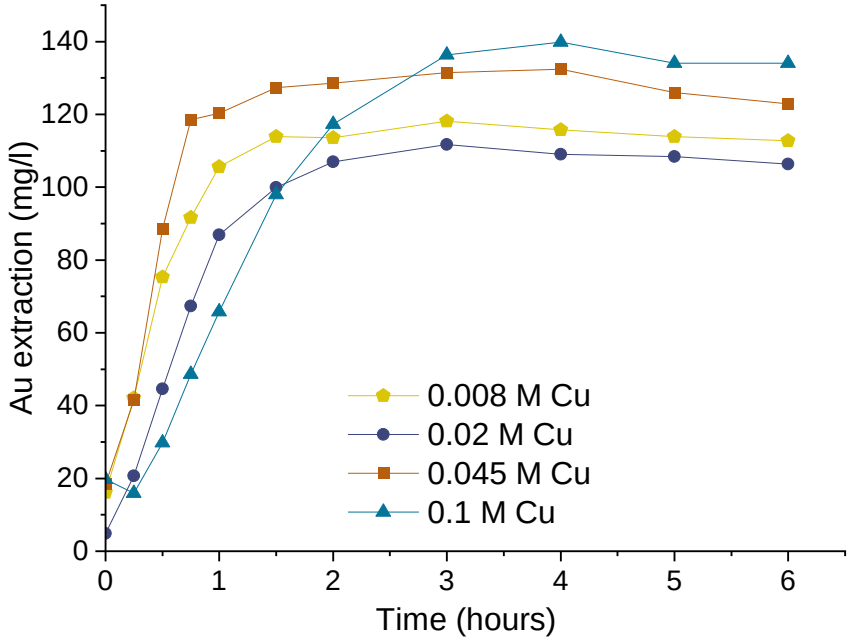


Figure 4.4: Gold extraction from gold powder dissolution at various background Cu concentrations (0.008 M, 0.02 M, 0.045 M and 0.1 M)

Table 4.1 summarises the gold extraction and the initial rate after 6 hours and 1 hour respectively for each background copper concentration. The results convey gold extraction in some experiments as greater than 100% which is associated with the residual error referred to in Section 3.5. The trend is depicted in Figure 4.4. The fastest initial dissolution rate was that of the 0.045 M Cu concentration whilst the slowest was 0.1 M Cu after 1 hour. The fastest

initial dissolution rate in the 0.045 M Cu experiment achieved the second highest amount of gold extracted after 6 hours compared to the other Cu experiments. This shows that a high concentration of background copper can further enhance the gold dissolution in the experiment within a set amount of time. Gold extractions across all experiments were in the range of 95% to 100%. Thus, the results substantiate the effectiveness of the ammonia-ammonium thiosulphate system in recovering gold in a fairly short period of time.

Table 4.1: Gold extraction (after 6 hours) and initial dissolution rate (after 1 hour) at various Cu concentrations (0.008 M, 0.02 M, 0.045 M and 0.1 M)

| Copper concentration (M) | Gold extraction (%) | Initial dissolution rate (mg/h) |
|---|---|---|
| 0.008 | 101 | 52.8 |
| 0.02 | 94.9 | 43.4 |
| 0.045 | 110 | 60.2 |
| 0.1 | 120 | 32.9 |

The gold extraction trend for gold powder dissolution followed a similar pattern for all copper concentrations; a sharp increase within the first 2 hours, with peak extractions reached at 3 hours, thereafter a slight decrease in gold extraction until 6 hours. The extractions in the presence of 0.045 M background Cu showed the fastest extraction reaching 119 mg/L in less than an hour correlating to a gold dissolution rate of 60.2 mg/h for the first hour. The slowest gold extraction over the 6 hours period was the experiment conducted in the presence of 0.1 M background Cu. This experiment reached its maximum extraction in 4 hours. Gold extractions were relatively low in solutions with low background Cu concentrations when comparing 0.1 M and 0.045 M. However, the same did not apply when inspecting the gold extractions in the presence of 0.008 M and 0.02 M background Cu. The gold extraction in the 0.008 M Cu experiment was consistently higher than the 0.02 M Cu experiment over the 6 hour period which was unexpected. This may be attributed to the higher gold extraction in the 0.008 M Cu experiment at the start of the experiment compared to the 0.02 M Cu experiment. Thus, allowing the gold extraction to proceed at a higher extraction rate owing to the initial high extraction at the start of the experiment.

At high concentrations of background Cu (0.1 M), gold extraction increased slowly after the first hour. This was in agreement with Abbruzzese et al. (1995) findings where similar Cu background concentrations were used at a higher ammonia concentration (1 M) at ambient temperature. Abbruzzese et al. (1995) found that at high Cu background concentrations of 0.1 M, the gold extraction increased slowly from 70% to 77% between 1 and 3 hours. At lower concentrations in Figure 4.4, such as 0.008 M and 0.02 M of background Cu, the gold extractions were much lower compared to the higher background Cu concentration experiments. This trend correlated with PCB experiments conducted in Tripathi et al. (2012) at similar background Cu concentrations of 0.016 M and 0.024 M. Tripathi et al. (2012) stated that at around 6 hours, gold extractions for 0.016 M and 0.024 M was much lower reaching only 10% whilst at higher background Cu concentrations of 0.04 M, gold extraction was faster reaching up to 35%. In addition, when comparing the gold extraction for the 0.1 M and the 0.045 M in Figure 4.4, additional time was required in the 0.1 M experiment to achieve the same concentration however the gold extraction from the 0.1 M experiment eventually

surpassed the gold extraction from the 0.045 M just before 3 hours. This indicated that although the initial dissolution rate was slower, the overall extraction was eventually higher.

Figure 4.5 below presents the same Cu background concentrations on PCB leaching experiments. In addition, 0 M background Cu concentration was introduced into the tests to determine the effect on the gold extraction rate with copper being extracted from the PCB only.

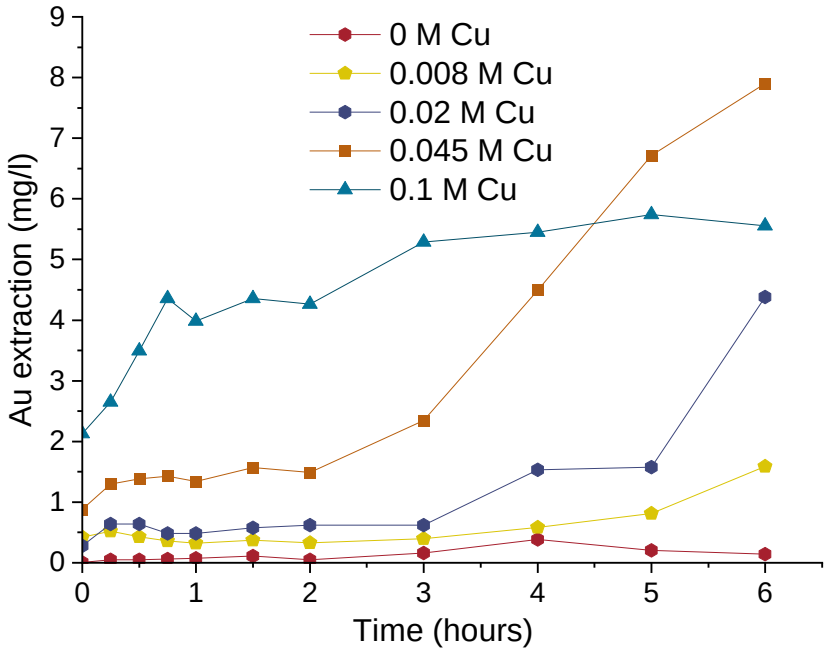


Figure 4.5: Gold extraction from PCB leaching at various background Cu concentrations (0 M, 0.008 M, 0.02 M, 0.045 M and 0.1 M)

The lowest extraction after 6 hours was displayed by the 0 M Cu graph line. It was clear that an initial amount of copper present in the solution was necessary to enhance the gold dissolution rate via the formation of the copper (II) amine complexes. The cathodic area, in Figure 2.2 Section 2.4.4.1, shows the formation of the cupric-ammonia complex along with the thiosulphate ion as a product. The thiosulphate ion was required in the anodic area to produce the aurothiosulphate ion. With the absence of background copper in solution, the reduction reaction has to be that of oxygen which has poor kinetics whereas in the presence of copper, the cupric/cuprous couple is a better redox mediator and hence the reaction will have a lag until sufficient copper has dissolved from the PCB to allow the cupric/cuprous couple to act as the redox mediator for the cathodic reaction. This was confirmed by the low gold extraction of 1.66% after 6 hours for the 0 M background Cu experiment (Table 4.2). Gold extraction was found to increase up to 90% with the addition of 0.045 M background Cu. The highest gold extraction was 7.9 mg/L at 6 hours in the presence of 0.045 M background Cu. This value was much higher than the 25% gold extraction at 0.04 M background Cu in the copper leaching experiments conducted by Tripathi et al. (2012) at 0.1 M ammonium thiosulphate after 6 hours. The authors, Tripathi et al. (2012), attributed the low extraction value of 25% to the slow agitation rate of 250 rpm used in the investigation in comparison to the 400 rpm speed used to produce the results in Figure 4.5. Background Cu concentrations at 0.045 M, 0.02 M and 0.008 M show that at 6 hours, the gold extraction was still increasing whilst background Cu concentrations at 0.1 M and 0 M reveal that gold extraction was slowly reaching stability. This

suggests that values outside the range of 0 M to 0.045 M background Cu would not be beneficial for high gold extractions.

A background copper concentration of 0.1 M was expected to have a higher gold extraction than 0.045 M similar to the results from the gold dissolution experiment and those reported in Abbruzzese et al. (1995) at ambient temperature and 4 M $NH_3$, however this was not demonstrated by the experiments. Therefore, it can be said that at very high background Cu concentrations, the gold extraction becomes independent of the copper concentration when incorporating PCBs. These results were consistent with those reported by Hung Ha et al. (2010) who found that after 2 hours at concentrations higher than 0.015 M background Cu, the leaching of gold remained around 30% gold extraction. There was a significant difference in gold extraction between 0.02 M and 0.045 M Cu from the start of the experiment up to 2 hours. After 2 hours, gold extraction in the 0.045 M Cu experiment occurred at a much faster rate than the 0.02 M Cu experiment. This was similar to the results reported by Tripathi et al. (2012) where the gold extraction increased at a faster rate from 10% to 30% after 8 hours. Furthermore, lower gold extractions were expected for the 0.008 M Cu experiment due to limited amount of copper in the system in comparison to the 0.02 M Cu experiment. This assumption is validated by Figure 4.5. Low copper concentrations result in a slow reaction in forming the aurothiosulphate ion in the system (Tripathi et al., 2012). This is because copper sulphate in the system catalyses the reaction and enhances gold dissolution in the system therefore low copper concentrations would cause a slow reaction.

Recalling gold extraction results from both Figure 4.4 and Figure 4.5 conveys that there was possibly a threshold background Cu concentration required for the reaction to proceed. Concentrations below this threshold indicate that the kinetics were sluggish and thus minimal gold was extracted and beyond the threshold excessive thiosulphate degradation takes place. Tripathi et al. (2012) found that at background copper concentrations between 0.032 M and 0.048 M similar gold extractions of around 30% - 35% after 8 hours of leaching were measured. Therefore, showing no significant increase in gold extraction with an increase in background copper concentration between 0.032 M and 0.048 M. Hung Ha et al. (2010) stated that at 0.005 M, gold extraction was excessively slow attaining below 5% gold extraction with 0.2 M thiosulphate concentration. The study also stated that background Cu concentrations above 0.015 M showed no effect on gold extraction. This was attributed to the high cupric-ammonia complex concentration causing higher losses of thiosulphate through its degradation into tetrathionate. The threshold for the results shown in Figure 4.5 was found to be 0.045 M background Cu concentration at ambient temperature and 0.5 M ammonia and ammonium thiosulphate. Background Cu concentrations above 0.045 M resulted in lower gold extractions and below 0.045 M resulted in slower kinetics and reduced gold extraction.

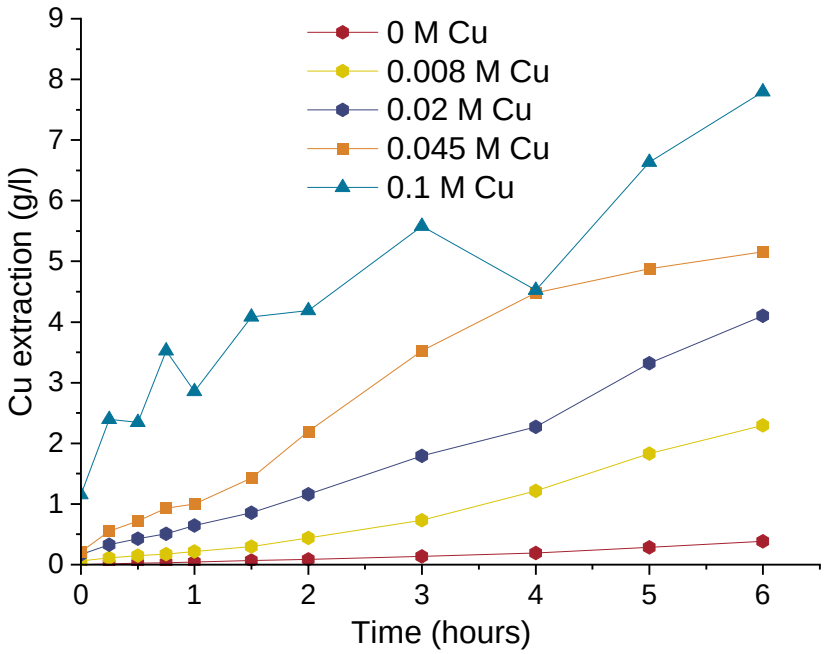


Figure 4.6: Copper extraction from PCB leaching at various Cu concentrations (0 M, 0.008 M, 0.02 M, 0.045 M and 0.1 M)

Figure 4.6 illustrates the copper extraction from copper found on the PCB after size reduction. Copper extraction was much higher than gold extraction reaching values of 8 g/L equating to 33% extraction. The highest extraction was from the 0.1 M Cu experiment. The lowest extraction (1.64%) was attained from the 0 M Cu experiment. The concentration from both these experiments (0.1 M and 0 M) after 6 hours were 7.8 g/L and 0.39 g/L respectively. All copper experiments showed a steady increase in copper extraction over 6 hours except for the 0.1 M Cu experiment. This experiment showed a sharper but erratic copper extraction over the 6 hours. The trend observed may be due to the large amount of background copper in the system competing with the gold for the thiosulphate ions in solution thus resulting in varying copper concentrations throughout the 6 hours. Another possibility causing the erratic extraction can be that since the background copper extraction was already high, determining the marginal additional copper extracted from leaching the PCB would be more susceptible to error. Gold extraction for this 0.1 M Cu experiment did not increase at such a fast rate and was slower than the other experiments after 2 hours therefore indicative that it was indeed competing with copper to form a thiosulphate complex. This competition occurred by copper being preferentially leached from the PCBs over the gold present on the surface hence the low gold extraction. Leaching copper instead of gold resulted in the formation of the copper-thiosulphate complex over the copper-amine complex. Furthermore, copper would leach in an ammonia solution without ammonium thiosulphate. All background cupric ions can dissolve the same amount of solid copper, therefore additional cupric ions are formed through the re-oxidisation of the cuprous ions present in solution provided by the air present in the reactor during the reaction. To an extent, this reaction is autocatalytic which could cause a faster reaction later in the leaching experiment. The formation of the aurothiosulphate complex is a side reaction that may be promoted or inhibited depending on the conditions.

The opposite trend was observed for the 0.045 M Cu experiment. In this instance, the copper extraction slowed down around 4 hours whilst gold extraction increased dramatically. This can

be explained by the electrocatalytic role of the Cu(II)/Cu(I) redox couple which is stable in the ammonia-ammonium thiosulphate system. The stable copper-amine complexes were being sufficiently regenerated by the cuprous-thiosulphate complex and oxygen thus allowing for the formation of the aurothiosulphate ion on the anode side as indicated by Equation 2.4 and Equation 2.7. Cupric ions are required to oxidise the gold however there is competition between gold and the copper for the formation of the cupric ions. In addition, this relates to the available surface area on the PCBs. As the gold is leached from the top layer of the PCB, copper underneath might be exposed which could dissolve preferentially.

Table 4.2 tabulates the gold and copper extractions for all PCB experiments where the background Cu solution concentration was varied. From Table 4.2, it was evident that the experiment with 0.045 M background Cu concentration resulted in the highest gold extraction and fairly low copper extraction from the PCBs. There was 11% more copper extracted from the PCBs when using a copper concentration of 0.1 M as opposed to 0.045 M. Gold extraction almost doubled between 0.02 M Cu and 0.045 M Cu whilst copper extraction increased by 4.5%. Therefore, a background Cu concentration of 0.045 M was ideal as this resulted in a small amount of copper being leached whilst giving the highest gold extractions.

Table 4.2: Gold and copper extractions (after 6 hours) from leaching PCBs with 5 different Cu concentrations

| Copper concentration (M) | Gold extraction (%) | Copper extraction (%) |
|---|---|---|
| 0 | 1.7 | 1.64 |
| 0.008 | 18.8 | 9.76 |
| 0.02 | 52.0 | 17.43 |
| 0.045 | 93.7 | 21.91 |
| 0.1 | 65.8 | 33.13 |

Recalling from Figure 4.4 and Figure 4.5, the effect of background copper on gold extraction was evident in that an increase in background copper concentration resulted in an increase in gold and copper extraction from the PCBs. However, above a certain background copper concentration (0.045 M), the effect of copper had no increasing effect on gold extraction. This indicates that copper was indeed essential to promote gold extraction in thiosulphate solutions but between a specific range for copper concentration (Abbruzzese et al., 1995). Jeffrey (2001) suggested that at very low copper concentrations (less than 0.005 M) the reaction rate is limited by the diffusion of $Cu^{2+}$ to the surface of the gold whilst at higher copper concentrations the reaction rate is chemically controlled. This effect on extraction rates was substantiated by the 0.1 M Cu experiment where the gold extraction was independent of Cu concentration after 3 hours. Furthermore, the high extractions achieved using 0.045 M as opposed to the 0.1 M Cu in the dissolution experiments can be attributed to the leached copper from the PCB. Thus, background concentrations at a threshold of 0.045 M Cu are needed for PCB leaching as additional copper from the board was provided via leaching due to the ammonium thiosulphate system dissolving both gold and copper.

In the 0.02 M background Cu experiment, it was evident that there was insufficient copper present at the start of the experiment to catalyse the reaction and produce a high gold recovery within the same 6 hours. The copper extraction of 17.4% was reasonably close to the copper extraction (21.2%) in the 0.045 M Cu experiment and almost 8% higher than the 9.8% extraction in the 0.008 M Cu experiment. This implies that though the additional copper

extracted from the board was similar to additional copper extracted in the 0.045 M Cu experiment, it was still insufficient in catalysing the reaction (due to the low background Cu concentration at the start) to produce a higher gold extraction than the 0.045 M Cu experiment.

The leaching results shown in Figure 4.7 and Figure 4.8 are from a PCB leach over 3 hours at two different $NH_3$ concentrations of 0.5 M and 1 M containing 0.02 M $CuSO_4$ and 0.5 M $(NH_4)_2S_2O_3$. Further experimental conditions are described in Chapter 3 Table 3.4. Figure 4.7 below conveys the gold extraction over a 3 hour period. The highest gold extraction after 3 hours was attained using a starting concentration of 1 M $NH_3$. This correlated to 3.08 mg/L as opposed to 0.8 mg/L from the 0.5 M $NH_3$ experiment. The high gold extraction at the start of the 1 M $NH_3$ experiment was thought to have been due to an error in sample analysis and can be disregarded as an outlier. From 15 minutes onwards, there was a steady increase in the gold extraction for the 1 M $NH_3$ experiment whilst the gold extraction remained stable below 1 mg/L for the 0.5 M $NH_3$ experiment.

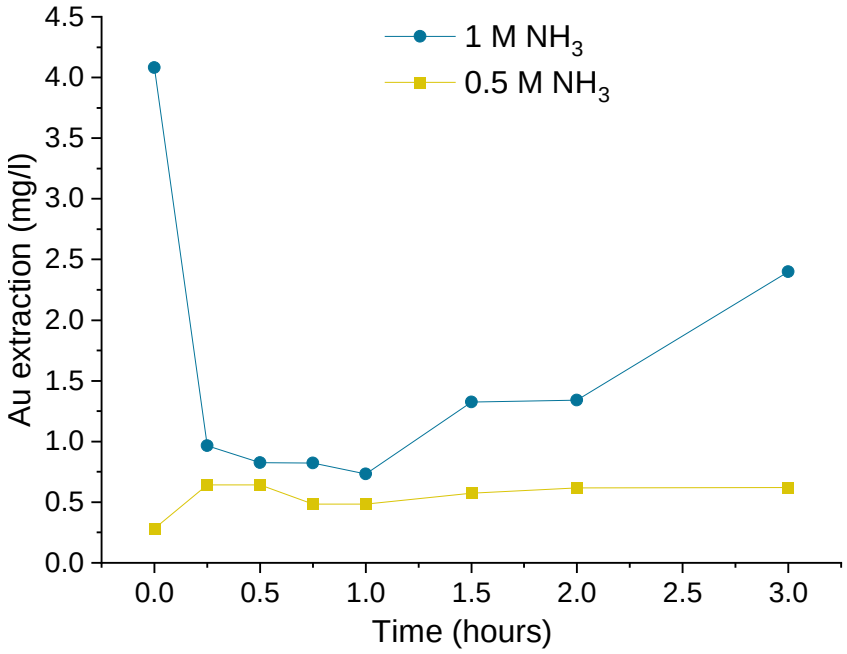


Figure 4.7: Gold extraction from PCB 3 hour leach at 0.5 M and 1 M $NH_3$

The ammonia to ammonium thiosulphate ratio in the 1 M and 0.5 M $NH_3$ experiments were 1:0.5 and 1:1 respectively. This was well within the 1-2 $NH_3$ : $(NH_4)_2S_2O_3$ ratio stated by Molleman & Dreisinger (2002). The ideal $NH_3$ concentration was important in these experiments as ammonia solubilises the copper as the copper-amine complexes. A large ratio might stabilise the copper as the copper (II) amine complex only and a small ratio might stabilise the copper as the copper (I) thiosulphate complex only thereby inhibiting the catalytic gold extraction in both instances (Molleman & Dreisinger, 2002). An ammonia concentration of 1 M which is closer to the higher end ratio of 2 resulted in a greater gold extraction. However, further increase in ammonia would defy the ratio range of 1-2 and result in lower gold extractions as seen by Breuer & Jeffrey (2000) where an increase in ammonia concentration from 0.2 M to 0.6 M resulted in a significantly lower leaching rate at a concentration of 0.1 M thiosulphate.

Figure 4.8 illustrates the copper extraction for the same 3 hour period. Similar to the gold extraction, there is a higher copper extraction in the 1 M $NH_3$ experiment as opposed to the 0.5 M $NH_3$ experiment. The copper extraction values, as well as the gold extractions, are stated in Table 4.3. In Figure 4.8, the trend for both experiments were similar however for the 0.5 M $NH_3$ experiment, the copper increase was a lot slower reaching only 1.79 g/L in 3 hours, whereas in the 1 M $NH_3$ experiment, between 1 and 3 hours, copper extraction increased significantly and was almost double its concentration at 3 hours (3.8 g/L).

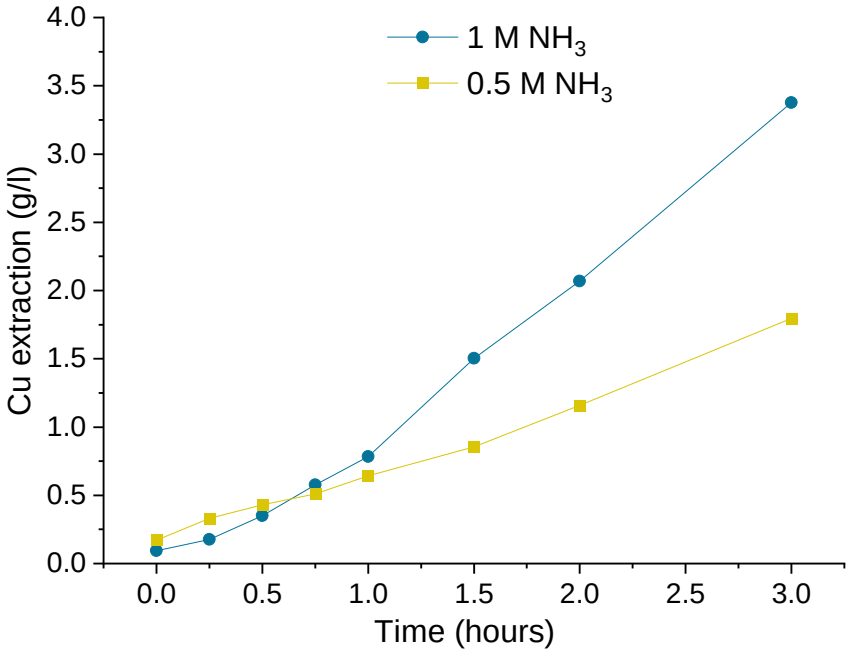


Figure 4.8: Copper extraction from PCB 3 hour leach at 0.5 M and 1 M $NH_3$

From both Figure 4.7 and Figure 4.8, gold extraction for the 0.5 M $NH_3$ experiment was stable remaining below 1 mg/L whilst the copper extraction showed a steady increase. The same trend was observed for the copper and gold extraction in the 0.1 M Cu experiment where copper was most likely being preferentially leached over the gold from the PCBs. It was also clear that an increase in ammonia concentration (0.5 M to 1 M) resulted in an increase in both gold and copper concentration (Table 4.3). This was expected as the ammonia to ammonium thiosulphate ratio was within the range of 1-2 (Molleman & Dreisinger, 2002). Furthermore, the leaching of copper by the cupric-ammonia complex is promoted by the higher ammonia concentration thus causing high copper extractions. However, a further increase in ammonia above 1 M would most likely have resulted in a decrease in leaching rate. A high ammonia concentration would result in equilibrium being favoured to the left (Equation 2.5 in Section 2.4.4.1) therefore reducing gold extraction. This trend was observed in both Abbruzzese et al. (1995) and Lampinen, Laari & Turunen (2015). In the case of Abbruzzese et al. (1995), an increase in ammonia concentration from 1 M to 4 M resulted in an increase in gold extraction (up to 78.8%) however further increase in ammonia resulted in lower gold extractions. Lampinen, Laari & Turunen (2015) observed that at low concentrations an increase in ammonia concentration from 0.1 to 0.2 M resulted in higher gold extractions. However, further increasing the ammonia concentration to 0.3 M did not result in an increase in gold dissolution rate or extraction.

Table 4.3: Gold and copper extractions after 3 hours from leaching PCBs with two different $NH_3$ concentrations

| $NH_3$ concentration | Gold extraction (%) | Copper extraction (%) |
|---|---|---|
| 0.5 M | 7.36 | 7.63 |
| 1 M | 28.4 | 14.3 |

It has been proposed by both Lee (2003) and Wan & LeVier (2003) that ammonia is necessary to prevent gold passivation by being preferentially adsorbed on the gold surface over thiosulfate therefore bringing gold into the solution as the gold-amine complexes (Equation 2.4). Most importantly, at high ammonia concentrations and subsequently high pH, solid copper species such as CuO and $Cu_2O$ are known to form due to the reduced stability of the copper-amine and copper-thiosulphate complexes (Abbruzzese et al., 1995). This affects gold dissolution by coating the PCB gold surface (Abbruzzese et al., 1995; Aylmore & Muir, 2001). On the other hand, for a pH greater than 9, gold leaching was dependent on ammonium thiosulphate concentration suggesting that the predominant species is $Au(S_2O_3)_2^{3-}$ instead of $Au(NH_3)_2{}^+$ (Hung Ha et al., 2010; Lampinen, Laari & Turunen, 2015).

## 4.2. SEM-EDS analysis

Additional ammonia-ammonium leaching was conducted on pre-treated PCBs at the conditions stated in Table A.1 for 24 hours and SEM-EDS (Scanning Electron Microscopy with Energy Dispersive Spectroscopy) analysis was conducted on a sample of the leached PCBs. This analysis was conducted on three solid materials following leaching to determine if there was any gold residual on the board. A small piece of the pre-treated PCB after leaching was retained for SEM-EDS analysis as well as the filter paper present in the 0.2 µm nylon syringe filter used to filter the sample solutions before depositing the solution into the sample bottle. A small piece of the filter paper, used to separate the liquid from the PCBs and any residual particles, by means of vacuum filtration, was also included in the SEM-EDS analysis. These three materials were analysed for the presence of gold in the Electron Microscope Unit at the University of Cape Town. The figures below (Figure 4.9 - Figure 4.11) depict the presence of gold, if any, that was found on all three materials. Additional images and detailed gold elemental compositions can be found in Appendix D.2.

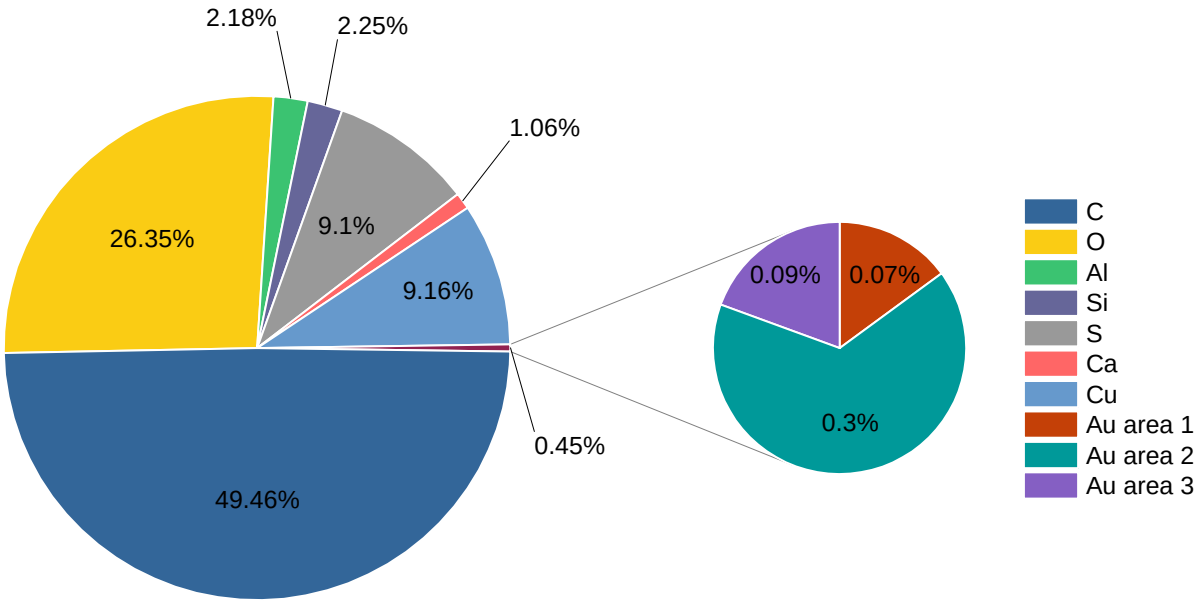


Figure 4.9: Pie chart indicating EDS composition analysis on the leached PCB piece

SEM-EDS analysis was conducted on one leached piece of PCB at three randomly selected different areas: Area 1, Area 2, Area 3. Investigation on six different spectra for Area 1 was conducted whilst Area 2 and 3 had only four sites of investigation. The pie chart above summarises the mean wt% of all three areas investigated. Table 4.4 lists the gold composition at each site or spectrum for the PCB pieces as well as the syringe filter. Area 2 reported the highest percentage of gold at 0.29% whilst Area 3 and 1 reported a value of 0.09% and 0.07% respectively. It is also clear, from Figure 4.9, that the PCB composition was largely from the carbon present on the PCB surface at 49.5%. Copper and sulphur were also common, making up about 9.16% and 9.10% each respectively. The leaching done in an ammonia-ammonium thiosulphate system was not expected to remove significant amounts of the copper found on the board, particularly because no effort had been made to liberate it. Furthermore, the copper content found in the top layer by Chirume (2019) using QEMSCAN was 11% which is fairly close to the value of 9.16% obtained from SEM-EDS and the difference between the two values could be because some of the copper present on the board had been leached and dissolved into solution in the ammonium-thiosulphate leaching process. This is possible if the solder mask layer dissolves during thiosulphate leaching. Sulphur was detected via SEM-EDS analysis and this is possibly due to the presence of polythionates such as sulphides forming within the system onto the PCB due to the decomposition of thiosulphate during leaching.

Figure 4.10 below shows the images of Area 2 and 3 on the PCB piece. Multiple sites were investigated within each area. Area 2 and 3 had a total of four sites each that were investigated. Gold was found on three out of the four sites in Area 2 and in only one out of the four sites in Area 3. Six sites were investigated in Area 1 of which only two reported the presence of elemental gold. Appendix D.2 contains images with the labels for each site investigated on all three areas.

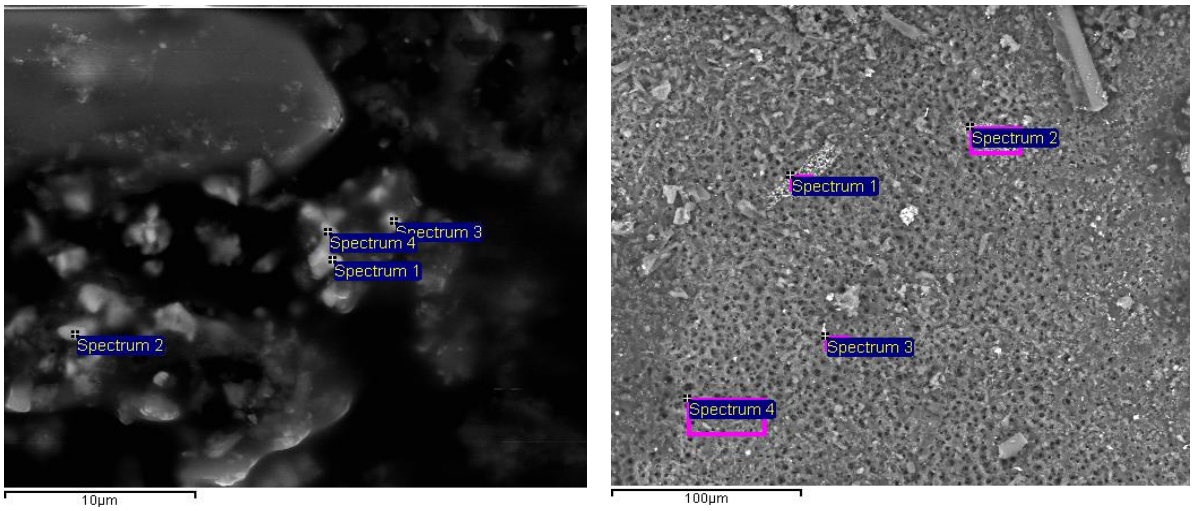


(a) (b)

Figure 4.10: (a) SEM-EDS of Area 2 on a PCB piece (b) SEM-EDS of Area 3 on a PCB piece

It was also found that the gold present at these sites was present on the surface where the gold-nickel alloy was plated as well as on the green ink mask part of the PCB. This was indicative that during leaching gold was dissolved into solution from the surface of the PCB but thereafter it precipitated or adsorbed onto the PCB.

Table 4.4: Gold elemental composition from leached PCB and syringe filter in wt%

| | PCB (wt%) | | | Syringe filter (wt%) | |
|---|---|---|---|---|---|
| | Area 1 | Area 2 | Area 3 | Area 1 | Area 2 |
| Spectrum 1 | 0.63 | 0.99 | 0.00 | 0.00 | 0.71 |
| Spectrum 2 | 0.56 | 1.41 | 1.03 | 1.43 | 1.13 |
| Spectrum 3 | 0.00 | 0.00 | 0.00 | 0.82 | 0.66 |
| Spectrum 4 | 0.00 | 1.11 | 0.00 | 0.00 | - |
| Spectrum 5 | 0.00 | - | - | - | - |
| Spectrum 6 | 0.00 | - | - | - | - |
| Average | 0.2 | 0.88 | 0.26 | 0.56 | 0.83 |

SEM-EDS analysis from the syringe filter and filter paper are shown in Figure 4.11. Figure 4.11 (a) depicts the imaging from one out of the two areas investigated on the syringe filter. Both areas of the filter paper revealed the presence of gold with 0.56% and 0.83% for Area 1 and 2 respectively. Area 2 had a greater amount of gold than Area 1. Figure 4.11 (b) depicts the imaging obtained from investigating the filter paper used in vacuum filtration. Multiple points were investigated, however there was no presence of gold on any of the sites. This suggests that the filtration allowed the remaining gold particles to pass through and remain in the leached solution whilst larger particles from the PCBs were separated out.

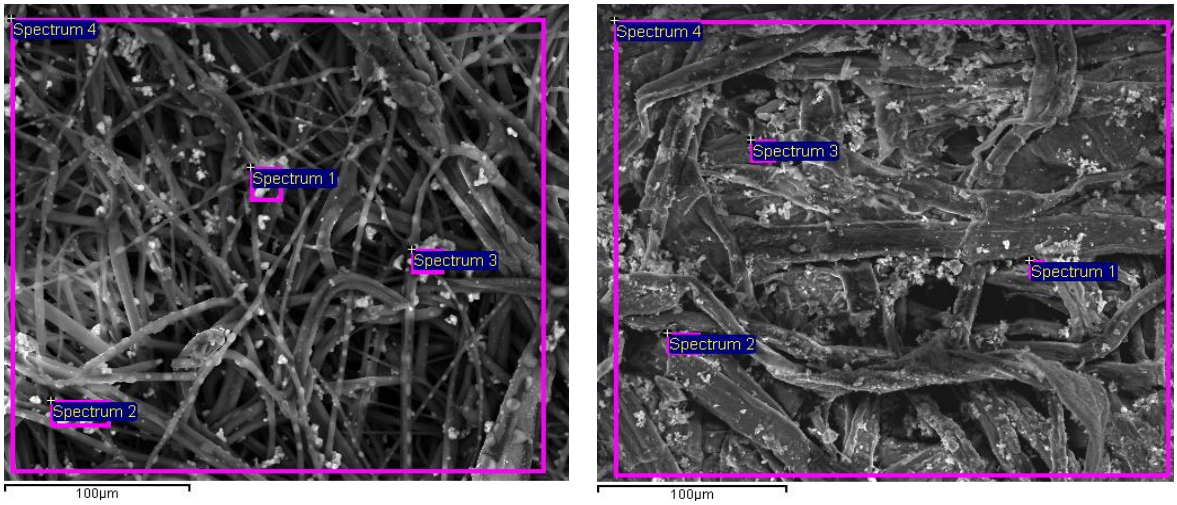


Figure 4.11: (a) SEM-EDS imaging from syringe filter of Area 1 (b) SEM-EDS imaging from filter paper used in vacuum filtration of Area 1

The imaging results from the syringe filter experiment reveal that small gold particles were present on the syringe filter when filtering the solution sample and that the particles were greater in size than the 0.2 µm syringe filter hence the presence of gold particles larger than 0.2 µm on the filter paper. It was clear that some particles had not yet completely dissolved into solution and thus the experimental conditions can be altered to ensure complete leaching of gold into solution.

## 4.3. Ion exchange experimentation

Ion exchange experimentation was conducted on three resins: AuRIX®100 resin and two Purogold™ resins, MTA5013SO4 and MTA5011SO4. Unless otherwise stated, all experiments were repeated three times. The results from all three investigations on the resin are presented and discussed in Section 4.3.1 to 4.3.3.

### 4.3.1. AuRIX®100 resin

Capacity, loading and elution tests were conducted on the AuRIX®100 resin. The resin was investigated due to its applicability in alkaline solutions given its use in the aurocyanide system to remove gold. The results are shown below.

#### 4.3.1.1. Capacity test results

Two different methods were used to investigate the capacity of the AuRIX®100 resin. In the first method, three tests were conducted to determine the operating resin capacity whilst in the second method, two tests were conducted. The details of the experiment can be found in Chapter 3 Section 3.3.3.2. In the first method, the test ran in an open circuit with the 0.1 M NaCl solution undergoing only a single pass through the resin. NaOH at 1 M concentration was then passed through the ZLC to dislodge the loaded $Cl^-$ ions. The $Cl^-$ ions in the NaOH effluent were monitored. In the second method, no NaOH was used and 0.1 M NaCl solution was passed through the ZLC in a closed circuit with $Cl^-$ ions being monitored at the end in the effluent solution. In both tests, the FWSV was 5.2 mL.

Table 4.5 shows the chloride ion concentration in equivalents per litre resin. Method 1 values were chloride ion concentrations that were eluted using 1 M NaOH solution. Method 2 values

were chlorides ion concentrations loaded onto the resin after passing through NaCl solution in a closed circuit. The Method 2 values were the difference in chloride ion concentration in solution at the start and end of the experiments.

Table 4.5: Comparison of two methods for capacity testing on the AuRIX®100 resin in terms of chloride ion concentration (eq/L)

| | Method 1<br>Chloride ions (eq/L) | Method 2<br>Chloride ions (eq/L) |
|---|---|---|
| Test 1 | 0.070 | 0.861 |
| Test 2 | 0.125 | 0.439 |
| Test 3 | 0.125 | - |
| Average | 0.107 | 0.650 |
| Standard Deviation | 0.031 | 0.299 |

Method 2 showed a much higher average resin capacity (0.65 eq/L) as compared to Method 1 (0.11 eq/L). This could be attributed to the open circuit used in Method 1 for an allocated time of 40 minutes. The contact time between the fresh solution in an open circuit and resin was limited to 40 minutes owing to the flowrate of 25 mL/min. The solution used was considered to be an infinite solution as the test was conducted in an open circuit. In addition, the first deionised water wash step after loading the resin with NaOH solution did not remove all traces of excess $OH^-$ ions as the pH was still slightly above 10 for all three tests (Appendix D.4). This would have resulted in the inhibition of maximum absorption of the $Cl^-$ ions, in the NaCl loading step. It was necessary to monitor the pH of the deionised water step as attaining a low pH provided an indication of whether all excess $OH^-$ ions had been removed from the ZLC (Nesbitt, 2016). If excess $OH^-$ ions were removed, the loading of NaCl solution onto the resin would not be inhibited.

Method 2 was conducted in a closed circuit at 25 mL/min for the same amount of time and in this instance a set solution volume was allowed to circulate between the solution and resin in the ZLC. The general resin capacity provided by the MSDS of the AuRIX®100 resin was 0.3 eq/L (Appendix C.1). The results from the two tests carried out using this method showed the resin to exceed the 0.3 eq/L capacity indicated by the manufacturer. This could be attributed to the NaCl solution being conducted in a closed circuit as the solution was allowed to circulate over the 40 minutes thus allowing the maximum possible $Cl^-/OH^-$ ion exchange on the resin. Based on the results from tests conducted using Method 2, the resin capacity of the AuRIX®100 resin was taken to be 0.65 eq/L for all further experiments.

Zhang & Dreisinger (2002) suggested that the low capacity values in weak-base and medium-base resins is due to their weak-base nature in requiring the resin to be protonated first. This translates to the functional amine groups on the resin and their interaction in strong alkaline solutions. It was proposed that the amine groups tend to stay in the free-base form in strong alkaline solution and therefore lose their ion-exchange ability. This is substantiated by the low capacities in Table 4.5 and the high pH of the deionised water step.

#### 4.3.1.2. Loading and elution results

Loading and elution tests were conducted on the AuRIX®100 to investigate the efficiency of the resin in extracting the aurothiosulphate ion in the ammonia-ammonium thiosulphate

system. Loading occurred of 0.5 L of aurothiosulphate solutions made by dissolving 56 mg of gold powder in 0.5 M ammonia-ammonium thiosulphate solutions (Section 3.3.2.2 contains the detailed method). Gold and background copper concentration was approximately 112 ppm and 0.02 M. The FWSV of the resin was 5.2 mL. Table 4.6 summarises the gold and copper loading of the resin. Loading values were based on the decrease in either gold or copper ions in solutions. The loaded resin capacity values were the percentage of resin active sites occupied by the aurothiosulphate and copper-thiosulphate ion respectively. The total resin capacity was the percentage of resin occupied by the gold and copper ions together.

Table 4.6: Gold and copper loading values from AuRIX®100 testing

| | Au loaded (eq/L) | Au-loaded resin capacity (%) | Cu loaded (eq/L) | Cu-loaded resin capacity (%) | Total resin capacity used (%) |
|---|---|---|---|---|---|
| Test 1 | 0.00879 | 1.35 | 0.132 | 20.3 | 21.65 |
| Test 2 | 0.00890 | 1.37 | 0.286 | 44.0 | 45.41 |

The concentration of gold loaded onto the resin was 0.0088 and 0.0089 eq/L for test 1 and test 2. This correlated to 6 mg/L and 6.08 mg/L loaded onto the resin. Loading values of 2 mg/L and 1.64 mg/L were found in an aurocyanide ion exchange system with 25 mL of AuRIX®100 resin (Gray, Hughes & Abols, 2005). This shows that the resin can recover much higher gold concentrations from the aurothiosulphate solution despite being suited for the aurocyanide system only. Test 2 loaded a higher concentration of the aurothiosulphate ion onto the resin than Test 1 despite Test 1 using fresh resin and Test 2 using the resin eluted after conducting Test 1. While Test 1 and Test 2 give similar results for Au, more than double the Cu was loaded in Test 2. In both tests, the copper loading was much higher than the gold loading given a loading time of 20 minutes across all AuRIX®100 sets of experiments. Results from Gray, Hughes & Abols (2005) reported that in the cyanide system over an extended period of time (greater than 30 minutes) copper was adsorbed and eventually displaced by hydroxyl ions in solution whilst similar effects were not observed on resin loaded with gold. This indicates that the resin has a higher affinity for gold than copper as gold remained attached to the resin whilst copper was displaced. Provided that the resin would behave in a similar manner in a thiosulphate system it can be assumed that had the loading time been increased, the Cu ions could possibly be displaced by hydroxyl ions which would result in the aurothiosulphate ion competing with the hydroxyl ion for the active sites.

Both copper and gold were present as thiosulphate complexes with a negative charge and therefore both complexes could attach onto the resin. The AuRIX®100 resin was manufactured for the alkaline aurocyanide system and was therefore suitable for application between a pH of 8 and 11.5 despite it being a medium-base anion resin which would typically not be suited within this range (Gray, Hughes & Abols, 2005). Given that this resin was a weak- to medium-base anion exchange resin, high gold loading values (above 98%) were not expected as the aurothiosulphate ion is much larger than the aurocyanide ion and the guanidine group on the resin is suited to extract the small aurocyanide ion (Gray, Hughes & Abols, 2005).

In both instances for Test 1 and Test 2 only about 22% and 45% of the resin was loaded with gold and copper assuming the capacity values established in Section 4.3.1.1. The low loading efficiency could be attributed to the hydroxyl ions that were loaded in the initial step and were

then not displaced when loading the resin with the gold saturated solution. Furthermore, the polythionates in solution can limit gold ion attachment by competing for resin active sites. In addition, due to the complex chemistry of the thiosulphate system (both hydroxyl and aurothiosulphate ions form in the overall reaction), there was a possibility of additional hydroxyl ions added into the ZLC from the gold saturated solution in accordance with Equation 2.7 and Equation 2.8.

Table 4.7 compares the elution concentration values (equivalents per litre resin) for gold and copper. NaOH at 0.5 M was used as an eluant and the results reveal that the eluant was effective in removing gold. This is similar to the results from Gray, Hughes & Abols (2005) where a combination of sodium hydroxide, sodium benzoate and sodium cyanide was used for elution. The results from this study showed that 99.6% and 75.7% of gold loaded onto the resin were eluted for Test 1 and Test 2 respectively. Copper was not eluted as easily as the gold with only 43.1% and 18.5% of loaded copper for Test 1 and 2 respectively being removed. In Test 1, only 22% of the resin capacity was occupied whilst Test 2 showed 46% occupancy. This relatively higher resin occupancy (46%) measured in Test 2 is mainly attributed to the concentration of copper loaded onto the resin. Thus, indicating that the resin can indeed use all its active sites if sufficiently eluted.

Table 4.7: Gold and copper elution values from AuRIX®100 testing

| | Au eluted (eq/L) | Au eluted from resin (%) | Cu eluted (eq/L) | Cu eluted from resin (%) |
|---|---|---|---|---|
| Test 1 | 0.0087 | 99.6 | 0.057 | 43.1 |
| Test 2 | 0.0067 | 75.7 | 0.053 | 18.5 |

NaOH proved to be an effective eluant for the gold ions however there was a significant amount of copper that remained on the resin after elution. This again may be due to the short elution time of 20 minutes and there is a possibility that copper elution could have improved if given more time due to the displacement of hydroxyl ions as indicated by Gray, Hughes & Abols (2005).

Table 4.8 shows the recoveries for both steps and the overall ion exchange process from loading to elution. The overall ion exchange efficiency was calculated based on the concentration of gold or copper in the eluant relative to the concentration of gold or copper in the standard solution at the start of the loading step.

Table 4.8: Average gold and copper recoveries from loaded solution

| | Recovery after loading (%) | Recovery after elution (%) | Overall Ion exchange efficiency (%) |
|---|---|---|---|
| Gold | 3.46 | 87.7 | 1.09 |
| Copper | 5.05 | 30.8 | 0.67 |

Overall, the AuRIX®100 resin does indeed load Au and Cu onto the resin. However, given that only 6 ppm Au was removed from the gold solution, this makes for an adsorption efficiency of 3.5% which is very low (Table 4.8). In addition, copper was adsorbed preferentially over gold however this was marginally higher at 69 ppm loaded onto the resin from a solution containing 1352 ppm copper. A loading recovery of 3.5 % was calculated for gold in the loading step as

compared to 5.1% for copper loading. Despite the low recoveries, there is the possibility of a higher loading rate given a FWSV greater than the 5.2 mL used in the experiment. Overall ion exchange efficiencies were also extremely low for both gold (1.09%) and copper (0.67%).

Given the low gold mass present on a PCB (4.22 mg), the AuRIX®100 resin can indeed recover over 50% of the gold present in a leached PCB solution as indicated by the loading gold values of around 3 mg (0.009 eq/L). The resin (5.2 mL) was able to recover 72% of gold present on a single PCB which is not far from the value of 98% gold recovery in a 13.4 ppm gold-cyanide solution with 93 mL of resin stated by Virgen et al. (2004). However, the recovery of 6 ppm relative to the 175 ppm gold solution is extremely low. This can possibly be attributed to the small resin volume (5.2 mL) utilised. On an industrial scale, the gold concentration would be much higher than that of a single PCB and thus the recovery of 6 ppm is what this study considers as low. In addition, the traditional approach of carbon adsorption has shown to reach recoveries of 95% with a traditional gold-bearing leach liquor thus indicating that the ion exchange approach would most likely not be able to compete due to its low recoveries (Grosse et al., 2003). The low percentage of active sites (1.35%) being occupied by the aurothiosulphate ion is concerning. Furthermore, Cu was shown to be preferentially loaded onto the resin (at the expense of Au ions). Thus, it is concluded that the AuRIX®100 resin was not suited for the thiosulphate. Hence, a medium-base anion resin was ill-fitted and a strong-base anion resin was required to achieve higher gold loading concentrations. NaOH was a suitable eluant in removing loaded gold however it was not as effective in removing copper from the resin.

### 4.3.2. Purogold™ MTA5013 Resin

Capacity, loading and elution in addition to kinetic and equilibrium tests were conducted on the strong-base anion exchange MTA5013 resin from Purogold™. The results from these investigations are presented below.

#### 4.3.2.1. Capacity test results

Capacity tests were conducted in an open circuit to determine the operating capacity of the MTA5013 resin. These tests were conducted using a titration with HCl and methyl red as an indicator. NaCl solution was used to displace the hydroxyl ions attached onto resin and the effluent solution was then titrated with HCl to determine the concentration. A total of three tests were conducted to determine the capacity in terms of $Cl^-$ ions. The capacity for each test was calculated using Equation 3.1. The FWSV of the resin was 5.2 mL.

Table 4.9: Capacity results on MTA5013SO4 resin

| Test | Chloride ions (eq/L) |
|---|---|
| Test 1 | 0.769 |
| Test 2 | 0.769 |
| Test 3 | 0.769 |
| Average | 0.769 |
| Standard Deviation | $3.98 \times 10^{-15}$ |

The general capacity provided by in the MSDS of the MTA5013 resin was 1.15 eq/L in chloride ion form (Appendix C.2). Strong-base anion exchange resins with a quarternary ammonium group are known to be between 1 eq/L and 1.4 eq/L at volume capacity (Zhang & Dreisinger,

2002; De Dardel & Arden, 2012). The operating capacity calculated from the results presented in Table 4.9 is much lower at 0.77 eq/L. This value was consistent across all three tests and its low value could be due to several factors. The significant deviation of the calculated resin capacity relative to that specified by the manufacturer (1.15 eq/L) could be due to the difference in methods used to measure the resin capacity. The manufacturing company, Purolite® conducts a two staged test whereby the weight capacity is determined via titration with silver nitrate and potassium dichromate as an indicator and the volume capacity using the weight capacity (Purolite, 1987, 1995).

In this study, a method presented by Nesbitt (2016) which uses NaOH and NaCl to determine the resin capacity in eq/L was used. This approach was used in place of the manufacturer's approach due to time constraints in addition to being a simpler approach and easily available chemical reagents for titration. Thus, the difference in methodologies could be a possible reason as to the low capacity of 0.77 eq/L being attained. In addition, the HCl concentration used in the titration experiments was 1 M. A concentration of 1 M was used as it followed the approach stipulated by Nesbitt (2016). This resulted in much smaller volumes of HCl required to neutralise the slightly basic solution as opposed to using a lower concentration such as 0.1 M or 0.025 M in the experimentation. However, given that the capacity test method provided by Nesbitt (2016) is a well-established method, the value of 0.77 eq/L is what this study considers acceptable. Furthermore, the measured or actual capacity of the resin in practice is often fairly lower or higher than the general capacity. This is attributed to the property of strong-base anion resins in that these resins are never 100% regenerated at the beginning of a cycle (De Dardel & Arden, 2012).

Furthermore, the actual capacity of the AuRIX®100 was 0.65 eq/L in comparison to the 0.77 eq/L obtained for the MTA5013 resin. Generally weak- to medium-base anion resins are often around 0.8 eq/L for general resin capacity and in the case of the AuRIX®100 resin specifically, the general capacity was 0.3 eq/L. According to Zhang & Dreisinger (2002), a higher resin capacity was expected for the strong-base anion resin and this was verified via the capacity tests which showed the actual capacity of the MTA5013 resin to be 0.77 eq/L.

#### 4.3.2.2. Loading and elution results

Loading and elution tests were conducted on the MTA5013 resin at various flowrates (10 mL/min, 25 mL/min and 50 mL/min) as well as using two eluants ($NH_3$ and $NH_4NO_3$). The results are shown in Table 4.10. One test each was conducted for flowrates 25mL/min and 50 mL/min. Three tests were conducted at the 10 mL/min flowrate and in this case, the average of the three tests was reported. The ion exchange loading results at the three different flowrates tested are shown in Table 4.10.

Table 4.10: Ion exchange loading results on MTA5013SO4 resin at 3 different flowrates: 10 mL/min, 25 mL/min and 50 mL/min

| Flowrate | Au loaded (meq/L) | Au-loaded resin capacity (%) | Cu loaded (meq/L) | Cu-loaded resin capacity (%) | Total resin capacity (%) |
|---|---|---|---|---|---|
| 10 mL/min | 8.06 | 1.05 | 150 | 19.54 | 20.58 |
| 25 mL/min | 7.73 | 1.01 | 56.9 | 7.40 | 8.40 |
| 50 mL/min | 6.97 | 0.906 | 69.6 | 1.34 | 2.24 |

The highest loading of gold onto the resin was at the flowrate of 10 mL/min. This correlated to 1.1% of the resin capacity being occupied by the aurothiosulphate ion. Whilst 20% was occupied by the copper-thiosulphate ion. The lowest loading was at the flowrate 50 mL/min with only 6.97 meq/L and 1.34 meq/L of gold and copper respectively being loaded onto the resin. Thus, it can be said that lower flowrates aided in higher gold loading ability onto the resin. However, only about 2.2% – 20.6% of the resin was loaded with both gold and copper over all three flowrates. This correlated to between 79.4% and 97.8% of the resin active sites being loaded with other ions besides gold and copper.

In this study there were very few other anionic species that could compete for the resin active sites. Similar to what was investigated with the AuRIX®100 resin, the remaining active sites could have been occupied by hydroxyl ions from the deionised water step prior to loading or by polythionates present in the solution. This was substantiated by the high pH (around 10.4) of the deionised water at the end of the wash water step. On the other hand, weak- or medium-base resins such as AuRIX®100 are required to be protonated before loading the targeted ion while strong-base resins such as MTA5013/5011 can easily adsorb the targeted ion without having to be protonated first (De Dardel & Arden, 2012). Therefore, it was possible that had the experiments been conducted with a larger amount (above 1 L) of deionised water to lower the pH and remove the excess hydroxyl ions, it could have resulted in a greater loading ability of the aurothiosulphate ion. Therefore, the poor metal loading on the resin for both gold and copper could imply that the resin required even lower solution flowrates so as to increase the contact time or that the resin volume was in effective for the purposes of removing gold and/or copper from solution.

In addition, polythionates present in a leach solution are generally at high concentrations and are poisonous to some resins (Zhang & Dreisinger, 2002). It was found by Zhang & Dreisinger (2002) that gold loading ability can drop by nearly 90% in the presence of tetrathionate due to the active sites being occupied by this species. This suggests that tetrathionate preferentially adsorbs onto the resin and competes with the gold thiosulphate complex for active ion exchange sites. The order of affinity proposed by Nicol & O'Malley (2001) states: gold thiosulphate > sulphite > tetrathionate, trithionate, thiosulphate > sulphate. Furthermore, Nicol & O'Malley's (2002) study did not mention the effect of concentration to the proposed order. While this order predicts gold being preferentially adsorbed, when using solutions similar to what was used in Table 4.10 experiments which contained low gold concentrations relative to polythionate concentrations, it could be that a high concentration of polythionates can impact the loading of gold by being preferentially adsorbed. Thus, resulting in a low gold loading ability and a reduced number of active sites being occupied by the aurothiosulphate ion.

Table 4.11: Ion exchange recovery values for gold and copper after loading step

| Flowrate | Au standard solution concentration (ppm) | Au recovery after loading (%) | Cu standard solution concentration (ppm) | Cu recovery after loading (%) |
|---|---|---|---|---|
| 10 mL/min | 143 | 3.84 | 1315 | 3.78 |
| 25 mL/min | 119 | 4.43 | 1330 | 1.41 |
| 50 mL/min | 119 | 4.02 | 1269 | 1.81 |
| Average | 127 | 4.09 | 1305 | 2.33 |

Table 4.11 provides the gold and copper recovery over the loading step of the resin. Prior to the ion exchange loading step, 127 ppm and 1305 ppm of gold and copper respectively were present in the solution. Only about 4.1% of total gold was recovered from the solution and in the case of copper 2.3% was recovered across all flowrates in the loading step relative to the FWSV of 5.2 mL and a solution volume of 0.5 L. Due to the low solid to liquid ratio (1:100) of resin volume to loading solution, minute changes in solution concentrations do not allow for accurate determination of the isotherms. Though the ion exchange method utilising the ZLC with a small volume of resin is an established method by Nesbitt (2016), revised experimentation with much higher resin volumes are required to determine better recoveries. This was not investigated due to time constraints of the study.

In the absence of competing anions, gold loading ability has been known to be between 60 – 90 g/L of resin which translates to 0.31 and 0.46 g of gold loaded onto 5.2 mL of resin (Nicol & O'Malley, 2002). In the ion exchange loading experiment, 2.75 mg, 2.6 mg and 2.38 mg of gold was loaded onto 5.2 mL of resin for each flowrate (10 mL/min, 25 mL/min and 50 mL/min). This was much smaller than the range of 0.31 - 0.46 g of gold that strong-base anion resins generally load. Results from Nicol & O'Malley (2001) suggest that given a solution containing 30 ppm Cu and 20 ppm Au, after 20 minutes 4 g/L of gold was loaded on the resin using a strong-base resin Amberjet 4200. Compared to the results obtained from loading experiments, this was much greater. Nicol & O'Malley (2001) also suggested that after 6 hours of loading, polythionates replaced the previous loaded gold. Thus, it could be possible that these loading solutions contained a high polythionate concentration and therefore gold was unable to be adsorbed from the start of the experiment due to the competition between the gold-thiosulphate complex and the high polythionate concentration.

In addition, Nicol & O'Malley's (2001) solutions had a much larger ratio of gold to copper concentration (0.67:1) than the ratio in present loading experiments (0.088:1). From Table 4.11, gold was preferentially adsorbed over copper. The higher loading recovery rates of the gold imply that the resin has a higher affinity for gold over copper similar to what was suggested by Dong et al. (2017). Dong et al. (2017) stated that the affinity of common gold extraction resins for the aurothiosulphate ion is much greater than that for the copper thiosulphate complex. The mass of gold loaded onto the resin was significantly smaller than the copper loaded (24.8 mg, 9.4 mg and 11.5 mg) for the 10/25/50 mL/min flowrates respectively. The concentration of the copper thiosulphate anion is generally much higher than the aurothiosulphate ion in solution resulting in lower gold loading values than copper loading but higher gold loading recoveries (Dong et al., 2017).

PCB leach solutions contained up to 4.22 mg of leached gold in solution from previous leaching experiments (Section 3.1.2.2). Ion exchange results from gold loading experiments on the MTA5013 resin showed that all three flowrates (10/25/50 mL/min) had the ability to recover more than 50% of the gold present in a PCB leached solution (4.22 mg) in the loading step as indicted in Table 4.11 despite only occupying 1% of the resin active sites with the aurothiosulphate ion. However, on an industrial scale the gold leached solution would generally contain gold concentrations much higher than a single PCB thus indicating that the resin is ineffective in removing large amounts of gold given a high gold concentration solution in the loading step and the same resin volume. Furthermore, lower flowrates and higher resin volumes are indeed necessary to recover more gold in the loading step however flowrates below 10 mL/min can be seen as impractical on an industrial scale and high resin volumes can be expensive.

Table 4.12 below shows the results obtained from the elution step using ammonium nitrate. The results from the 10 mL/min flowrate were obtained from an average of three tests while those from the 25 mL/min and 50 mL/min were obtained from 1 test each. Appendix D.4 contains the individual results for the 10 mL/min flowrate experiment.

Table 4.12: Ion exchange elution results on MTA5013SO4 resin at 3 different flowrates: 10 mL/min, 25 mL/min and 50 mL/min

| Flowrate | Au eluted (meq/L) | Au eluted from resin (%) | Cu eluted (meq/L) | Cu eluted from resin (%) |
|---|---|---|---|---|
| 10 mL/min | 4.96 | 65.6 | 22.4 | 24.4 |
| 25 mL/min | 5.80 | 75.0 | 38.4 | 67.5 |
| 50 mL/min | 5.11 | 73.3 | 20.3 | 29.1 |

Utilising a flowrate of 25 mL/min resulted in the highest amount of gold eluted from the resin (5.8 meq/L) with the 10 mL/min correlating to the least eluted gold of 4.96 meq/L. This was unexpected as the loading results showed that a lower flowrate resulted in higher gold loading values and thus it was expected that the same would apply for elution. In the case of copper elution, the greatest copper concentration eluted was in the 25 mL/min flowrate experiment whilst the lowest copper eluted was in the 50 mL/min experiment. The ammonium nitrate eluant removed most of the gold (up to 75%) attached onto the resin whilst in the case of copper it varied between 24% – 68%. Therefore, it was clear that the ammonium nitrate solution was effective in eluting gold from the MTA5013 resin. This was in agreement with gold results reported by Nicol & O'Malley (2001) who used an Amberjet 4200 strong-base anion resin and a solution containing 85 ppm of gold. In 20 minutes, 80% of gold had been extracted and 100% of gold extracted after 3 hours for 6 mL of resin (O'Malley, 2002).

One of the clear observations between the elution and loading step was that in the same amount of time higher gold recoveries are seen in elution than in loading thus indicating that the elution step was more efficient than the loading step. Zhang & Dreisinger (2002) suggests that another way to increase the elution in a short time period was to elevate the temperature at which elution occurs. However, this requires more energy which may not be beneficial in comparison to the ambient temperature experiments conducted.

Table 4.13 lists the total gold and copper recovered in the elution step for the overall process. It is thus clear that the method of eluting with ammonium nitrate is preferential for gold recovery. Copper recovery efficiency was much lower at 0.68% whilst gold was around 2.9%. Despite the low overall gold recoveries, the MTA5013 has been shown to have the ability to remove the aurothiosulphate ion from solution. However, this ion exchange method still needs to be refined to produce higher gold recoveries. There are several ways in which optimisation can occur such as reducing the flowrates as well as increasing the concentration of copper to 0.045 M. Previous experiments have shown that gold dissolution at lower background Cu concentration aids in gold recovery (Tripathi et al., 2012). This can be beneficial in downstream ion exchange processes as the reduced amount of Cu present will thus reduce the loading of the copper ions on to the resin. Thereby allowing less competition between the aurothiosulphate ions and the copper complexes in solution (Section 0). In the instance of PCB leaching, it is not necessarily easy to control the Cu concentration as copper is leached simultaneously with gold. Thus, the background copper concentration in the leaching experiment needs to be sufficiently high to introduce fast kinetics in the leaching system whilst not inhibiting gold recovery in the ion exchange downstream processes and it is possible that the 0.045 background Cu concentration proposed in the leaching experiments in Section 0 can achieve this.

Table 4.13: Overall gold and copper recoveries from loaded synthetic gold solution

| Flowrate | Au standard solution concentration (ppm) | Overall Au efficiency (%) | Cu standard solution concentration (ppm) | Overall Cu efficiency (%) |
|---|---|---|---|---|
| 10 mL/min | 143 | 2.36 | 1315 | 0.564 |
| 25 mL/min | 119 | 3.32 | 1330 | 0.954 |
| 50 mL/min | 119 | 2.94 | 1269 | 0.527 |
| Average | 127 | 2.88 | 1305 | 0.681 |

Additional experiments were conducted at 25 mL/min flowrate for loading and elution however elution was conducted in two stages. Ammonia was used in the first elution step to remove copper and ammonium nitrate was used in the second step to elute gold. Each step was conducted three times and the results reported are averaged.

Table 4.14 compares the gold to the copper loading values at 25 mL/min on the MTA5013 resin. Similar to the results from varying flowrate (Table 4.13), gold loading recovery from the synthetic gold solution was measured to be 3.52% (Table 4.16). Copper loading recovery was slightly higher at 5.49% closer to the copper loading recovery obtained from the 10 mL/min flowrate experiment (3.78%). In total, 30% of the resin was occupied by both copper and gold complexes (Table 4.14). This value is relatively high when compared to 8.4% calculated for the 25 mL/min flowrate experiment in Table 4.10. This could be attributed to the large amount of copper that was loaded onto the resin as a result of the large number of copper species in the solution therefore competing with gold for the active sites present on the resin. In addition, 70% of the resin capacity could possibly be attributed to the attachment of polythionates on the resin which further impede the attachment of gold onto the active sites by poisoning the

resin. This result is analogous to what was measured in the 10/25/50 mL/min flowrate experiments.

Table 4.14: Ion exchange loading results from MTA5013SO4 resin at 25 mL/min

| Flowrate | Au loaded (meq/L) | Au loaded resin capacity (%) | Cu loaded (meq/L) | Cu loaded resin capacity (%) | Total resin capacity (%) |
|---|---|---|---|---|---|
| 25 mL/min | 6.9 | 0.897 | 222 | 28.9 | 29.8 |

Table 4.15 shows the elution results for both copper and gold. Elution tests were run at the same flowrate of 25 mL/min using 1 M ammonia in the first step and 1 M ammonium nitrate in the second step. In the first step, 22% of gold and 1.9% of copper loaded was eluted. Though ammonia was introduced to remove copper prior to removing gold, very little copper was removed in the first elution step. Copper at a concentration of 0.81 ppm and 0.7 ppm of gold was eluted from the resin in the first step. Experiments conducted by O'Malley (2002) using the same concentration of ammonia as those used in the current study (0.5 M) and an Amberjet resin loaded with 1000 ppm Cu and 1600 ppm Au, reported only 35 ppm of copper eluted. This correlated to 3.5% of copper being recovered which was close to the 1.88% copper recovery achieved in Table 4.15. The low recovery of copper could be due to the low ammonia concentration used in this study and thus further investigation into higher ammonia concentrations could result in much higher copper recoveries. This was established by O'Malley (2002) who compared 1 M and 2 M ammonia on the elution of gold and copper and found that 2 M ammonia solution removed all copper from the loaded resin with no gold being removed. However, in the ammonia elution step of this study, 22% of the loaded gold was removed.

Table 4.15: Ion exchange elution results for MTA5013SO4 resin at 25 mL/min with 2 eluants: 1 M Ammonia and 1 M Ammonium nitrate

| Eluant | Elution | Au eluted (meq/L) | Au Eluted from resin (%) | Cu eluted (meq/L) | Cu Eluted from resin (%) |
|---|---|---|---|---|---|
| $NH_3$ | Step 1 | 0.761 | 21.7 | 2.44 | 1.88 |
| $NH_4NO_3$ | Step 2 | 1.37 | 52.3 | - | - |
| Total | | 2.13 | 54.9 | 2.44 | 1.88 |

Elution with ammonium nitrate in step 2 removed 52.3% (0.94 ppm) of the gold adsorbed on the resin and overall 55% of the loaded gold on the resin was removed after both step 1 and step 2. Copper removal in step 2 was negligible and this could be due to the low ammonium nitrate concentration (1 M) used as opposed to the higher ammonium nitrate concentration (2 M) used in the prior elution experiments. Elution results at 1 M and 2 M ammonium nitrate, conveyed that a higher ammonium nitrate concentration was required to remove most of the loaded gold effectively. Thereby suggesting that the high nitrate ion concentration competes with the loaded aurothiosulphate ion for the active sites on the resin. Moreover, lower concentrations of ammonium nitrate could thus result in lower gold elution efficiencies.

Table 4.16: Gold and copper recoveries over each step in the ion exchange process

| | Starting solution concentration (ppm) | Recovery after loading (%) | Recovery after elution (%) | Overall Ion exchange efficiency (%) |
|---|---|---|---|---|
| Gold | 133.9 | 3.52 | 54.9 | 1.21 |
| Copper | 1338 | 5.49 | 2.44 | 0.0603 |

Table 4.16 summarises the gold and copper recoveries over each step. The overall ion exchange efficiency was calculated to be the total amount of gold or copper adsorbed and eluted throughout the ion exchange process. The resin operating capacity of 0.77 eq/L conveys that it does have available active sites to load all gold present in the starting solution and produce 100% loading recovery however only 3.5 % of gold was loaded onto the resin in this step. In addition, the concentration of ammonium nitrate as an eluant does influence the elution of gold with a recovery of 52.3% as opposed to 75% in the prior elution experiment at the same flowrate. This is further substantiated by work conducted by Nicol & O'Malley (2002) where a higher concentration of 2 M, as opposed to 1 M, produced a higher concentration of gold (110 ppm in contrast to 40 ppm). It was also found that using a lower concentration required twice the volume of eluant to remove all the gold loaded on the resin.

#### 4.3.2.3. Kinetic and equilibrium Results

Kinetic and equilibrium tests were conducted to investigate the resin performance over an extended period (2 hours and 4 hours) in a closed circuit. Various flowrates were introduced (10 mL/min, 25 mL/min and 50 mL/min) and the gold and copper concentrations were monitored.

Kinetic tests were investigated over 2 hours in a closed circuit as stated in Chapter 3.3.3.4. This experiment was conducted to determine the loading ability of the resin towards the aurothiosulphate ion at various flowrates. The results for both gold and copper at the three different flowrates (10 mL/min, 25 mL/min and 50 mL/min) are shown in Figure 4.12 and Figure 4.13.

Figure 4.12 depicts the gold concentration in solution over 2 hours using a closed circuit. The loaded gold solution was obtained from experimentation conducted in Chapter 3.3.2.2. Over 2 hours, all three flowrates showed a decline in concentration thereby indicating that the MTA5013 resin did remove aurothiosulphate ions in solution. The highest loading recovery of gold was 5.67% in the 10 mL/min investigation. The lowest loading recovery of 3.24% was measured at the 25 mL/min flowrate (Table 4.17). A gold concentration of 10.7 meq/L was removed from solution in the 10 mL/min flowrate whilst 5.18 meq/L and 7.63 meq/L were removed from the 25mL/min and 50 mL/min investigations respectively. The loading recoveries were still low given the resin operating capacity of 0.77 eq/L and that the experiment was conducted over 2 hours in a closed circuit in comparison to 50 minute kinetic tests investigated by Nesbitt (2016). It was expected that the aurothiosulphate ions would readily occupy the resin active sites given the higher affinity for the ion as stated in Nicol & O'Malley (2002) however the results from this study state otherwise. O'Malley (2002) found that after 2 hours using 30 ppm Cu, 0.5 M $NH_3$ and two strong-base anion resins, the gold recovery was between 12% - 25%. Zhang & Dreisinger (2004) found that in a solution containing 500 ppm Cu and 0.1 M ammonium thiosulphate, the gold recovery was 80% over

24 hours. Therefore, it is possible that the loading time was insufficient in removing a significant amount of gold from the solution especially considering the high concentration of copper in solution of 1270 ppm. Moreover, the low recoveries could be the result of polythionates occupying the active sites on the resin thereby poisoning the resin as indicated by Zhang & Dreisinger (2002).

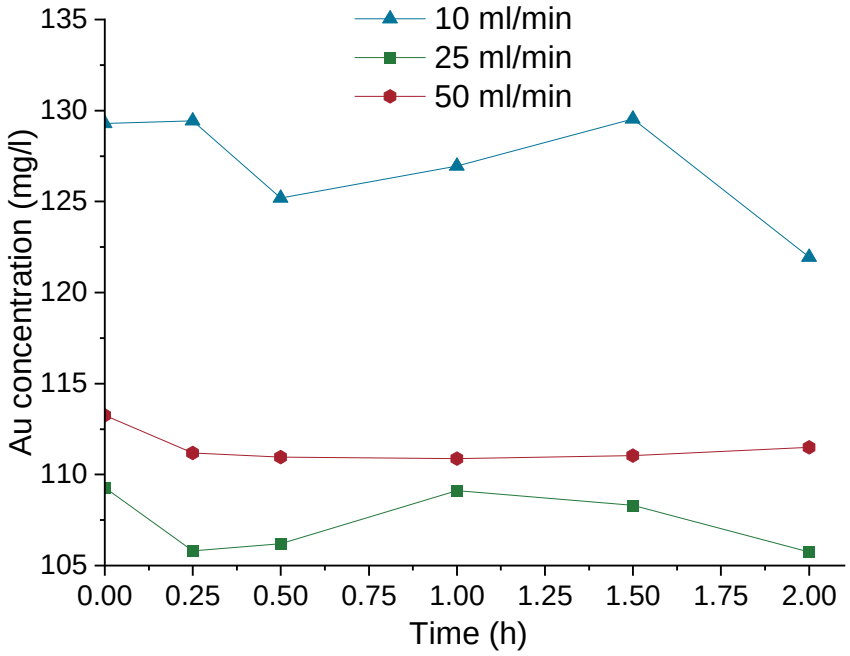


Figure 4.12: Gold solution concentration in mg/L at 3 different flowrates (10 mL/min, 25 mL/min and 50 mL/min) over 2 hours

In Figure 4.12, the gold solution concentration for the 10 mL/min showed an overall decline (7.33 mg/L) over the 2 hours whereas the gold concentration for the 50 mL/min experiment showed a slight initial decline (1.75 mg/L) then remained fairly stable between 30 minutes and 2 hours. The fluctuation in the gold concentration for the 25 mL/min experiment was similar to that of the 10 mL/min. Both experiments revealed high gold concentrations between 1 and 1.5 hours. The starting concentrations for all three flowrates varied as synthetic gold powder solutions were used in the ion exchange process thus each solution contained different gold extraction values at the start of the experiment.

Figure 4.13 below depicts the copper concentration in solution over 2 hours at various flowrates. There was a slight overall decrease in solution of 0.024 g/L and 0.009 g/L concentration for flowrates 10 mL/min and 50 mL/min respectively however the copper concentration for the 25 mL/min experiment showed no overall change over the 2 hours. The curve increased first before decreasing. This was unexpected given that the Cu concentration at the start of the experiment in solution was the highest concentration expected in solution. The increase thereafter could possibly be attributed to Cu ions that remained on the resin after elution in the previous step therefore indicating the elution step did not remove all Cu ions as intended. As mentioned previously in Section 4.3.2.1, regeneration of the resin in practice is hardly ever 100%. Furthermore, the resin utilised for the 25 mL/min was not fresh resin and had been regenerated after conducting the 10 mL/min experiment thus suggesting that Cu ions were still present on the resin and desorbed in the loading step of the 25 mL/min experiment.

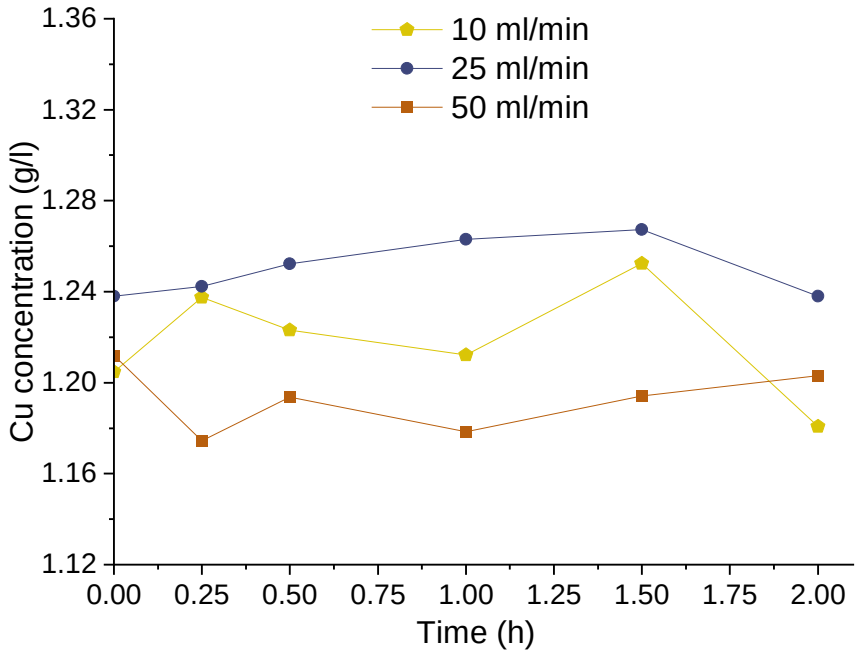


Figure 4.13: Copper solution concentration in g/L at 3 different flowrates (10 mL/min, 25 mL/min and 50 mL/min) over 2 hours

The highest recovery was measured in the 10 mL/min flowrate with 2% of the starting copper concentration being loaded onto the resin. The 25 mL/min flowrate showed no change in copper concentration over the 2 hours and the 50 mL/min flowrate resulted in a loading recovery of 0.73%. Both recovery values were low but as expected the lower flowrate did slightly increase the loading concentration of copper onto the resin. The lower flowrate of 10 mL/min as opposed to 50 mL/min resulted in a longer solution retention time and therefore a more complete ion exchange reaction compared to the 50 mL/min experiment.

Figure 4.14 depicts the gold and copper solution concentration comparison for all 3 flowrates and Table 4.17 below lists the recoveries over 2 hours for the kinetic experiments.

Table 4.17: Gold and copper recoveries for kinetic experiments at 3 flowrates (10 mL/min, 25 mL/min and 50 mL/min)

| Flowrate | Au recovery (%) | Copper recovery (%) |
|---|---|---|
| 10 mL/min | 5.67 | 2.00 |
| 25 mL/min | 3.24 | - |
| 50 mL/min | 1.55 | 0.73 |

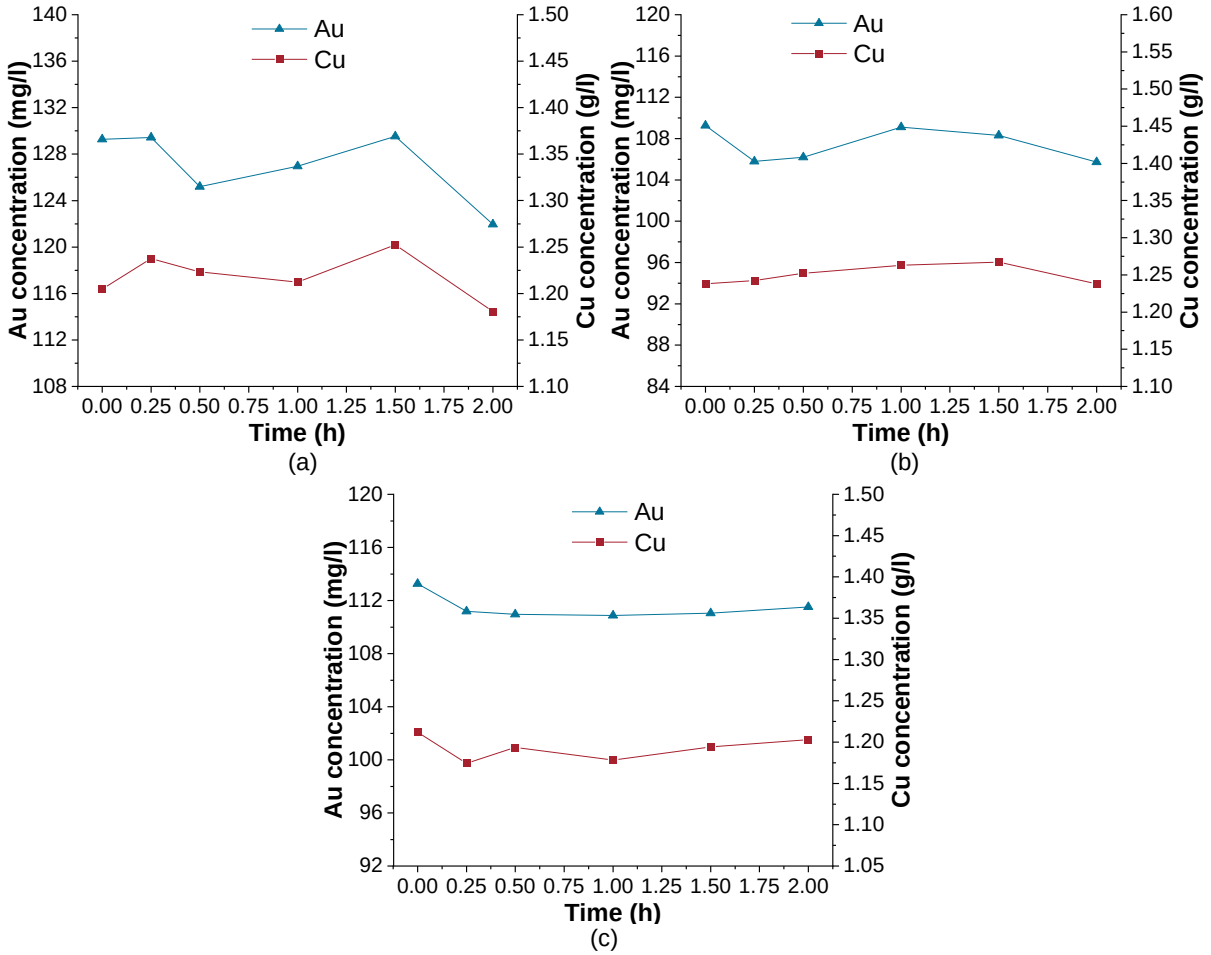


Figure 4.14: (a) Gold and copper solution concentration comparison for 10 mL/min flowrate (b) Gold and copper solution concentration comparison for 25 mL/min flowrate (c) Gold and copper solution concentration for 50 mL/min flowrate

Figure 4.14(a) compares the copper and gold solution concentration at the 10 mL/min flowrate. Au loading recovery was calculated to be 5.67% whilst Cu loading recovery was 2% as shown in Table 4.17. It can be concluded that the adsorption of gold on the resin for the 10 mL/min flowrate although small was much better than that of copper. Therefore, this was suggestive that the resin had selective loading for gold over copper.

Figure 4.14(b) depicts the gold and copper solution concentration for the 25 mL/min flowrate. The copper results showed no apparent change in copper solution concentration over the 2 hours. This could be the result of gold being preferentially adsorbed over the copper however the gold concentration in solution was still relatively low with only 3.54 ppm of gold removed from a 112 ppm solution. Therefore, it can be concluded that the resin was loaded with other ions possibly polythionates in place of both the gold and copper thiosulphate complexes. Polythionates in solution, as mentioned in Section 0, are detrimental to the adsorption of gold. Given the concentration of copper in solution and the possibility of polythionates being present, the adsorption of gold was hindered. In addition, it was clear that the system required to be operated at lower flowrates for it to be effective.

Figure 4.14(c) depicts the gold and copper solution concentration at a much higher flowrate of 50 mL/min. It was expected that minimal to no gold loading on the resin would occur and this was substantiated with the gold loading recovery of 1.55% from the solution correlating to 1.75

ppm of gold removed. Copper loading recovery was around 0.73% which was relatively lower than the copper recovery of 2% in the 10 mL/min flowrate. Both gold and copper loadings were very low and this was directly attributed to the change in flowrate.

The slight decrease in concentration for gold and copper across all three flowrates was indicative that the resin can load both ions effectively however the time given to load resin may have resulted in insufficient loading of the resin consequently low recoveries were obtained. O'Malley (2002) used flowrates as low as 25 mL/h over 4 hours for elution in a resin column however these low flowrates become impractical when introduced on an industrial scale with large solution volumes. In addition, there was a direct relation between gold and copper and the solution flowrate in this study. A lower flowrate resulted in relatively higher though still poor loadings for gold and copper. Furthermore, given that a single PCB leached solution would contain around 4.22 mg of gold, the loading of 7.33 ppm achieved in the 10 mL/min flowrate could thus be sufficient in removing majority of gold from the leached solution provided the same resin volume (5 mL). However, the lower concentration in the leach liquor would also have meant a lower driving force for mass transfer. This assumes that the competing anions present in the gold powder dissolution solution are similar to that of the leached solution and that other thiosulphate complexes such as $Zn(S_2O_3)_2^{3-}$ or even $Ag(S_2O_3)_2^{3-}$ that could form in PCB leached solutions would not further impede the loading of the aurothiosulphate ion on the resin. Zhang & Dreisinger (2004) found that the loading of the resin is predominantly determined by the affinity of the resin for the aurothiosulphate ion over other anions in solution. Furthermore, the resin affinity for gold over silver and zinc is important as stated by Eusebius, Ghose & Dey (1981). However, industrial scale leached solutions would contain gold from many PCBs. This suggests that the resin is effective in removing gold from highly saturated gold solutions provided that a much higher resin volume than 5 mL is utilised. This may be less practical due to the costs associated with large resin volumes though theoretically still possible to extract most of the gold from solution.

Equilibrium tests were conducted for 4 hours on the resin using NaCl solution to elute the aurothiosulphate loaded resin. Three different chloride concentrations were used: 318 ppm, 425 ppm and 637 ppm. These values correlated to 50%, 100% and 200% excess resin capacity with 5.2 mL of resin. A detailed description of the method can be found in Chapter 3.3.3.4. Calculations for the model can be found in Appendix B.2.

The mass action law model was fitted to the data based on the findings reported by Gomes, Almeida & Loureiro (2001). This law accounts for the concentrations of both anions competing for the active sites in both the solution and resin phases (Nesbitt, 2016). Figure 4.15 below depicts the fraction of gold present on the resin obtained from the equilibrium experiments ($\bar{X}_{Au}\ data$) against the fraction of gold present on the resin using the mass action law model ($\bar{X}_{Au}\ model$). A straight line starting at the origin is expected indicating that the data matches the model however Figure 4.15 depicts scattered points thus indicative that the equilibrium data does not fit the mass action law model.

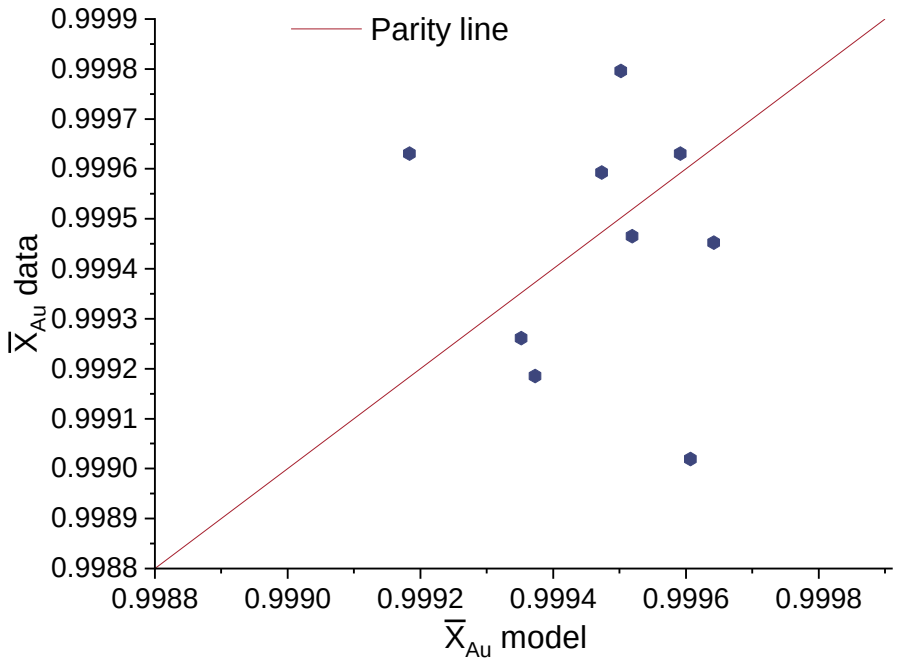


Figure 4.15: Mass action law model fitted to equilibrium data from gold on the resin in the presence of chloride ions

The data points are quite close to the parity line however all the data points cluster at the top right hand corner indicating that the resin holds tightly onto the aurothiosulphate ion which substantiates that the data is not a good fit for the model. The selectivity coefficient ($K_{Au}^{Cl}$) was calculated to be 1.34 x$10^{14}$ using the equations in Appendix B.2. This is extremely high for a selectivity coefficient value where a value of 9.44 was found by Gomes, Almeida & Loureiro (2001) in an ion exchange between the aurocyanide ion and the hydroxyl ion. O'Malley (2002) reported values between 0.0005 and 0.338 depending on the anion being exchanged with the aurothiosulphate ion. Some of the anions used in the ion exchange were thiosulphate, nitrate and even polythionates such as tetrathionate. All of which are much larger anions and therefore provide a greater degree of competition between the aurothiosulphate ion loaded on the resin and the anion in solution. The mass action law model therefore does not predict the equilibrium data accurately.

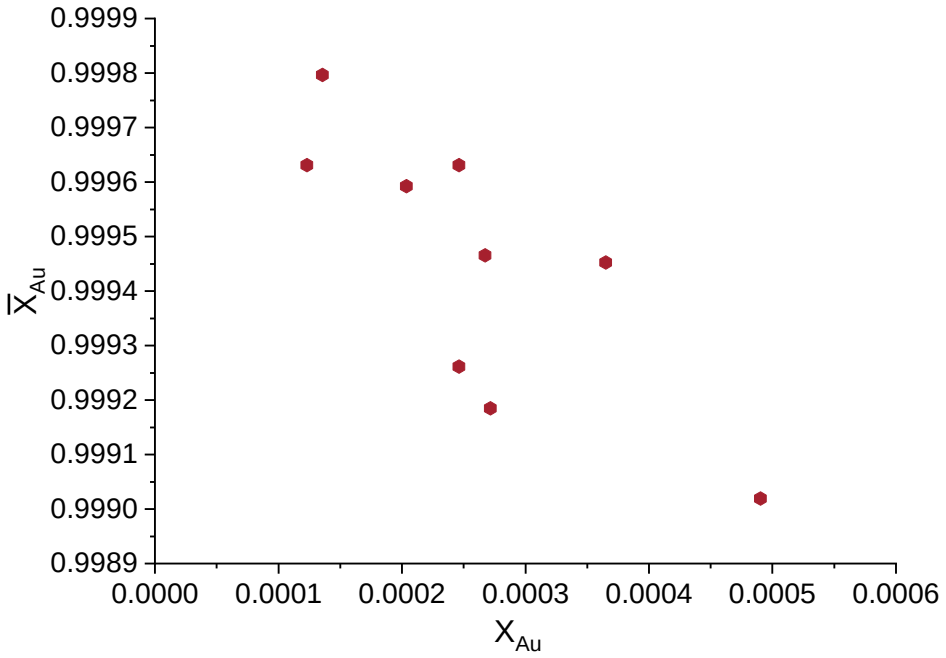


Figure 4.16: Equilibrium experimental data of gold isotherms in the presence of a competing chloride ion

Figure 4.16 depicts the fraction of gold in resin ($\bar{X}_{Au}$) against the fraction of gold in solution ($X_{Au}$). The bow curve expected is not depicted in the experimental data. The data is scattered and affirms that the loading of chloride ions between a concentration of 300 – 640 ppm has no substantial effect on the displacement of the aurothiosulphate ions. The resin therefore holds strongly onto the aurothiosulphate ion in low chloride concentration solutions. It is assumed that higher chloride concentrations are required to displace the aurothiosulphate ions possibly around 1 M. Figure 4.16 is fairly different from the mass action isotherm predicted by Gomes, Almeida & Loureiro (2001). Furthermore, it was expected that the resin would show a greater affinity for the chloride resin given its small size relative to the large aurothiosulphate ion however this was not depicted. This can be attributed to the resin holding tightly onto the aurothiosulphate ion and that in fact an anion of similar size would therefore compete easily for the active sites such as the tetrathionates or trithionate ions. Therefore, a solution containing either of these anions might display a better fit for the mass action law similar to the good correlation when incorporating polythionates found by Muslim (2010) for the Langmuir and Freundlich models.

In general, contact time between the resin and the anion is an important variable in adsorption in addition to the adsorption of competing anions. The loading of the resin increases with time and at some stage it reaches a constant value. At this stage, the anions being adsorbed onto the resin is matched by the anions entering the solution. This is known as dynamic equilibrium. The equilibrium tests in Figure 4.16 were conducted over 4 hours whilst those conducted by Muslim (2010) were 5 hours using 200 mL solutions and 0.333 g of resin. Therefore, the time allocated may have been low however the low loading recoveries obtained from gold can be attributed to the competing anion of choice, in this instance the chloride ion.

Muslim (2010) investigated the adsorption of thiosulphate, tetrathionate and trithionate with a strong-base anion resin in the chloride form. The study investigated the equilibrium constant for the reaction between the chloride ion and the thiosulphate ion. It was found that the

equilibrium constant between chloride and the thiosulphate ion decreased with a change in thiosulphate concentration. This was indicative that there was no competition between chloride and thiosulphate. It was suggested that the chloride ion is a weak anion compared to thiosulphate, tetrathionate and trithionate and therefore cannot occupy the active site of the resin to maintain the static equilibrium. Similarly, to Figure 4.16, the chloride ion in solution does not compete with the aurothiosulphate ion as indicated by the large fraction of gold on the resin after 4 hours. Therefore, it can be assumed that the chloride is a weak anion in comparison to the aurothiosulphate ion and that a stronger anion such as tetrathionate or trithionate might be better suited to compete with the resin active sites.

The equilibrium results substantiate the poor resin performance due to the presence of polythionates in the gold powder synthetic solutions used in previous experiments (Section 4.3.2.2). Low gold loading recoveries were measured and stated in Table 4.11 and Table 4.16. These results were attributed to the high concentration of polythionates in solution. In the equilibrium experiments, between 11% and 12% of the available resin active sites for all experiments were occupied by gold and copper ions therefore indicating that possible polythionate ions were present on the resin making up the remaining 89% – 88%. In the instance that no polythionates were present in the loading solution, the chloride ion would easily attach itself onto the available resin active sites with no competition of larger ions however this was not observed. Instead, chloride ions remained in solution therefore demonstrating that the resin had an affinity for polythionates over the chloride ion. These strong polythionates such as tetrathionate and trithionate compete with gold for the resin active sites thereby inhibiting gold adsorption onto the resin resulting in an ineffective resin and a lower gold loading concentration (Zhang & Dreisinger, 2002). Therefore, introducing a weak anion such as chloride at a later stage to compete for the active sites occupied by the polythionates and the active sites occupied by the aurothiosulphate ion was ineffective.

### 4.3.3. Purogold™ MTA5011 resin

Further experimentation was carried out on the MTA5011 resin obtained from Purogold™. These tests were conducted purely for confirmatory results of the MTA5013 experiments. The main difference noted between the MTA5011 and MTA5013 resin was the particle size range.

#### 4.3.3.1. Capacity test results

Capacity tests were conducted on the resin before loading and elution. The same method used in determining the MTA5013 capacity was used for the MTA5011 capacity experiment. The results obtained from the MTA5011 capacity test were similar to those obtained for the MTA5013 resin (0.77 eq/L). The operating capacity of the MTA5011 resin was taken to be 0.76 eq/L. This value was much smaller than the general capacity value of 1.15 eq/L reported in the MTA5011 MSDS in Appendix C.3.

Table 4.18: Capacity results on MTA5011SO4 resin

| Test | Chloride ions (eq/L) |
|---|---|
| Test 1 | 0.796 |
| Test 2 | 0.741 |
| Test 3 | 0.741 |
| Average | 0.759 |
| Standard Deviation | 0.0321 |

The capacity result of 0.76 eq/L was expected given the same method as the MTA5013 capacity experiment was employed. Despite the operating capacity being lower than the general capacity, the method used by Nesbitt (2016) and incorporated in this study, is a well-established method and thus the operating capacity was considered to be acceptable

Zhang & Dreisinger (2002) utilised a similar strong-base anion exchange resin (Purolite® A500/2788) in their experiments with a particle size range of 800 to 1300 µm and found that in comparison to other strong-base resins, with a particle size ranging from 300 – 800 µm, it showed noticeably lower capacity values (1.15 eq/L opposed to 1.4 eq/L and 1.35 eq/L). This may be due to the macroporous nature of the resin. However, since both MTA5013 and MTA5011 are macroporous resins, the slight difference in capacity of the MTA5011 resin can possibly be attributed to the resin bead size.

#### 4.3.3.2. Loading and elution results

Loading and elution experiments were conducted at a flowrate of 25 mL/min. Further details regarding the experiment method can be found in Chapter 3.3.3.3. A total of three tests were conducted and the average results are reported below. Gold at a concentration of 10 ppm (14.7 meq/L) was loaded onto the resin, whilst copper loading amounted to 44 ppm (129 meq/L). The gold values were higher than that of the MTA5013 resin at the same flowrate whilst the copper values were lower (Table 4.14). Therefore, it is possible that a smaller particle size could result in higher gold loading concentrations as 10 ppm was the highest concentration of gold loaded in all the loading experiments. The total resin capacity occupied by gold and copper was 19% and this fits well within the range of 8.4% - 29.8% obtained at the same flowrate for the MTA5013 resin. A possible explanation could be that gold adsorbs more rapidly and is then gradually displaced by copper or polythionates. The smaller beads have a larger surface area per unit volume, so the displacement will occur more pronouncedly that in larger resins where gold penetrates more deeply into the subsurface and would thus be more slowly displaced.

Table 4.19: Ion exchange loading results for the MTA5011 resin at 25 mL/min

| MTA5011 | Au loaded (meq/L) | Au loaded resin capacity (%) | Cu loaded (meq/L) | Cu loaded resin capacity (%) | Total resin capacity (%) |
|---|---|---|---|---|---|
| Test Average | 14.7 | 1.93 | 129 | 17.0 | 19 |

Moreover, the loading of 5 mg in a gold dissolved solution substantiates the possible loading of gold from PCB leached solutions with a gold content of 4.22 mg. However, this loading recovery is still too low and thus a large bed volume of resin is required for higher recoveries when accounting for process design PCB leached solutions containing gold much higher than 4.22 mg found on a single board.

Table 4.20 shows the results from elution with 2 M ammonium nitrate. The results for gold were similar to the results obtained in Table 4.12 for the 25 mL/min flowrate with 75% of loaded gold being eluted. Copper results were the lowest elution results obtained over all experiments with only 21.8% of the loaded copper being eluted. This further substantiates the choice of 2 M ammonium nitrate being suited for gold elution recovery over copper elution recovery.

Table 4.20: Ion exchange elution results for the MTA5011 resin at 25 mL/min

| MTA5011 | Au eluted (meq/L) | Au Eluted from resin (%) | Cu eluted (meq/L) | Cu Eluted from resin (%) |
|---|---|---|---|---|
| Test Average | 8.95 | 71 | 15.3 | 21.8 |

The MTA5013 and MTA5011 resins performed in a similar manner which was expected given the difference between the two resins was the particle size range. However, the highest gold loading and elution concentrations were recorded for the MTA5011 resin with 10 ppm being loaded and 6.3 ppm being eluted. This was associated with the nature of the resin bead and its effect on gold loading ability.

# 5. Conclusions

This study investigated the ammonium-thiosulphate system for the dissolution of gold powder and leaching of gold from PCBs. In addition, the effect of background copper concentrations on gold leaching was studied using PCB leaching tests and by dissolving pure gold to avert the influence of other foreign ions which would be expected in leaching PCBs. Ion exchange using three different resins was researched including the effect of the ammonium-thiosulphate system on gold recovery.

In setting up the leach experiments, considerable difficulty was encountered with accurately determining the gold content in thiosulphate solutions due to rapid decomposition and precipitation of gold. It was found that the ratio of thiosulphate to copper and ammonia to thiosulphate significantly influences the stability of the solution. Increasing the ammonia and thiosulphate concentration relative to the copper concentration by means of 1:1 ammonia and ammonium thiosulphate dilution reduced the tendency of the solution to precipitate. Therefore, samples were immediately diluted and refrigerated before being analysed in an effort to limit precipitation of gold from the solution.

It was found that the ammonium-thiosulphate system was promising for the dissolution of gold as indicated by the high extractions of 100% (141 mg/L) after 24 hours of dissolving gold powder in solution but this is still subject to optimisation. Furthermore, from the gold powder dissolution experiments it was established that the presence of 0.1 M Cu resulted in the highest gold extraction whilst PCB leaching experiments achieved highest gold extractions at 93.7% using 0.045 M background Cu. The lower background Cu concentration needed for optimal leaching of the PCBs is attributed to the additional leaching of copper from the board as the reaction proceeds. This additional leaching of copper was not present in the gold powder dissolution experiment hence a higher background Cu concentration was needed. Moreover, SEM-EDS analysis of the residual PCBs confirmed that gold was leached and some was precipitated onto the board possibly due to thiosulphate decomposition. A threshold background Cu concentration of 0.045 M was recommended such that below this threshold the kinetics of the gold reactions were slow and above the threshold thiosulphate degradation and preferential leaching of copper over gold was prevalent.

The medium-base anion exchange resin, AuRIX®100, was ill-suited for recovering the gold ion in the ammonia-thiosulphate system. Extremely low gold loading recoveries and higher copper loading recoveries demonstrated that copper was adsorbed preferentially over the aurothiosulphate ion. Strong-base anion exchange resins were more appropriate than the AuRIX®100 though still poor for the system reaching gold loadings of around 2.6 mg and in some cases only up to 5 mg. Further investigation revealed that low flowrates (10 mL/min) allowed for better loading and elution of the resin due to a greater retention time and thus a better ion exchange between species. However, further reducing the flowrates to below 10 mL/min to increase gold loading recovery is impractical on a larger scale. Overall loading of both gold and copper ions on the resin was low with between 2% and 30% of the resin capacity occupied by both gold and copper ions. This might be the result of a high concentration of polythionates in solution thereby competing with the aurothiosulphate ion despite the resins affinity for thiosuphate over polythionates and therefore poisoning the resin.

Elution with ammonium nitrate at 2 M removed up to 75% of gold and 68% of copper which was much higher than elution with 1 M ammonia. Minimal copper was removed using ammonia as opposed to ammonium nitrate despite previous investigations detailing the use of ammonia specifically for copper removal (Nicol & O'Malley, 2002) . It was also found that a higher concentration of ammonium nitrate was more suited in removing the aurothiosulphate ion due to the high concentration of nitrate ions thereby competing for the resin actives sites.

Kinetic data revealed that 2 hours was insufficient in loading gold and copper ions, achieving recoveries of only 5.7% and 2%. This was a consequence of the small resin volume used relative to the solution. A period of 2 hours and high flowrates of 50 mL/min resulted in a short solution retention time and an incomplete ion exchange reaction hence the low recoveries. In addition, it concluded that the active sites were occupied by other ions besides the aurothiosulphate ion and copper-thiosulphate ion. These other ions could possibly be the polythionates in solution. Modelling of the equilibrium data using the mass action law model did not prove to be successful. This is mainly due to the extremely low concentration of chloride ions in solution competing with the loaded aurothiosulphate ion and possibly the attached polythionates on the resin. The data was inaccurately modelled as the chloride ion proved to be a weak anion in competition with the aurothiosulphate ion. Stronger anions such as tetrathionate, trithionates or thiosulphate ions would be more suited in competing with the aurothiosulphate ion.

In summary, the ammonium-thiosulphate is effective in removing gold from PCBs into solution. The system has been validated with high extractions in both the gold powder dissolution experiments and the PCB leaching experiments. Furthermore, strong-base anion resins can recover some dissolved gold from standard synthetic solutions however this process still requires an in-depth analysis in order to be effective and compete with established commercial processes such as carbon adsorption. The MTA5011 and MTA5013 did not show high selectivities of the aurothiosulphate ion over possible polythionates in solution and only loaded 5 mg of a 112 ppm gold synthetic solution therefore indicating that significantly larger volumes of resin would be required to achieve higher recoveries of gold from solution as what was employed in the ion exchange experiments. This is easy to address in an operational context but may render the process expensive due to the large volume of resin required. Moreover, competition of anions in the system was an underestimated challenge in the system. Elution of both gold and copper was favourable using ammonium nitrate at 2 M and it is thus concluded that both anions can successfully be eluted.

Overall, the study has provided an in-depth analysis into the ammonium-thiosulphate system for leaching and the performance of medium- and strong-base anion exchange resins in recovering gold. The assessment completed on both these aspects will significantly increase the attraction in recycling e-waste in a formal and safe manner in the South African context thereby alleviating the growing e-waste problem.

## Recommendations

Throughout this study there have been various elements requiring further investigation and possible alterations to improve the test work and any future work around the e-waste ammonium-thiosulphate system. These are summarised below.

Dilution of samples immediately after sampling helped alleviate the precipitation of the solution however analysis of ammonium-thiosulphate sample solutions should be conducted immediately (under 24 hours) after sampling. This limits the time for the solution to decrease in stability and metal precipitates to form.

Careful management of copper concentration in the PCB leach solution is required so to maximise extraction and minimise thiosulphate degradation. In the context of a comprehensive PCB flowsheet, strict separation of copper and gold leaching is necessary to manage this. A higher ammonia concentration will also contribute to a faster leaching time provided that the thiosulphate to ammonia ratio is still obeyed. In addition, leaching time can be increased above 24 hours to determine the effect of time on the ammonium-thiosulphate system. This would first require additional research.

Investigation into the consumption of thiosulphate in solution and thus the production of polythionate concentrations, during gold dissolution should be conducted. This will indicate the extent to which polythionates play a role in the ammonium-thiosulphate system and will therefore indicate the challenges that may arise in the downstream ion exchange processes.

It was evident that during capacity testing that the values obtained for both MTA5013 and MTA5011 resins were quite low for strong-base-anion resins. Thus, applying the Purolite® capacity test method on the MTA5013 and MTA5011 should be attempted to compare operating capacities.

Stronger anions such as thiosulphate, tetrathionate and trithionate would be more appropriate in testing the competition between the aurothiosulphate ion for active sites on the resin. Another option is to increase the chloride ion concentration but at a much higher concentration of 1 M or 2 M to determine the effect on equilibrium.

MTA5013 and MTA5011 were the only strong-base anion exchange resins that were investigated and other strong-base anion exchange resins should be considered to determine their effectiveness in comparison, especially if they were not manufactured for the specific removal of the aurothiosulphate ion. In addition, a higher resin volume: solution volume ratio should be investigated in determining the effect on gold recoveries.

Overall, the research conducted in this study including the application of the above mentioned recommendations will further highlight the benefits of e-waste and e-waste recycling in the sustainable development context specifically from an economic, environmental and public safety and health perspective. In addition, it will provide low cost and efficient alternatives to the current established practices for gold recovery. Furthermore, developing countries such as South Africa will benefit from the additional revenue creating employment in the formal e-waste sector and promoting the circular economy principles.

# References

Abbruzzese, C., Fornari, P., Massidda, R., Vegliò, F. & Ubaldini, S. 1995. Thiosulphate leaching for gold hydrometallurgy. *Hydrometallurgy*. 39(1–3):265–276. DOI: 10.1016/0304-386X(95)00035-F.

Arslan, F. & Sayiner, B. 2018. Ammoniacal thiosulphate leaching of Ovacik gold ore. *Mineral Processing on the Verge of the 21st Century*. 3(3):517–522. DOI: 10.1201/9780203747117-90.

Ayawei, N., Ebelegi, A.N. & Wankasi, D. 2017. Modelling and Interpretation of Adsorption Isotherms. *Journal of Chemistry*. 2017. DOI: 10.1155/2017/3039817.

Aylmore, M.G. & Muir, D.M. 2001. Thiosulfate leaching of gold - a review. *Minerals Engineering*. 14(2):135–174. DOI: 10.1016/S0892-6875(00)00172-2.

Aylmore, M.G. & Staunton, W.P. 2014. Effect of minerals on the stability of gold in copper ammoniacal thiosulfate solutions - The role of copper, silver and polythionates. *Hydrometallurgy*. 143:12–22. DOI: 10.1016/j.hydromet.2013.12.001.

Balde, C.P., Forti, V., Gray, V., Kuehr, R. & Stegmann, P. 2017. *The global e-waste monitor 2017*. DOI: 10.1016/j.proci.2014.05.148.

Baldé, C.P., van den Brink, S., Forti, V., Schalk, A. Van Der & Hopstaken, F. 2020. The Dutch WEEE Flows 2020. (November):10. Available: https://www.scycle.info/the-dutch-weee-flows-2020-what-happened-between-2010-and-2018/.

Behnamfard, A., Salarirad, M.M. & Veglio, F. 2013. Process development for recovery of copper and precious metals from waste printed circuit boards with emphasize on palladium and gold leaching and precipitation. *Waste Management*. 33(11):2354–2363. DOI: 10.1016/j.wasman.2013.07.017.

Birloaga, I., De Michelis, I., Ferella, F., Buzatu, M. & Vegliò, F. 2013. Study on the influence of various factors in the hydrometallurgical processing of waste printed circuit boards for copper and gold recovery. *Waste Management*. 33(4):935–941. DOI: 10.1016/j.wasman.2013.01.003.

Black, S.B. 2006. The Thermodynamic Chemistry of the Aqueous Copper-Ammonia Thiosulfate System. Murdoch University.

Breuer, P.L. & Jeffrey, M.I. 2000. Thiosulphate leaching kinetics of gold in the presence of copper and ammonia. *Minerals Engineering*. 13(10):1071–1081.

Chaparro, M., Munive, G., Guerrero, P., Parga, J.R., Vazquez, V. & Valenzuela, J.L. 2015. Gold Adsorption In Thiosulfate Solution Using Anionic Exchange Resin. *Journal of Multidisciplinary Engineering Science and Technology (JMEST)*. 2(8):3159–3199. Available: www.jmest.org.

Chirume, B.H. 2019. Investigation of a Hydrometallurgical Process Route to Recover Metals from Waste Printed Circuit Boards. Available: https://open.uct.ac.za/handle/11427/31434.

Choo, W.L. & Jeffrey, M.I. 2004. An electrochemical study of copper cementation of gold(I) thiosulfate. *Hydrometallurgy*. 71(3–4):351–362. DOI: 10.1016/S0304-386X(03)00087-2.

Cui, H. & Anderson, C.G. 2016. Literature Review of Hydrometallurgical Recycling of Printed Circuit Boards (PCBs). *Journal of Advanced Chemical Engineering*. 6(1). DOI: 10.4172/2090-4568.1000142.

Cui, J. & Zhang, L. 2008. Metallurgical recovery of metals from electronic waste: A review.

*Journal of Hazardous Materials*. 158(2–3):228–256. DOI: 10.1016/j.jhazmat.2008.02.001.

De Dardel, F. & Arden, T. V. 2012. Ion Exchangers. In *Ullmann's Encyclopedia of Industrial Chemistry*. 473–545. DOI: 10.1002/14356007.a14.

Dong, Z., Jiang, T., Li, Q., Xu, B. & Yang, Y. 2017. Recovery of Gold from Pregnant Thiosulfate Solutions by the Resin Adsorption Technique. *Metals*. 7(12):555. DOI: 10.3390/met7120555.

Dönmez, B., Sevim, F. & Çolak, S. 2001. Study on recovery of gold from decopperized anode slime. *Chemical Engineering and Technology*. 24(1):91–95. DOI: 10.1002/1521-4125(200101)24:1<91::AID-CEAT91>3.0.CO;2-A.

Eusebius, L.C.T., Ghose, A.K. & Dey, A.K. 1981. Thiosulphate as a complexing agent in the separation of cations by cation-exchange chromatography. *The Analyst*. 106(1262):529–536. DOI: 10.1039/AN9810600529.

Feng, D. & van Deventer, J.S.J. 2006. Ammoniacal thiosulphate leaching of gold in the presence of pyrite. *Hydrometallurgy*. 82(3–4):126–132. DOI: 10.1016/j.hydromet.2006.03.006.

Ficeriová, J., Baláž, P. & Gock, E. 2011. Leaching of gold, silver and accompanying metals from circuit boards (PCBs) waste. *Acta Montanistica Slovaca*. 16(2):128–131.

Fleming, C. a, McMullen, J., Thomas, G.K. & Wells, J. a. 2003. Recent advances in the development of an alternative to the cyanidation process : Thiosulfate leaching and resin in pulp. *Minerals and Metallurgical Processing*. 20(February 2003):1–9. DOI: 10.1007/BF03403107.

Forti, V., Baldé, C.P., Kuehr, R. & Bel, G. 2020. *The Global E-waste Monitor 2020*. Available: http://ewastemonitor.info/.

Gökelma, M., Birich, A., Stopic, S. & Friedrich, B. 2016. A Review on Alternative Gold Recovery Reagents to Cyanide. *Journal of Materials Science and Chemical Engineering*. (August):8–17.

Gomes, C.P., Almeida, M.F. & Loureiro, J.M. 2001. Gold recovery with ion exchange used resins. *Separation and Purification Technology*. 24(1–2):35–57. DOI: 10.1016/S1383-5866(00)00211-2.

Gray, A.H., Hughes, T. & Abols, J. 2005. The use of AuRIX®100 resin for the selective recovery of gold and silver from copper, gold and silver solutions. *Australasian Institute of Mining and Metallurgy Publication Series*. (November):53–58.

Grosse, A.C., Dicinoski, G.W., Shaw, M.J. & Haddad, P.R. 2003. Leaching and recovery of gold using ammoniacal thiosulfate leach liquors (a review). *Hydrometallurgy*. 69(1–3):1–21. DOI: 10.1016/S0304-386X(02)00169-X.

Guerra, E. & Dreisinger, D.. 1999. A study of the factors affecting copper cementation of gold from ammoniacal thiosulphate solution. *Hydrometallurgy*. 51(2):155–172. DOI: 10.1016/S0304-386X(98)00061-9.

Guo, C., Wang, H., Liang, W., Fu, J. & Yi, X. 2011. Liberation characteristic and physical separation of printed circuit board (PCB). *Waste Management*. 31(9–10):2161–2166. DOI: 10.1016/j.wasman.2011.05.011.

Ha, V.H., Lee, J.C., Huynh, T.H., Jeong, J. & Pandey, B.D. 2014. Optimizing the thiosulfate leaching of gold from printed circuit boards of discarded mobile phone. *Hydrometallurgy*. 149:118–126. DOI: 10.1016/j.hydromet.2014.07.007.

Hadi, P., Xu, M., Lin, C.S.K., Hui, C.W. & McKay, G. 2015. Waste printed circuit board recycling techniques and product utilization. *Journal of Hazardous Materials*. 283:234–243.

DOI: 10.1016/j.jhazmat.2014.09.032.

Hiskey, J.B. & Lee, J. 2003. Kinetics of gold cementation on copper in ammoniacal thiosulfate solutions. *Hydrometallurgy*. 69(1–3):45–56. DOI: 10.1016/S0304-386X(03)00003-3.

Hung Ha, V., Lee, J., Jeong, J., Trung Hai, H. & Jha, M.K. 2010. Thiosulfate leaching of gold from waste mobile phones. *Journal of Hazardous Materials*. 178:1115–1119. DOI: 10.1016/j.jhazmat.2010.01.099.

Iguchi, A. 1958. The Separation of Polythionates with Anion-Exchange Resins. *Bulletin of the Chemical Society of Japan*. 31(5):597–600. DOI: 10.1246/bcsj.31.597.

Jeffrey, M.I. 2001. Kinetic aspects of gold and silver leaching in ammonia-thiosulfate solutions. *Hydrometallurgy*. 60(1):7–16. DOI: 10.1016/S0304-386X(00)00151-1.

Jeffrey, M.I., Breuer, P.L. & Choo, W.L. 2001. A kinetic study that compares the leaching of gold in the cyanide, thiosulfate, and chloride systems. *Metallurgical and Materials Transactions B: Process Metallurgy and Materials Processing Science*. 32(6):979–986. DOI: 10.1007/s11663-001-0086-7.

Jeffrey, M.I., Breuer, P.L. & Chu, C.K. 2003. The importance of controlling oxygen addition during the thiosulfate leaching of gold ores. *International Journal of Mineral Processing*. 72(1–4):323–330. DOI: 10.1016/S0301-7516(03)00108-X.

Jing-ying, L., Xiu-li, X. & Wen-quan, L. 2012. Thiourea leaching gold and silver from the printed circuit boards of waste mobile phones. *Waste Management*. 32(6):1209–1212. DOI: 10.1016/j.wasman.2012.01.026.

Kiddee, P., Naidu, R. & Wong, M.H. 2013. Electronic waste management approaches: An overview. *Waste Management*. 33(5):1237–1250. DOI: 10.1016/j.wasman.2013.01.006.

Kim, E.Y., Kim, M.S., Lee, J.C. & Pandey, B.D. 2011. Selective recovery of gold from waste mobile phone PCBs by hydrometallurgical process. *Journal of Hazardous Materials*. 198:206–215. DOI: 10.1016/j.jhazmat.2011.10.034.

Korhonen, J., Honkasalo, A. & Seppälä, J. 2018. Circular Economy: The Concept and its Limitations. *Ecological Economics*. 143:37–46. DOI: 10.1016/j.ecolecon.2017.06.041.

Kotze, M., Green, B., Mackenzie, J. & Virnig, M. 2005. Chapter 25: Resin-in-pulp and resin-in-solution. In *Advances in Gold Ore Processing*. 603–635. DOI: https://doi.org/10.1016/S0167-4528(05)15025-X.

Krinitsyn, D.O., Kononova, O.N., Krylov, A.S., Maznyak, N. V. & Kholmogorov, A.G. 2008. Recovery of gold(I) thiocyanate complexes by some anion-exchangers. *Russian Journal of Physical Chemistry A*. 82(3):429–433. DOI: 10.1134/S0036024408030199.

Lampinen, M., Laari, A. & Turunen, I. 2015. Ammoniacal thiosulfate leaching of pressure oxidized sulfide gold concentrate with low reagent consumption. *Hydrometallurgy*. 151:1–9. DOI: 10.1016/j.hydromet.2014.10.014.

Lee, J. 2003. Gold cementation on copper in thiosulfate solution: kinetic, electrochemical, and morphological studies. The University of Arizona.

Lu, Y. & Xu, Z. 2016. Precious metals recovery from waste printed circuit boards: A review for current status and perspective. *Resources, Conservation and Recycling*. 113(2016):28–39. DOI: 10.1016/j.resconrec.2016.05.007.

Lydall, M., Nyanjowa, W. & James, Y. 2017. Mapping South Africa's Waste Electrical and Electronic Equipment ( WEEE ) Dismantling, Pre-Processing and Processing Technology Landscape - Waste Research Development and Innovation Roadmap Research Report. *Futurespot.Co.Za*. (March):1–91.

Mecucci, A. & Scott, K. 2002. Leaching and electrochemical recovery of copper, lead and tin from scrap printed circuit boards. *Journal of Chemical Technology and Biotechnology*. 77(4):449–457. DOI: 10.1002/jctb.575.

Molleman, E. & Dreisinger, D. 2002. The treatment of copper-gold ores by ammonium thiosulfate leaching. *Hydrometallurgy*. 66(1–3):1–21. DOI: 10.1016/S0304-386X(02)00080-4.

Murakami, H., Nishihama, S. & Yoshizuka, K. 2015. Separation and recovery of gold from waste LED using ion exchange method. *Hydrometallurgy*. 157:194–198. DOI: 10.1016/j.hydromet.2015.08.014.

Muslim, A. 2010. Thiosulfate Leaching Process for Gold Extraction. Curtin University of Technology.

Nesbitt, A.B. 2016. A Study of the Decay of Acid Cationic Ion. University of Cape Town.

Nicol, M.J. & O'Malley, G. 2002. Recovering gold from thiosulfate leach pulps via ion exchange. *Jom*. 54(10):44–46. DOI: 10.1007/BF02709221.

O'Malley, G.P. 2002. Recovery of gold from thiosulfate solutions and pulps with ion-exchange resins. Murdoch University.

Pangum, L.S. & Browner, R.E. 1996. Pressure chloride leaching of a refractory gold ore. *Minerals Engineering*. 9(5):547–556. DOI: 10.1016/0892-6875(96)00042-8.

Petter, P.M.H., Veit, H.M. & Bernardes, A.M. 2014. Evaluation of gold and silver leaching from printed circuit board of cellphones. *Waste Management*. 34(2):475–482. DOI: 10.1016/j.wasman.2013.10.032.

Prestele, M.P. 2020. Assessment of a Shredding Technology of Waste Printed Circuit Boards in preparation for Ammonia-based Copper leaching. University of Cape Town.

Purolite. 1987. *Purolite International Ltd Document PITM 10*.

Purolite. 1995. *Purolite International Ltd Document PITM 9*.

Quinet, P., Proost, J. & Van Lierde, A. 2008. Recovery of precious metals from electronic scraps. *Minerals and Metallurgical Processing*. 22(04):1673–1677.

Sanapala, R. 2008. Characterization of FR-4 printed circuit board laminates before and after exposure to lead-free soldering conditions. University of Maryland.

Schwarzer, S., Bono, A.., Peduzzi, P., Giuliani, G. & Kluser, S. 2005. E-waste, the hidden side of IT equipment's manufacturing and use UNEP Early Warning on Emerging Environmental Threats. *United Nations Environmental Programme*. Available: https://archive-ouverte.unige.ch/unige:23132.

Senanayake, G. 2004. Analysis of reaction kinetics, speciation and mechanism of gold leaching and thiosulfate oxidation by ammoniacal copper(II) solutions. *Hydrometallurgy*. 75(1–4):55–75. DOI: 10.1016/j.hydromet.2004.06.004.

Sousa, R., Futuro, A., Fiúza, A., Vila, M.C. & Dinis, M.L. 2018. Bromine leaching as an alternative method for gold dissolution. *Minerals Engineering*. 118(January):16–23. DOI: 10.1016/j.mineng.2017.12.019.

Sullivan, A.M. & Kohl, P.A. 1997. Electrochemical Study of the Gold Thiosulfate Reduction. *Journal of The Electrochemical Society*. 144(5):1686–1690. DOI: 10.1149/1.1837660.

Tao, J., Jin, C. & Shi, X. 1993. Electrochemistry and mechanism of leaching gold with ammoniacal thiosulfate. *Publications of the Australasian Institute of Mining and Metallurgy*. 3/93(XVIII International Mineral Processing Congress, 1993, Vol. 5):1141–1146.

Thermo Fischer Scientific. 2021. Available: https://www.thermofisher.com/za/en/home/industrial/spectroscopy-elemental-isotope-analysis/spectroscopy-elemental-isotope-analysis-learning-center/trace-elemental-analysis-tea-information/icp-oes-information/icp-oes-sample-preparation.html [2021, October 26].

Tripathi, A., Kumar, M., C. Sau, D., Agrawal, A., Chakravarty, S. & R. Mankhand, T. 2012. Leaching of Gold from the Waste Mobile Phone Printed Circuit Boards (PCBs) with Ammonium Thiosulphate. *International Journal of Metallurgical Engineering*. 1(2):17–21. DOI: 10.5923/j.ijmee.20120102.02.

Virgen, M.., Picardo, J., Mackenzie, J.M.., Katsikaros, N. & Gray, S. 2004. The Use of AuRIX®100 Resin and Gekko Systems Technology for the Recovery of Gold. *Systems Technology*. (May):1–24.

Wan, R.Y. & LeVier, K.M. 2003. Solution chemistry factors for gold thiosulfate heap leaching. *International Journal of Mineral Processing*. 72(1–4):311–322. DOI: 10.1016/S0301-7516(03)00107-8.

Xia, C. 2000. Thiosulphate Stability In Gold Leaching Process. DOI: 10.16953/deusbed.74839.

Xu, B., Kong, W., Li, Q., Yang, Y., Jiang, T. & Liu, X. 2017. A review of thiosulfate leaching of gold: Focus on thiosulfate consumption and gold recovery from pregnant solution. *Metals*. 7(6). DOI: 10.3390/met7060222.

Zhang, H. & Dreisinger, D.B. 2002. The adsorption of gold and copper onto ion-exchange resins from ammoniacal thiosulfate solutions. *Hydrometallurgy*. 66(1–3):67–76. DOI: 10.1016/S0304-386X(02)00077-4.

Zhang, H. & Dreisinger, D.B. 2004. The recovery of gold from ammoniacal thiosulfate solutions containing copper using ion exchange resin columns. *Hydrometallurgy*. 72(3–4):225–234. DOI: 10.1016/S0304-386X(03)00183-X.

Zhang, S. & Forssberg, E. 1997. Mechanical separation-oriented characterization of electronic scrap. *Resources, Conservation and Recycling*. 21(4):247–269. DOI: 10.1016/S0921-3449(97)00039-6.

Zhang, Y., Liu, S., Xie, H., Zeng, X. & Li, J. 2012. Current Status on Leaching Precious Metals from Waste Printed Circuit Boards. *Procedia Environmental Sciences*. 16:560–568. DOI: 10.1016/j.proenv.2012.10.077.

Zhao, J., Wu, Z. & Chen, J.C. 1998. Solvent extraction of gold in thiosulfate solutions with mines. *Solvent Extraction and Ion Exchange*. DOI: 10.1080/07366299808934538.

# Appendices

## A. Appendix A: Analysis of Gold and Copper in Thiosulphate Solution

Current available methods for gold analysis are generally unsuited to the ammonium thiosulphate system, mainly because of the use of ultra-pure $HNO_3$ in acidifying the solution sample prior to analysis. Early pre-liminary leaching experiments had shown that analysing the solution sample neat, without employing acidification, proved to be quite unreliable and unstable, and hence further experiments to improve the stability of the solution before being analysed were needed. Subsequently, an investigation into different sample preparation for gold analysis was required before any extensive ammonia-ammonium leaching experiments were conducted. This involved investigating the different dilution methods to maintain the stability of gold in solution as well as observing the precipitation from the unstable solution over a period of time. Two leaching experiments were conducted on PCBs and gold powder and various dilutions were completed immediately after sampling before being analysed in the analysis laboratory. The conditions for both leaching experiments are shown below in Table A.1.

The gold powder dissolution experiment was conducted for 51 hours. The starting copper sulphate concentration was 10 ppm and was increased to 100 ppm and 200 ppm at the 2 hour and 48 hour mark. Copper was added at extremely low concentrations (10 ppm - 200 ppm) to ensure that the reaction can proceed at a fast rate whilst at the same time promoting the formation of the aurothiosulphate ion in place of the copper thiosulphate ion (Section 2.4.4.1). Copper was added in gradual increments as visual inspection of the solution revealed that all gold had not dissolved completely into the solution and copper is known to aid the dissolution reaction as an oxidant (Fleming et al., 2003). Gold powder weighing 56 mg was added at the start of the experiment as a proxy for the gold present on a single PCB. Gold concentration in the solution was 112 ppm.

The PCB leaching experiment was conducted using the same method as the gold powder dissolution experiment except for the experiment duration and background copper concentration. The experiment was conducted over 24 hours at 0.02 M copper sulphate concentration as stated in Table A.1. The PCBs and leachate were filtered using a vacuum filter and Buchner funnel after leaching and dried on filter paper before recording its weight.

Table A.1: Conditions for gold analysis leaching experiment

| Lixiviants/Conditions | Units | Values |
|---|---|---|
| $(NH_4)_2S_2O_3$ concentration | M | 0.5 |
| $NH_3$ concentration | M | 1 |
| $CuSO_4.5H_2O$ concentration | M | 0.02* |
| Temperature | °C | 25 |
| Time | Hours (h) | 24/51 |
| Stirring speed | Revolutions per minute (rpm) | 400 |
| Volume | mL | 500 |
| Compressed air flowrate | L/min | 0.17 |
| Solid to liquid ratio | - | 1:10 |

*PCB experiment only

Conventional methods employ the use of Ultra-pure $HNO_3$ at 2% concentration for acidification of liquid samples when analysing with Inductively Coupled Plasma Atomic Emission Spectroscopy (ICP-AES) or Microwave Plasma Atomic Emission Spectroscopy (MP-AES). The use of an acid in diluting the ammonium-thiosulphate solution sample presented a considerable challenge. This was mainly because the reduced pH of the solution sample results in the decomposition of the thiosulphate ion and thus precipitation of the metals in solution (Section 2.4.4.1). This hindered any valuable analysis of the solution sample. Thus, a different approach to acidifying the solution samples was undertaken.

This approach consisted of utilising other reagents to dilute or “acidify” the samples at various dilution ratios. These reagents included deionised water, aqua regia, ammonia and ammonium thiosulphate solutions. Seven samples each from both experiments were collected at the end and immediately underwent various dilutions before being refrigerated. Refrigeration of samples was required because the analysis was completed by external laboratories who could not analyse samples immediately and who, due to challenges with staff availability as a result of COVID-19, would at times refrigerate samples for extended periods. These samples and the dilution methods incorporated immediately after the experiment are listed in Table A.2 and Table A.3. In addition, both tables include the gold concentration in mg/L from the analysis using MP-AES and ICP-AES. MP-AES was utilised in the University of Cape Town (UCT) Analytical Laboratory (AL) whilst ICP-AES analysis was performed in the Central Analysis Facility (CAF) at the University of Stellenbosch (US). Initial dilution refers to the dilution conducted immediately after sampling in the hydrometallurgy laboratory whilst additional dilution refers to the second dilution conducted by the Analytical laboratory. The results stated in Table A.2 and Table A.3 have already accounted for both dilution steps and as such are the final gold concentrations.

Reverse aqua regia dilution samples contained 55% $HNO_3$ and 32% HCl. Reverse aqua regia was introduced at a strong concentration due its high digestive ability. Dilutions with ammonia-ammonium thiosulphate solutions utilised the same concentration as that in the leaching experiments i.e 0.5 M ammonium thiosulphate and 1 M ammonia. The detection limit for the MP-AES and ICP-AES was 20 ppb and 50 ppb respectively.

All ICP-AES samples were further diluted by a factor of 50 in the CAF laboratory with deionised water before being analysed. The samples sent for MP-AES underwent various additional

dilutions using deionised water in the UCT Analytical laboratory. The additional dilutions are stated in Table A.2 and Table A.3.

For the deionised water sample in Table A.3, 2% $HNO_3$ was used at a dilution factor of 10 as precipitation occurred when using deionised water at the same dilution factor. Thus, a value of 2.19 mg/L gold was reached much lower than the expected 8.44 mg/L. A dilution factor of 100 was required with 2% $HNO_3$ for the 1:2 reverse aqua regia sample in Table A.3. Prior attempts to diluting the sample 10 times, with both 2% $HNO_3$ and deionised water, resulted in precipitation. The 100 dilution factor resulted in no precipitation however the sample could not be analysed as the metal ion concentration dropped to below the detection limit for MP-AES analysis. Some samples such as the reverse aqua regia dilution (Table A.2) and the ammonium thiosulphate and ammonia dilution (Table A.2 and Table A.3) were not analysed by ICP-AES.

Table A.2: Gold powder (112 mg/L Au) experiment results for various dilution methods (ND = below detection limit)

| Initial dilution solution | Initial dilution Factor | UCT AL | | CAF | |
|---|---|---|---|---|---|
| | | Additional dilution | MP-AES (mg/L) | Additional dilution | ICP-AES (mg/L) |
| No dilution | - | 1:5♦ | ND | 1:50♦ | ND |
| Reverse aqua regia | 1:1 | 1:10 $HNO_3$ | 31.7 | 1:50♦ | - |
| | 1:2 | | 19.3 | | 34.1 |
| $(NH_4)_2S_2O_3$ and $NH_3$ | 1:1 | 1:10♦ | 50.2 | 1:50♦ | 55.3 |
| | 1:2 | | 35.1 | | 40.2 |
| | 1:3 | | 26.5 | | - |
| Deionised water | 1:1 | 1:10♦ | 54.9 | 1:50♦ | 57.4 |

♦Deionised water

Samples that were diluted with reverse aqua regia and subsequently 2% $HNO_3$ showed relatively lower concentrations than the expected 112 mg/L from the gold powder leach experiment with the highest extraction value of 51% for ICP-AES analysis. It is also clear that increasing the dilution factor of ammonia-ammonium thiosulphate solution, decreases the gold concentration values in both analyses. Dilution with water proved to be the most appropriate dilution method across both MP-AES and ICP-AES analysis with the closest gold concentration values of 54.9 mg/L and 57.4 mg/L respectively to the expected 112 mg/L. These concentration values were much higher than the other experiments and this dilution was taken to be the most appropriate in comparison to the other dilutions.

Table A.3: PCB (8.44 mg/L Au) dilution experiment results for various dilution methods

| Initial dilution solution | Initial dilution Factor | UCT AL | | CAF | |
|---|---|---|---|---|---|
| | | Additional Dilution | MP-AES (mg/L) | Additional Dilution | ICP-AES (mg/L) |
| No dilution | - | 1:5♦ | ND | 1:50♦ | ND |
| Reverse aqua regia | 1:1 | 1:100 $HNO_3$ | ND | 1:50♦ | 4.1 |
| | 1:2 | | ND | | 3.64 |
| $(NH_4)_2S_2O_3$ and $NH_3$ | 1:1 | 1:10♦ | 3.14 | 1:50♦ | - |
| | 1:2 | | 2.14 | | 2.3 |
| | 1:3 | | 1.59 | | 1.78 |
| Deionised water | 1:1 | 1:10 $HNO_3$ | 2.19 | 1:50♦ | 2.4 |

♦Deionised water

Gold concentration values for the PCB experiment were in the range of 1.6 ppm to 4.1 ppm. The highest gold concentration value (4.1 mg/L) received utilised the reverse aqua regia method with a dilution factor of 1:1 that underwent further 50 times dilution in the analysis laboratory using deionised water. Dilution with ammonia-ammonium thiosulphate solution (3.14 mg/L) in a 1:1 ratio and further dilution with deionised water at UCT AL proved to be the closest concentration to the expected 8.44 mg/L present on a PCB for the MP-AES analysis.

The dilution method incorporating ammonia-ammonium thiosulphate solution in a 1:1 ratio at the time of sampling was the preferred method to use for both gold powder and PCB experiments. After which, the samples would be refrigerated before being analysed. Further dilution, if required by the analysis laboratory, would utilise deionised water only.

Experimentation on precipitation formation such as sulphides or copper oxides in the ammonia-ammonium thiosulphate system at different copper concentrations was also conducted. This consisted of preparing five standard 1 M $NH_3$ and 0.5 M $(NH_4)_2S_2O_3$ solutions of various copper concentrations listed in Table A.4 with no gold present. All solutions were placed in tightly sealed 20 mL McCarthy glass bottles and placed in the refrigerator for one week. Observations were conducted on day one, day three and day seven. This experimentation was conducted mainly to observe the precipitation of metal and instability of the ammonium thiosulphate solution.

Table A.4: Copper concentrations for 5 samples on metal formation observation experiment

| Sample bottle number | Copper concentration (M) |
|---|---|
| Sample 1 and 5 | 0.04 |
| Sample 2 | 0.03 |
| Sample 3 | 0.05 |
| Sample 4 | 0.01 |

Table A.5 below contains images and observations documented over seven days. Five samples were observed with Sample 5 being a repeat of Sample 1.

Table A.5: Observations over 3 days of ammonium thiosulphate solutions

| Timeline | Illustration | Observation |
|---|---|---|
| Day 1 |  | In all McCarthy bottles, solution was clear with no evidence of precipitation. Small white particles were present in solution that eventually settled to the bottom of the bottles. These particles were present in reagent preparation. |
| Day 3 |  | The same particles observed in Day 1 were still present at the bottom of the flasks. Solution colour in all flasks had become noticeably clearer. |
| Day 7 |   | Precipitates were observed in significant quantities in Sample 1 and 5 with barely any precipitates in Sample 2. Sample 4 showed evidence of some precipitates whilst Sample 3 had little to no precipitates. Precipitates were of a brown colour in all bottles. |

The ammonia to thiosulphate ratio remained the same for all samples bottles however the ammonia to copper ratio changed for each change in copper concentration. On Day 7, hardly any precipitates were present in Sample 2 (0.03 M) which is peculiar as the copper concentration was between 0.01 M (Sample 4) and 0.05 M (Sample 3). This potentially points to a metastable system and the presence of a catalyst. The increasing copper concentration resulted in a high cuprous-thiosulphate complex formation and increases the possibility of precipitate formation in solution especially since there is a lack of gold in solution. Thus, there is a limit to the stabilising effect of ammonia on the system with an increase in copper in solution.

# B. Appendix B: Gold Analysis Calculations

## B.1. Leaching calculations

For 1 L standard ammonium thiosulphate solution

Table B.1: Conditions for preparing a 1 L standard solution

| Reagents | Conditions |
|---|---|
| 98wt% Ammonium thiosulphate | 0.5 M |
| 25% Ammonia | 0.5 M |
| Copper sulphate | 0.02 M |

Table B.2: Physical properties of ammonium thiosulphate, ammonia and copper sulphate

| Physical properties | |
|---|---|
| Ammonium thiosulphate molar mass (g/mol) | 148.21 |
| Ammonia molar mass (g/mol) | 17.031 |
| Ammonia density (g/cm$^3$) | 0.9 |
| Copper sulphate pentahydrate molar mass (g/mol) | 249.68 |

For ammonium thiosulphate:

$$m = n \times M$$

$$= 0.5 \frac{mol}{L} \times 148.21 \frac{g}{mol} \times 1\ L$$

$$= 74.105\ g$$

$$actual\ mass = \ 74.105\ g \div 98\% = 75.62\ g$$

For ammonia:

$$m = n \times M$$

$$= 0.5 \frac{mol}{L} \times 17.031 \frac{g}{mol} \times 1\ L$$

$$= 8.516\ g$$

$$V = \frac{m}{\rho}$$

$$= \frac{8.5155 g}{0.9\ g/cm^3}$$

$$= 9.462\ ml$$

$$actual\ volume = 9.4617\ \div 25\% = 37.85\ ml$$

For copper sulphate

$$m = n \times M$$

$$= 0.02 \frac{mol}{L} \times 249.68 \frac{g}{mol} \times 1\ L$$

$$= 4.994\ g$$

## B.2. Ion exchange calculations

**Calculating 50% excess capacity for 1 L NaCl solution**

Table B.3: Physical properties of sodium chloride, chloride ion and the resin bed

| Physical properties | |
|---|---|
| Resin Capacity (eq/L) | 1.15 |
| Resin bed mL | 5.2 |
| Chloride equivalent weight g/eq | 35.5 |
| Chloride molar mass (g/mol) | 35.5 |
| Sodium chloride molar mass (g/mol) | 58.44 |

$$Capacity = 1.15\frac{eq}{l} \times 0.0052\ l$$

$$= 0.00598\ equivalents$$

$$Chloride\ mass = 35.5\frac{g}{eq} \times 0.00598\ eq$$

$$= 0.21229\ g$$

$$Excess\ capacity = 0.21229\ g \times 50\%$$

$$= 0.106145\ g$$

$$Total\ Cl\ mass = 0.21229\ g + 0.106145\ g$$

$$= 0.31843\ g$$

$$n = \frac{m}{M}$$

$$= 35.5\frac{g}{mol} \div 0.31843\ g$$

$$= 0.00897\ mol$$

$$Total\ NaCl\ mass = 58.44\frac{g}{mol} \times 0.00897\ mol$$

$$= 0.5242\ g$$

**Calculations for Recovery after loading, elution and overall ion exchange efficiency**

$$Recovery\ after\ loading\ (\%) = \frac{Gold\ on\ resin\ after\ loading\ at\ T = 20\ mins}{Gold\ in\ loading\ solution\ at\ T = 0} \times 100$$

$$Recovery\ after\ elution\ (\%) = \frac{Gold\ in\ eluant\ after\ elution\ at\ T = 20\ mins}{Gold\ on\ resin\ after\ loading\ at\ \ T = 20\ mins} \times 100$$

$$Recovery\ after\ loading\ (\%) = \frac{Gold\ in\ eluant\ after\ elution\ at\ T = 20\ mins}{Gold\ in\ loading\ solution\ at\ T = 0} \times 100$$

**Mass action law model calculations**

$$\frac{\overline{X_{Au}}}{(1-\overline{X_{Au}})^3} = K_{Au}^{Cl} \times \left(\frac{\bar{C}}{C}\right)^2 \times \frac{X_{Au}}{(1-X_{Au})^3} \qquad \text{Equation 2.21}$$

Rearranging into: $AX^3 + BX^2 + CX + D = 0$

Produces: $A = -1$

$B = 3$

$C = -\left(K_{Au}^{Cl} \times \left(\frac{\bar{C}}{C}\right)^2 \times \frac{X_{Au}}{(1-X_{Au})^3}\right)^{-1} - 3$

$D = 1$

Solving for a third order polynomial required the following equations where:

$$X = \sqrt[3]{W + \sqrt[2]{W^2 + Z^3}} + \sqrt[3]{W - \sqrt[2]{W^2 + Z^3}} - V \qquad \text{Equation B.1}$$

With: $W = -\frac{B^3}{27A^3} + \frac{BC}{6A^2} - \frac{D}{2A}$

$Z = \frac{C}{3A} - \frac{B^2}{9A^2}$

$V = \frac{B}{3A}$

# C. Appendix C: MSDS of Resins

## C.1. AuRIX®100 MSDS

cognis
www.cognis.com

# AuRIX®100

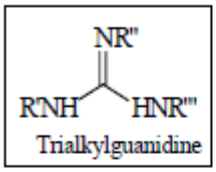

Trialkylguanidine

AuRIX 100 ion exchange resin is based on a styrene di-vinylbenzene based macroreticular resin bead functionalized with guanidine groups. Guanidines are strong organic bases especially suited to the extraction of aurocyanide from typical alkaline cyanide leach liquors. Upon contact with an aqueous solution, the guanidine will extract a proton from water at pH's typically less than 11.5 to form a guanidinium cation, which can then form an ion pair with auro-cyanide resulting in extraction. At pH's above 13, the guanidinium cation gives up its proton to re-form the neutral guanidine group resulting in transfer of the aurocyanide back into the aqueous resulting in stripping. The overall process is described in the following equations:

**Extraction**

$$RG_{(resin)} + H_2O \rightleftharpoons RGH^+_{(resin)} + OH^-_{(aq)}$$

$$RGH^+_{(resin)} + Au(CN)_2^-{}_{(aq)} \rightleftharpoons RGH^+Au(CN)_2^-{}_{(resin)}$$

**Stripping**

$$RGH^+Au(CN)_2^-{}_{(resin)} + OH^-_{(aq)} \rightleftharpoons RG_{(resin)} + Au(CN)_2^-{}_{(aq)} + H_2O$$

**TYPICAL PROPERTIES**

**A. Physical Properties:**

| | |
|---|---|
| Appearance | Tan Spherical Beads |
| Resin Bulk Density | |
| As shipped – wet | 620-700 gpl |
| Dry basis | 330 gpl |
| Moisture Retention (Cl) % | 47-53 % |
| Particle Size (% < 0.60 mm) | 0.01 |

**B. Performance Properties:**

| | |
|---|---|
| Volume Capacity | 0.25-0.35 eq/l |
| Recommended Gold Loading in Extraction | 2,000 – 10000 gm/ton |
| Typical Eluted Resin Values | 300 gm/ton Au |
| Typical Elution Time | 12-24 hours |
| Typical Residence Time per Stage in RIP | 15-30 mins |

### Selectivity

While quite selective for gold, AuRIX 100 will extract other anionic metal cyanide complexes. The order of extraction is as follows:

$$Au > Ag > Zn \sim Ni > Cu > Co > Fe$$

The observed selectivity is to some extent dependent upon the pH of the incoming aqueous feed solution as might be expected for an ion pair extraction type mechanism.

## TYPICAL OPERATING CONDITIONS

AuRIX 100 ion exchange resin is ideally suited for recovery of gold from typical alkaline cyanide leach liquors having a pH of 9.0-11.5. AuRIX 100 is well suited for extraction of gold from clear solutions in the Resin-in-Solution(RIS) process and from pulps in the Resin-in-Pulp(RIP) process. Attrition tests in an Anglo American pump cell contactor have shown that no detectable break down of AuRIX resin beads occurred during the processing of 800 tons of pulp.

The resin is shipped as the hydrochloride form. Before beginning any test work to evaluate the effectiveness of AuRIX 100 on a given leach solution, it is recommended that the resin be first converted to the free base form by two contacts with 1 molar sodium hydroxide (2 volumes of aqueous caustic/volume of resin beads) followed by washing with water until the pH of the wash water is neutral. Resin amounts must be determined on a volume measurement basis. Drying the resin beads in an attempt to obtain a dry weight will result in destruction of the resin upon re-exposure to water.

Stripping is achieved by contacting the loaded resin with a caustic solution containing 0.5M sodium hydroxide, 0.5M sodium benzoate and 100 ppm of sodium cyanide at 55-60oC. The gold values are recovered from the eluent by electrowinning.

For assistance in developing a test program for evaluating the application of AuRIX 100 ion exchange resin to a particular leach solution, please contact your Cognis technical representative.

## TOXICITY

Material Safety Data Sheet available upon request.

## C.2. Purogold ™ MTA5013SO4 MSDS

**PRODUCT DATA SHEET**

# Purogold™ MTA5013SO4

**Polystyrenic Macroporous, Type I Strong Base Anion Resin, Sulfate form, RIP Grade**

### PRINCIPAL APPLICATIONS
- Gold recovery from thiosulphate leach liquors and pulps

### ADVANTAGES
- Superior Mechanical Strength
- Large bead size

### SYSTEMS
- Resin-In-Pulp (RIP) Process

### TYPICAL PACKAGING
- 1 ft³ Sack
- 25 L Sack
- 5 ft³ Drum (Fiber)
- 1 m³ Supersack
- 42 ft³ Supersack

### TYPICAL PHYSICAL & CHEMICAL CHARACTERISTICS:

| | |
|---|---|
| Polymer Structure | Macroporous polystyrene crosslinked with divinylbenzene |
| Appearance | Spherical Beads |
| Functional Group | Type I Quaternary Ammonium |
| Ionic Form | $SO_4^{2-}$ |
| Total Capacity | 1.15 eq/L (25.1 Kgr/ft³) ($Cl^-$ form) |
| Moisture Retention | 54 - 61 % ($Cl^-$ form) |
| Particle Size Range | 1000 - 1600 µm |
| < 1000 µm (max.) | 10 % |
| < 850 µm (max.) | 1 % |
| Specific Gravity | 1.09 |
| Shipping Weight (approx.) | 670 - 700 g/L (41.9 - 43.8 lb/ft³) |
| Temperature Limit | 100 °C (212.0 °F) ($SO_4^{2-}$ form) |

Purolite

**Americas**
T +1 610 668 9090
F +1 610 668 8139
americas@purolite.com

**EMEA**
T +44 1443 229334
F +44 1443 227073
europe@purolite.com

**Asia Pacific**
T +86 571 876 31382
F +86 571 876 31385
asiapacific@purolite.com

## C.3. Purogold™ MTA5011SO4 MSDS

**PRODUCT DATA SHEET**

# Purogold™ MTA5011SO4

**Polystyrenic Macroporous, Type I Strong Base Anion Resin, Sulfate form, RIP Grade**

### PRINCIPAL APPLICATIONS

- Gold recovery from thiosulphate leach liquors and pulps

### ADVANTAGES

- Superior Mechanical Strength
- Large bead size

### SYSTEMS

- Resin-In-Pulp (RIP) Process

### TYPICAL PACKAGING

- 1 ft³ Sack
- 25 L Sack
- 5 ft³ Drum (Fiber)
- 1 m³ Supersack
- 42 ft³ Supersack

### TYPICAL PHYSICAL & CHEMICAL CHARACTERISTICS:

| | |
|---|---|
| Polymer Structure | Macroporous polystyrene crosslinked with divinylbenzene |
| Appearance | Spherical Beads |
| Functional Group | Type I Quaternary Ammonium |
| Ionic Form | $SO_4^{2-}$ |
| Total Capacity | 1.15 eq/L (25.1 Kgr/ft³) ($Cl^-$ form) |
| Moisture Retention | 54 - 61 % ($Cl^-$ form) |
| Particle Size Range | 800 - 1300 µm |
| < 710 µm (max.) | 1 % |
| Reversible Swelling, $Cl^- \rightarrow OH^-$ (max.) | 25 % |
| Specific Gravity | 1.08 |
| Shipping Weight (approx.) | 670 - 700 g/L (41.9 - 43.8 lb/ft³) |
| Temperature Limit | 100 °C (212.0 °F) ($Cl^-$ form) |
| Temperature Limit | 60 °C (140.0 °F) ($OH^-$ form) |

Purolite

**Americas**
T +1 610 668 9090
F +1 610 668 8139
americas@purolite.com

**EMEA**
T +44 1443 229334
F +44 1443 227073
europe@purolite.com

**Asia Pacific**
T +86 571 876 31382
F +86 571 876 31385
asiapacific@purolite.com





m

# D. Appendix D: Further Experiment Results

## D.1. Size reduction results

Table D.1: Mass loss of all PCBs for the size reduction step

| PCB No. | Whole PCB (g) | Pre-Treated PCB (g) | Mass loss (g) | Mass loss (%) |
|---|---|---|---|---|
| 1 | 52,8 | 47,4 | 5,4 | 10,24 |
| 2 | 52,30 | 48,37 | 3,93 | 7,51 |
| 3 | 52,11 | 45,34 | 6,77 | 12,99 |
| 4 | 52,05 | 49,29 | 2,76 | 5,30 |
| 5 | 53,33 | 49,30 | 4,03 | 7,55 |
| 6 | 52,85 | 49,75 | 3,04 | 5,75 |
| 7 | 52,18 | 48,81 | 4,04 | 7,64 |
| 8 | 52,07 | 48,76 | 3,43 | 6,57 |
| 9 | 52,71 | 48,85 | 3,86 | 7,32 |
| 10 | 52,63 | 48,70 | 3,93 | 7,46 |
| 11 | 52,38 | 48,60 | 3,78 | 7,21 |
| 12 | 51,87 | 49,75 | 2,12 | 4,08 |
| 13 | 52,29 | 48,43 | 3,86 | 7,38 |
| 14 | 52,57 | 48,67 | 3,90 | 7,42 |
| 15 | 52,60 | 49,98 | 2,62 | 4,97 |
| 16 | 52,40 | 48,47 | 3,92 | 7,49 |
| 17 | 51,59 | 47,81 | 3,77 | 7,31 |
| 18 | 52,8 | 47,5 | 5,3 | 10,04 |
| 19 | 51,43 | 47,70 | 3,73 | 7,26 |
| 20 | 51,21 | 47,51 | 3,70 | 7,23 |
| 21 | 51,96 | 48,18 | 3,78 | 7,27 |
| 22 | 52,89 | 49,09 | 3,80 | 7,18 |
| 23 | 52,44 | 48,58 | 3,86 | 7,36 |
| 24 | 52,30 | 48,52 | 3,78 | 7,23 |
| 25 | 52,35 | 48,59 | 3,77 | 7,20 |
| 26 | 51,82 | 48,11 | 3,71 | 7,17 |
| 27 | 52,37 | 48,62 | 3,76 | 7,17 |
| 28 | 51,91 | 48,20 | 3,71 | 7,15 |
| 29 | 52,63 | 48,88 | 3,76 | 7,13 |

## D.2. SEM-EDS analysis results

Imaging results from all 3 materials: PCB. syringe filter and filter paper from vacuum filtration.

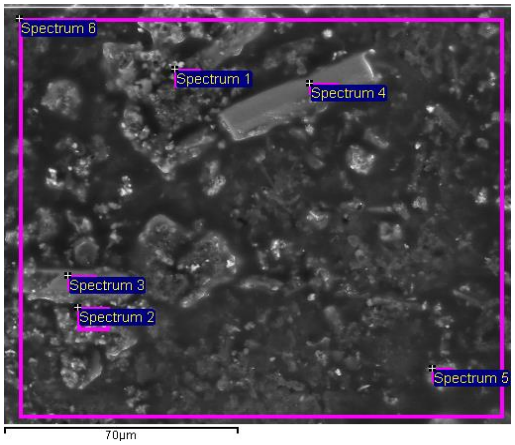


(a)

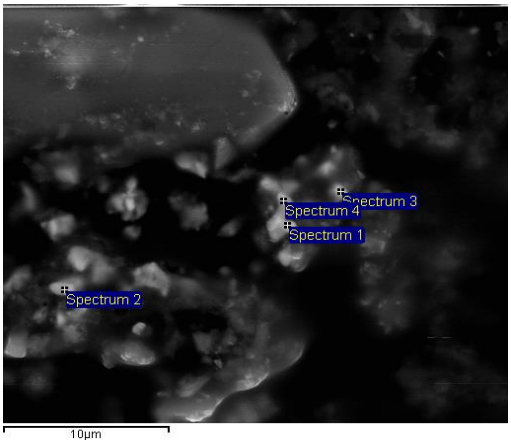


(b)

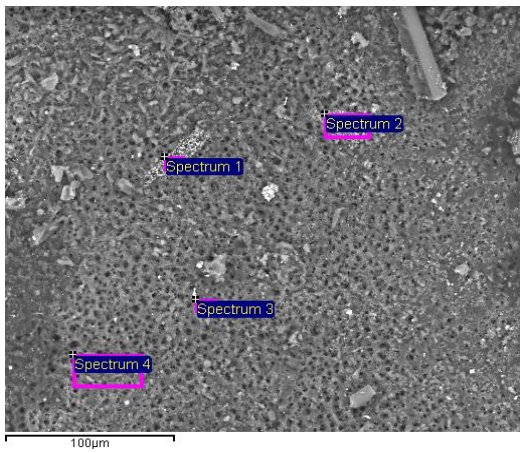


(c)

Figure D.1: (a) SEM-EDS images from leached PCB Area 1 (b) SEM-EDS images from leached PCB Area 2 (c) SEM-EDS images from leached PCB Area 3

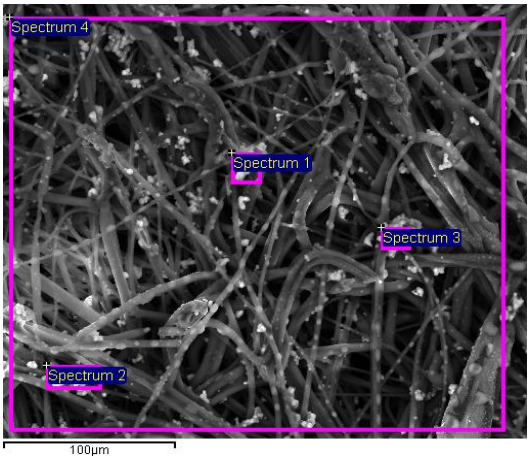


(a)

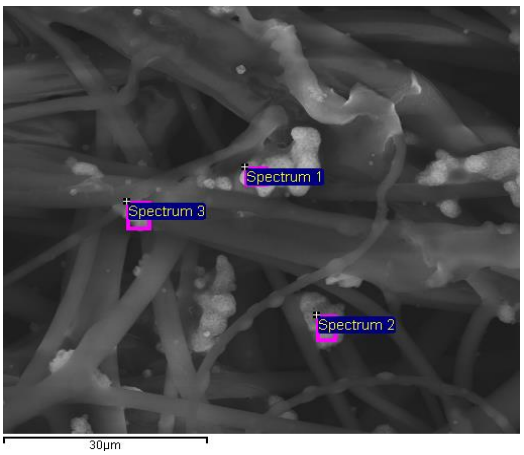


(b)

Figure D.2: (a) SEM-EDS images from syringe filter Area 1 (b) SEM-EDS images from syringe filter Area 2

The images below depict the areas investigated on the filter paper used to filtrate the solution from the PCBs. No gold was found on any of the spectrums investigated.

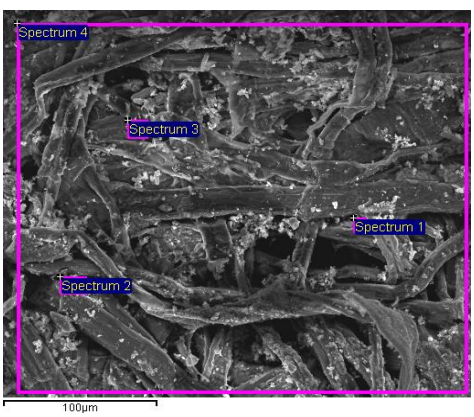


(a)

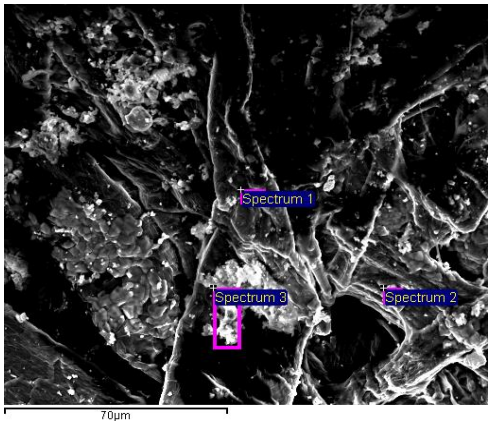


(b)

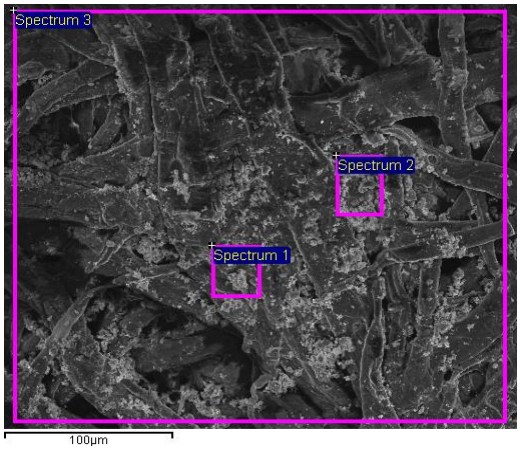


(c)

Figure D.3: (a) SEM-EDS images from filter paper Area 1 (b) SEM-EDS images from filter paper Area 2 (c) SEM-EDS images from filter paper Area 3

## D.3. Gold leaching results

All gold and copper recoveries were based on the equation below:

$$Gold\ recovered = \frac{Gold\ analysed\ in\ solution\ (mg)}{initial\ PCB\ gold\ mass\ or\ initial\ gold\ added\ (mg)}$$ Equation D.1

Table D.2: Table showing the recorded pH for gold powder dissolution experiments

| Gold powder experiment | Time (Hours) | pH | | |
|---|---|---|---|---|
| | | Reactor A | Reactor B | Reactor C |
| **24 hour** | 0 | 9.511 | 9.511 | 9.511 |
| | 24 | 9.441 | 9.544 | 9.331 |
| **0.008 M Cu** | 0 | 9.372 | 9.372 | 9.372 |
| | 3 | 9.357 | 9.452 | 9.395 |
| | 6 | 9.373 | 9.445 | 9.321 |
| **0.02 Cu** | 0 | 9.973 | 9.973 | 9.973 |
| | 3 | 9.405 | 9.435 | 9.356 |
| | 6 | 9.409 | 9.487 | 9.387 |
| **0.045 Cu** | 0 | 9.568 | 9.568 | 9.568 |
| | 3 | 9.450 | 9.398 | 9.287 |
| | 6 | 9.293 | 9.333 | 9.216 |
| **0.1 Cu** | 0 | 9.515 | 9.5151 | 9.515 |
| | 3 | 9.346 | 9.355 | 9.312 |
| | 6 | 9.340 | 9.355 | 9.310 |

Table D.3: Gold dissolution of gold powder experiments over 24 hours (mg/L)

| Time (hours) | Average Au recovered (mg/L) | Average Au recovered (%) |
|---|---|---|
| **0** | 0.0 | 0.0 |
| **0.25** | 16.7 | 14.8 |
| **0.5** | 40.4 | 36.0 |
| **0.75** | 71.8 | 64.0 |
| **1** | 94.5 | 84.2 |
| **1.5** | 124.7 | 111.2 |
| **2** | 141.4 | 126.0 |
| **3** | 139.7 | 124.5 |
| **4** | 143.2 | 127.6 |
| **5** | 142.3 | 126.8 |
| **6** | 140.5 | 125.2 |
| **21** | 146.9 | 130.9 |
| **22** | 136.2 | 121.4 |
| **23** | 132.9 | 118.5 |
| **24** | 133.6 | 119.1 |

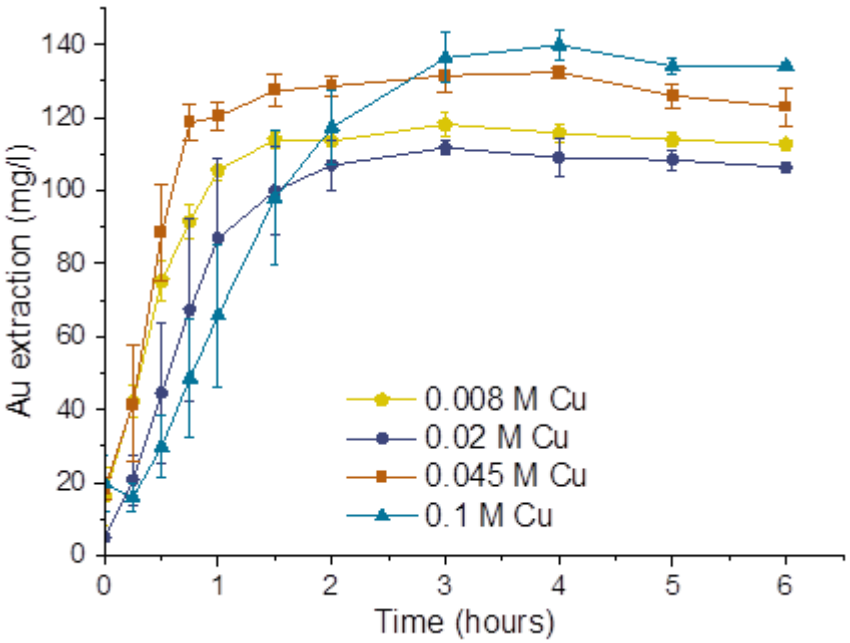


Figure D.4: Gold extraction from gold powder dissolution at various background Cu concentrations (0.008 M, 0.02 M, 0.045 M and 0.1 M

Table D.4: Gold powder dissolution for 0.008 M Cu and 0.02 M Cu gold powder experiments (mg/L)

| Time hours | 0.008M | | 0.02 M Cu | |
|---|---|---|---|---|
| | Au recovered (mg/L) | Au recovered (%) | Au recovered (mg/L) | Au recovered (%) |
| **0** | 16.1 | 14.4 | 4.9 | 4.3 |
| **0.25** | 42.1 | 37.6 | 20.7 | 18.5 |
| **0.5** | 75.3 | 67.2 | 44.6 | 39.8 |
| **0.75** | 91.6 | 81.8 | 67.3 | 60.1 |
| **1** | 105.6 | 94.3 | 86.9 | 77.5 |
| **1.5** | 113.9 | 101.7 | 99.9 | 89.2 |
| **2** | 113.6 | 101.4 | 106.9 | 95.5 |
| **3** | 118.1 | 105.4 | 111.7 | 99.8 |
| **4** | 115.7 | 103.3 | 109.1 | 97.4 |
| **5** | 113.9 | 101.7 | 108.4 | 96.8 |
| **6** | 112.8 | 100.7 | 106.3 | 94.9 |

Table D.5: Gold dissolution for 0.045 M Cu and 0.1 M Cu gold powder experiments (mg/L)

| Time hours | 0.045 M Cu | | 0.1 M Cu | |
|---|---|---|---|---|
| | Au recovered (mg/L) | Au recovered (%) | Au recovered (mg/L) | Au recovered (%) |
| **0** | 18.4 | 16.4 | 19.7 | 17.6 |
| **0.25** | 41.5 | 37.0 | 15.9 | 14.2 |
| **0.5** | 88.5 | 79.0 | 29.8 | 26.6 |
| **0.75** | 118.5 | 105.8 | 48.6 | 43.4 |
| **1** | 120.3 | 107.4 | 65.8 | 58.7 |
| **1.5** | 127.4 | 113.7 | 98.0 | 87.5 |
| **2** | 128.6 | 114.9 | 117.3 | 104.7 |
| **3** | 131.5 | 117.4 | 136.3 | 121.7 |
| **4** | 132.4 | 118.2 | 139.9 | 124.9 |
| **5** | 126.0 | 112.5 | 134.0 | 119.7 |
| **6** | 122.9 | 109.8 | 134.0 | 119.7 |

Table D.6: Table showing the recorded pH for all PCB experiments

| PCB Experiment | Time hours | pH | | |
|---|---|---|---|---|
| | | Reactor A | Reactor B | Reactor C |
| **24 hour** | 0 | 10.111 | 10.111 | 10.111 |
| | 24 | 9.395 | 9.586 | 9.162 |
| **0 M Cu** | 0 | 9.837 | 9.387 | 9.837 |
| | 3 | 9.827 | 9.829 | 9.740 |
| | 6 | 9.762 | 9.764 | 9.617 |
| **0.008 M Cu** | 0 | 9.557 | 9.557 | 9.557 |
| | 3 | 9.553 | 9.574 | 9.528 |
| | 6 | 9.586 | 9.532 | 9.543 |
| **0.02 Cu** | 0 | 9.845 | 9.845 | 9.845 |
| | 3 | 9.949 | 9.873 | 9.873 |
| | 6 | 9.845 | 9.929 | 9.883 |
| **0.045 Cu** | 0 | 9.593 | 9.593 | 9.593 |
| | 3 | 9.485 | 9.483 | 9.475 |
| | 6 | 9.356 | 9.570 | 9.415 |
| **0.1 Cu** | 0 | 9.576 | 9.576 | 9.576 |
| | 3 | 9.684 | 9.690 | 9.570 |
| | 6 | 9.406 | 6.656 | 9.494 |
| **0.5 M $NH_3$** | 0 | 9.845 | 9.845 | 9.845 |
| | 1.5 | 9.840 | 9.835 | 9.849 |
| | 3 | 9.845 | 9.929 | 9.883 |
| **1 M $NH_3$** | 0 | 10.009 | 10.009 | 10.009 |
| | 1.5 | 10.162 | 10.161 | 10.146 |
| | 3 | 10.163 | 10.158 | 10.117 |

Table D.7: Gold and copper leaching concentrations for PCB experiments (mg/L)

| Experiment | Time (hours) | Average Au recovered (mg/L) | Average Au recovered (%) | Average Cu recovered (g/L) | Average Cu recovered (%) |
|---|---|---|---|---|---|
| **24 hour experiment** | 0 | 0.26 | 0.33 | 0.35 | 0.87 |
| | 0.25 | 0.55 | 0.71 | 0.42 | 1.05 |
| | 0.5 | 0.22 | 0.28 | 0.49 | 1.22 |
| | 0.75 | 0.20 | 0.26 | 0.53 | 1.32 |
| | 1 | 0.28 | 0.37 | 0.62 | 1.55 |
| | 1.5 | 0.26 | 0.33 | 0.81 | 2.02 |
| | 2 | 0.23 | 0.29 | 1.11 | 2.78 |
| | 3 | 0.40 | 0.51 | 1.88 | 4.70 |
| | 4 | 0.98 | 1.26 | 3.13 | 7.82 |
| | 5 | 3.02 | 3.89 | 3.86 | 9.66 |
| | 6 | 4.04 | 5.20 | 4.58 | 11.46 |
| | 21 | 4.39 | 5.64 | 6.35 | 15.88 |
| | 22 | 4.18 | 5.37 | 6.90 | 17.27 |
| | 23 | 3.94 | 5.07 | 6.61 | 16.53 |
| | 24 | 4.00 | 5.14 | 6.56 | 16.42 |
| **0 M Cu** | 0 | 0.01 | 0.01 | 0.00 | 0.01 |
| | 0.25 | 0.05 | 0.06 | 0.01 | 0.03 |
| | 0.5 | 0.05 | 0.06 | 0.02 | 0.06 |
| | 0.75 | 0.06 | 0.08 | 0.03 | 0.08 |
| | 1 | 0.07 | 0.09 | 0.04 | 0.11 |
| | 1.5 | 0.11 | 0.15 | 0.07 | 0.16 |
| | 2 | 0.05 | 0.06 | 0.09 | 0.22 |
| | 3 | 0.16 | 0.21 | 0.13 | 0.34 |
| | 4 | 0.39 | 0.50 | 0.19 | 0.49 |
| | 5 | 0.21 | 0.27 | 0.28 | 0.71 |
| | 6 | 0.14 | 0.18 | 0.39 | 0.97 |
| **0.008 M Cu** | 0 | 0.42 | 0.54 | 0.06 | 0.15 |
| | 0.25 | 0.52 | 0.67 | 0.11 | 0.28 |
| | 0.5 | 0.43 | 0.55 | 0.15 | 0.38 |
| | 0.75 | 0.36 | 0.47 | 0.18 | 0.44 |
| | 1 | 0.33 | 0.42 | 0.22 | 0.54 |
| | 1.5 | 0.37 | 0.48 | 0.30 | 0.74 |
| | 2 | 0.33 | 0.43 | 0.44 | 1.11 |
| | 3 | 0.40 | 0.51 | 0.73 | 1.83 |
| | 4 | 0.58 | 0.75 | 1.21 | 3.04 |
| | 5 | 0.81 | 1.04 | 1.83 | 4.59 |
| | 6 | 1.59 | 2.04 | 2.30 | 5.75 |
| **0.02 Cu** | 0 | 0.28 | 0.36 | 0.17 | 0.43 |
| | 0.25 | 0.64 | 0.83 | 0.33 | 0.83 |
| | 0.5 | 0.64 | 0.83 | 0.43 | 1.07 |
| | 0.75 | 0.48 | 0.62 | 0.51 | 1.27 |
| | 1 | 0.48 | 0.62 | 0.64 | 1.61 |
| | 1.5 | 0.58 | 0.74 | 0.85 | 2.14 |

t

| | | | | | |
|---|---|---|---|---|---|
| | 2 | 0.62 | 0.80 | 1.16 | 2.90 |
| | 3 | 0.62 | 0.80 | 1.79 | 4.49 |
| | 4 | 1.53 | 1.97 | 2.27 | 5.68 |
| | 5 | 1.58 | 2.03 | 3.32 | 8.31 |
| | 6 | 4.38 | 5.64 | 4.10 | 10.26 |
| **0.045 Cu** | 0 | 0.88 | 1.14 | 0.21 | 0.53 |
| | 0.25 | 1.30 | 1.67 | 0.55 | 1.38 |
| | 0.5 | 1.38 | 1.78 | 0.72 | 1.81 |
| | 0.75 | 1.43 | 1.84 | 0.93 | 2.32 |
| | 1 | 1.34 | 1.73 | 1.00 | 2.50 |
| | 1.5 | 1.57 | 2.02 | 1.43 | 3.58 |
| | 2 | 1.49 | 1.92 | 2.20 | 5.50 |
| | 3 | 2.35 | 3.02 | 3.53 | 8.82 |
| | 4 | 4.49 | 5.78 | 4.48 | 11.21 |
| | 5 | 6.72 | 8.64 | 4.88 | 12.20 |
| | 6 | 7.90 | 10.16 | 5.16 | 12.90 |
| **0.1 Cu** | 0 | 2.13 | 2.73 | 1.15 | 2.88 |
| | 0.25 | 2.65 | 3.41 | 2.40 | 5.99 |
| | 0.5 | 3.50 | 4.50 | 2.35 | 5.87 |
| | 0.75 | 4.36 | 5.60 | 3.53 | 8.82 |
| | 1 | 3.98 | 5.12 | 2.86 | 7.15 |
| | 1.5 | 4.36 | 5.60 | 4.09 | 10.22 |
| | 2 | 4.26 | 5.48 | 4.19 | 10.48 |
| | 3 | 5.29 | 6.80 | 5.58 | 13.96 |
| | 4 | 5.45 | 7.01 | 4.53 | 11.32 |
| | 5 | 5.74 | 7.38 | 6.64 | 16.60 |
| | 6 | 5.55 | 7.14 | 7.80 | 19.51 |

Table D.8: Gold recoveries for gold dissolution experiments for ion exchange experiments (mg/L)

| | Time (hours) | Reactor A (mg/L) | Reactor B (mg/L) | Reactor C (mg/L) | Average Au (mg/L) | Au recovery % |
|---|---|---|---|---|---|---|
| Set 1 | 0 | 0 | 0 | 0 | 0 | 0 |
| | 24 | 165.1 | 156.0 | 170.9 | 164.0 | 146.4 |
| Set 2 | 0 | 0 | 0 | 0 | 0 | 0 |
| | 24 | 110.7 | 80.3 | 113.5 | 101.5 | 90.6 |
| Set 3 | 0 | 0.0 | 0.0 | 0.0 | 0.0 | 0.0 |
| | 24 | 113.2 | 126.3 | 125.8 | 121.8 | 108.7 |
| Set 4 | 0 | 10.5 | 17.5 | 18.5 | 15.5 | 13.8 |
| | 24 | 123.4 | 135.2 | 125.9 | 128.2 | 114.4 |
| Set 5 | 0 | 7.1 | 11.2 | 7.6 | 8.6 | 7.7 |
| | 24 | 109.3 | 127.6 | 124.4 | 120.4 | 107.5 |
| Set 6 | 0 | 14.2 | 17.9 | 19.7 | 17.3 | 15.4 |
| | 24 | 132.5 | 126.8 | 131.3 | 130.2 | 116.3 |
| Set 7 | 0 | 9.9 | 15.1 | 14.3 | 13.1 | 11.7 |
| | 24 | 125.6 | 118.1 | 126.0 | 123.2 | 110.0 |
| Set 8 | 0 | 7.1 | 6.9 | 7.9 | 7.3 | 6.5 |
| | 24 | 111.8 | 107.6 | 106.2 | 108.5 | 96.9 |
| Set 9 | 0 | 5.4 | 5.1 | 4.9 | 5.1 | 4.6 |
| | 24 | 111.3 | 110.7 | 120.8 | 114.3 | 102.0 |
| Set 10 | 0 | 7.8 | 6.5 | 5.4 | 6.6 | 5.9 |
| | 24 | 110.5 | 112.0 | 109.3 | 110.6 | 98.7 |
| Set 11 | 0 | 8.3 | 7.9 | 4.4 | 6.9 | 6.1 |
| | 24 | 137.9 | 135.1 | 140.2 | 137.7 | 123.0 |
| Set 12 | 0 | 9.6 | 8.8 | 6.6 | 8.4 | 7.5 |
| | 24 | 140.2 | 125.9 | 137.3 | 134.5 | 120.1 |
| Set 13 | 0 | 11.9 | 9.6 | 11.2 | 10.9 | 9.7 |
| | 24 | 137.5 | 131.3 | 149.1 | 139.3 | 124.4 |
| Set 14 | 0 | 13.3 | 10.6 | 9.7 | 11.2 | 10.0 |
| | 24 | 132.1 | 135.8 | 136.8 | 134.9 | 120.4 |
| Set 15 | 0 | 6.1 | 6.6 | 4.6 | 5.8 | 5.2 |
| | 24 | 135.7 | 149.6 | 131.9 | 139.1 | 124.2 |
| Set 16 | 0 | 2.1 | 3.1 | 0.5 | 1.9 | 1.7 |
| | 24 | 104.0 | 105.4 | 107.0 | 105.4 | 94.1 |

## D.4. Ion exchange results

Table D.9: Recorded pH for capacity tests on AuRIX®100 resin

| Method | Solution | Experiment step | Time (min) | pH | | |
|---|---|---|---|---|---|---|
| | | | | Test 1 | Test 2 | Test 3 |
| 1 | Deionised water | 2 | 0 | 7.132 | 7.132 | 7.192 |
| | | | 40 | 10.364 | 10.209 | 10.588 |
| 1 | Deionised water | 4 | 0 | 7.132 | 7.132 | 7.912 |
| | | | 40 | 9.164 | 8.958 | 9.625 |
| 2 | Deionised water | 2 | 0 | 7.888 | 7.888 | - |
| | | | 40 | 10.381 | 10.602 | - |

Table D.10: Chlorine concentration in mg/L for capacity tests on AuRIX®100 resin

| Method | Time (min) | Cl (mg/L) | | |
|---|---|---|---|---|
| | | Test 1 | Test 2 | Test 3 |
| 1 | 0 | 125 | 102 | 122 |
| | 40 | 138 | 125 | 145 |
| 2 | 0 | 3933 | 3943 | - |
| | 40 | 3774 | 3862 | - |

Table D.11: Gold and copper concentration (mg/L) and pH for AuRIX®100 loading and elution experiments

| Step | Time (min) | Test 1 | | | Test 2 | | |
|---|---|---|---|---|---|---|---|
| | | pH | Au (mg/L) | Cu (mg/L) | pH | Au (mg/L) | Cu (mg/L) |
| Loading | 0 | 9.930 | 170.4 | 1401 | 9.566 | 178.5 | 1302 |
| | 10 | 9.752 | 166.6 | 1315 | 9.281 | 167.7 | 1273 |
| | 20 | 9.376 | 164.6 | 1307 | 9.539 | 173.7 | 1258 |
| Elution | 0 | 12.238 | 0.0 | 7 | 13.997 | 2.3 | 1 |
| | 10 | 13.587 | 0.0 | 17 | 13.938 | 3.4 | 1 |
| | 20 | 13.800 | 3.0 | 9 | 13.680 | 2.3 | 9 |

Table D.12: Recorded pH for capacity tests on MTA5013 resin

| Experiment step | Solution | Time (min) | pH | | |
|---|---|---|---|---|---|
| | | | Test 1 | Test 2 | Test 3 |
| 1 | NaOH | 0 | 14.020 | 14.090 | 14.890 |
| | | 40 | 13.930 | 14.065 | 14.537 |
| 2 | Deionised water | 0 | 9.556 | 8.764 | 9.292 |
| | | 40 | 10.200 | 10.25 | 10.318 |
| 3 | NaCl | 0 | 8.200 | 8.300 | 8.200 |
| | | 40 | 11.23 | 11.591 | 11.712 |

Table D.13: Gold and copper concentration (mg/L) and pH for MTA5013 loading and elution experiment (10 mL/min)

| Step | Time (min) | Test 1 | | | Test 2 | | | Test 3 | | |
|---|---|---|---|---|---|---|---|---|---|---|
| | | pH | Au (mg/L) | Cu (mg/L) | pH | Au (mg/L) | Cu (mg/L) | pH | Au (mg/L) | Cu (mg/L) |
| Load | 0 | 9.868 | 145.5 | 1278 | 9.860 | 140.2 | 1349 | 9.774 | 144.3 | 1318 |
| | 10 | 9.680 | 134.1 | 1289 | 9.680 | 134.3 | 1275 | 9.514 | 133.7 | 1273 |
| | 20 | 9.660 | 135.4 | 1290 | 9.476 | 143 | 1300 | 9.292 | 148 | 1230 |
| Elution | 0 | 4.845 | 0 | 0 | 5.002 | 0 | 0 | 5.499 | 0 | 0 |
| | 10 | 6.985 | 6.500 | 7.748 | 7.252 | 3.100 | 7.800 | 7.100 | 2.800 | 8.880 |
| | 20 | 6.867 | 5.700 | 5.308 | 6.841 | 2.130 | 8.296 | 6.781 | 2.310 | 8.641 |

Table D.14: Gold and copper concentration (mg/L) and pH for MTA5013 loading and elution experiments (25 mL/min and 50 mL/min)

| Step | Time (min) | Test 1: 25 mL/min | | | Test 2: 50 mL/min | | |
|---|---|---|---|---|---|---|---|
| | | pH | Au (mg/L) | Cu (mg/L) | pH | Au (mg/L) | Cu (mg/L) |
| Loading | 0 | 9.779 | 119.3 | 1330 | 9.884 | 118.5 | 1269 |
| | 10 | 9.621 | 118.9 | 1351 | 9.573 | 120.7 | 1359 |
| | 20 | 9.458 | 114 | 1311 | 9.503 | 113.8 | 1246 |
| Elution | 0 | 4.748 | 0 | 0 | 5.152 | 0 | 0 |
| | 10 | 9.079 | 7.722 | 21.25 | 7.170 | 5.27 | 80.92 |
| | 20 | 6.721 | 3.961 | 12.69 | 6.921 | 3.49 | 6.694 |

Table D.15: Gold and copper concentration (mg/L) for loading and elution experiments with 2 eluants (ammonia and ammonium nitrate)

| Step | Time (min) | Test 1 | | | Test 2 | | | Test 3 | | |
|---|---|---|---|---|---|---|---|---|---|---|
| | | pH | Au (mg/L) | Cu (mg/L) | pH | Au (mg/L) | Cu (mg/L) | pH | Au (mg/L) | Cu (mg/L) |
| Load | 0 | 9.821 | 128.8 | 1301 | 9.920 | 135.3 | 1356 | 9.393 | 137.7 | 1378 |
| | 10 | 9.727 | 126.6 | 1307 | 9.683 | 133.7 | 1265 | 9.297 | 147.4 | 1312 |
| | 20 | 9.723 | 126.1 | 1182 | 9.681 | 136.3 | 1277 | 9.369 | 137.6 | 1356 |
| Elution 1 | 0 | 12.43 | 0 | 0 | 12.42 | 0 | 0 | 11.80 | 0 | 0 |
| | 10 | 11.73 | 1.10 | 1.822 | 11.79 | 1.1 | 0 | 11.28 | 0 | 0 |
| | 20 | 11.90 | 1.50 | 0.622 | 12.07 | 1.5 | 0.916 | 11.54 | 0.50 | 0.884 |
| Elution 2 | 0 | 7.977 | 0 | - | 5.616 | 0 | - | 7.890 | 0 | - |
| | 10 | 7.966 | 2.10 | - | 7.414 | 3.70 | - | 7.557 | 2.50 | - |
| | 20 | 7.636 | 1.24 | - | 7.315 | 0.70 | - | 7.310 | 0.80 | - |

Table D.16: Recorded pH for capacity experiments on the MTA5011 resin

| Experiment step | Solution | Time (minutes) | pH | | |
|---|---|---|---|---|---|
| | | | Test 1 | Test 2 | Test 3 |
| 1 | NaOH | 0 | 13.822 | 13.986 | 13.931 |
| | | 40 | 13.911 | 13.979 | 13.734 |
| 2 | Deionised water | 0 | 9.241 | 9.241 | 9.704 |
| | | 40 | 10.540 | 10.778 | 10.834 |
| 3 | NaCl | 0 | 9.426 | 8.673 | 9.528 |
| | | 40 | 11.754 | 11.587 | 11.535 |

Table D.17: Gold and copper concentrations (mg/L) for loading and elution experiments on the MTA5011 resin

| Step | Time (min) | Test 1 | | | Test 2 | | | Test 3 | | |
|---|---|---|---|---|---|---|---|---|---|---|
| | | pH | Au (mg/L) | Cu (mg/L) | pH | Au (mg/L) | Cu (mg/L) | pH | Au (mg/L) | Cu (mg/L) |
| Load | 0 | 9.598 | 129.1 | 1201 | 9.640 | 146.3 | 1306 | 9.638 | 139.8 | 1319 |
| | 10 | 9.537 | 128.3 | 1167 | 9.531 | 128.3 | 1234 | 9.328 | 138 | 1325 |
| | 20 | 9.530 | 119.4 | 1188 | 9.526 | 129.4 | 1208 | 9.440 | 135.3 | 1297 |
| Elution | 0 | 5.845 | 0 | 0 | 5.835 | 0 | 0 | 5.476 | 0 | 0 |
| | 10 | 7.469 | 8.613 | 8.498 | 7.354 | 11.05 | 7.015 | 7.136 | 9.29 | 15.49 |
| | 20 | 7.177 | 6.316 | 4.285 | 7.120 | 8.172 | 5.749 | 6.853 | 4.6 | 5.722 |